2348 #3

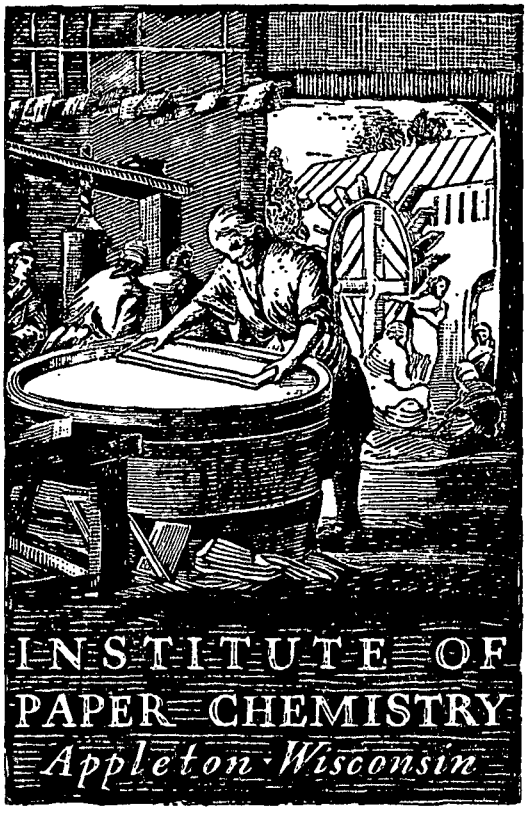

STUDIES OF THE SHEET-FORMING PROCESS

THE RETENTION OF FINE PARTICLES IN FIBER MATS

Project 2348

Report Three

A Progress Report to

MEMBERS OF GROUP PROJECT 2348

January 20, 1964

THE INSTITUTE OF PAPER CHEMISTRY
Appleton, Wisconsin

STUDIES OF THE SHEET-FORMING PROCESS

THE RETENTION OF FINE PARTICLES IN FIBER MATS

Project 2348

Report Three

A Progress Report to

MEMBERS OF GROUP PROJECT 2348

January 20, 1964

Members of Group Project 2348:

Consolidated Papers, Inc.

Crown Zellerbach Corporation

Eastman Kodak Company

The Eaton-Dikeman Company

P. H. Glatfelter Co.

International Paper Company

Kimberly-Clark Corporation

KVP Sutherland Paper Company

Longview Fibre Company

Marathon Division, American Can Company

The Mead Corporation

Personal Products Company

Riegel Paper Corporation

St. Regis Paper Co.

Scott Paper Company

Union Bag-Camp Paper Corporation

West Virginia Pulp & Paper Company

ERRATA

Page	Line	Correction
26	Equation (40)	$\underline{w}$ =
30	last equation	(31)
35	line 7	($\underline{A}$ =
42	first equation	(3)
	second equation	(62)
	third equation	(4)
50	Equation (64)	= $\underline{p_s}' \underline{W}$
61	Table X, first line	beaker x 10^{-2}
63	Table X, last line	$\underline{p_s}$
70	line 13	is more than 1 x 10^{-5}
71	line 4	$\alpha = \frac{(4.0 \times 10^{-3})}{(1.8 \times 10^{-5})^{2/3}} = 5.8$
	line 5	the value 5.8
	line 14, under α	5.8
79	line 6	the retention equation (61)
97	Equation (A-7)	exp[ ]
101	line 6	diffusion of
126	between $\underline{n}$ and $\underline{p}$	$\underline{n}'$ = exponent

TABLE OF CONTENTS

THE INSTITUTE OF PAPER CHEMISTRY
Appleton, Wisconsin

STUDIES OF THE SHEET-FORMING PROCESS

THE RETENTION OF FINE PARTICLES IN FIBER MATS

SUMMARY

The retention of fine particles in fiber mats in the sheet-forming process has long been of considerable interest. Previous work was confined largely to the physicochemical aspect of the problem, and no theory has ever been advanced which would adequately describe even the simplest case of particle retention. In this project it was proposed that the retention problem be attacked from the hydrodynamic standpoint which has been fruitfully employed in the field of aerosol filtration.

This report covers about a year's experimental work and theoretical development. Its main body consists of five chapters which are summarized below:

Introduction. The essentials of particle dynamics are briefly reviewed. The collection of particles by fibers is caused by the motion of particles relative to fibers, the collision of particles with fibers, and the adhesion of particles to fibers. The forces involved are of hydrodynamic, molecular, and colloidal nature. The retention process is therefore governed by these forces, the complexity of which is beyond complete comprehension in the present state of knowledge.

Of particular interest in the sheet-forming process is the retention of fines. A description of fines is attempted with regard to their origin, size, and shape. The fines pertinent to this work are crudely defined to be smaller than the pore sizes of fiber mats and much shorter and thinner than fibers.

The sheet-forming process is considered as one of filtration in the sense that solid particles are separated from the suspending water by a filter medium. The retention of fibers is by virtue of their elongated shape, while the retention of fine particles takes place as a result of their collisions with the deposited fibers during flow through the mat already formed.

Analysis. The concept of particle attenuation and the associated definition of collection efficiency are introduced from aerosol permeation of a stationary mat of cylindrical fibers. The resulting attenuation equation is then modified for swollen fibers of irregular cross-sectional shapes. For the filtration process a differential continuity equation is developed on the basis of particle conservation. Combined with the attenuation equation under the simplified conditions of forming an incompressible mat from a dilute suspension at constant rate, the resulting differential equation is solved for the prescribed boundary conditions to yield the solution:

$$\frac{p' - p_s'}{p_s} = 1 - \exp\left[-n_f L_f D_f E\left(\frac{W}{A}\right)\left(1 - \frac{w}{W}\right)\right]$$

showing the distribution of particles collected by fibers in a mat. The total amount of particles retained in the mat can be otained easily by integration once the distribution is known.

The differential equation of particle continuity is generalized by utilizing the continuity equations for water and fiber developed previously for the filtration process. The simple attenuation equation is further developed for the compressible case in which both water and deposited fibers are moving toward the wire screen. The resulting equations of attenuation and retention plus the

previously established equation of filtration completely describe the process of filtration for a system of fibers, particles, and water.

The solutions of these equations will yield porosity, velocity, pressure, and particle distributions, provided the compressibility function for the fiber mat is known. The process of solving these equations, however, is extremely complicated even with the aid of a computer.

In this report the generalized attenuation and retention equations are solved for the simplified conditions stated before. The result indicates that the particle distribution in a compressible mat is the same as that for the incompressible case.

Experiments. Dacron and classified sulfite fibers were chosen for incompressible and compressible mats, respectively. Particles used were either titanium dioxide or radioactive fines prepared from wet-ground sulfite fibers and tagged by silver-110. Both fibers and particles were dispersed in deaerated and distilled water to form a dilute suspension, to which certain ionic compounds (hydrogen, sodium, or calcium chloride) were added, singly or in combination, for adjusting particle retentivity.

For each particle-fiber system, permeation and filtration experiments were conducted under identical retention and flow conditions, using the constant-rate filtration apparatus developed and refined at the Institute. The particles retained in a mat or its sections were determined by colorimetry in the case of titanium dioxide or by a Geiger-Müller counter in the case of fines.

Results. The value of collection efficiency (E) was obtained from the permeation data. The cumulative amounts of bound particles (m') and

fibers (w) in the sections or layers of a mat formed by filtration were correlated by a smooth curve, from which the slopes representing the local bound particle-fiber ratio (p') were taken, the slope at the last data point (W) being the ratio (p_s') of particles already bound to the fibers in the approaching suspension. Other experimental values needed in the retention expression are the free particle-fiber ratio (p_s) in the approaching suspension, the number of fibers per unit mass (n_f), the length of fibers (L_f), the projected diameter or width of fibers (D_f), and the total cross-sectional area of the mat (A).

In filtration of incompressible mats, the values of E and p_s' were evaluated graphically as well as statistically. For compressible mats, a quantitative evaluation of the data could not be carried out to completion due to the complexity of the phenomena observed.

Discussion. The results from filtration experiments with titanium dioxide particles or tagged fines and incompressible dacron fiber mats are plotted as $-\ln [(p' - p_s')/p_s]$ vs. $(1 - w/W)$. For all runs a linear relationship is evident, in agreement with the form of the retention equation. The collection efficiency evaluated from the slope of the line agrees with the value obtained from permeation experiments within experimental errors of 15%. It is concluded that the retention equation is substantially valid. On comparison with the permeation results of previous work under identical hydrodynamic conditions and similar colloidal environments, retention in the present titanium dioxide-dacron system is about two times lower than the previous titanium dioxide-nylon system, indicating that the surface nature of both particles and fibers is the controlling factor in adhesion.

For compressible wood fiber mats, the initial experimental results deviate considerably from the retention equation. After careful examination of the data a hypothesis of fiber saturation with particles is advanced. Further experiments under conditions of reduced retention indicate closer and closer agreement with the theory. Upon more detailed analysis it is inferred that the distribution of particles in a compressible mat consists of three regions: a saturated region near the wire screen, in which the fibers have reached a state of equilibrium with the particles, a partially saturated region, in which the collection efficiency continuously decreases, and an unsaturated region near the mat face, where the collection efficiency remains constant as assumed in the theory. This analysis is also supported by the permeation results.

The complexity of the retention phenomena obviously requires further clarification. In the immediate continuing work it is suggested to study low retention in thin mats for the verification of the theory in its simple form, to explore the possibility of the migration of particles at high flow rates, and to investigate the effect of fine particles retained in a mat on drainage. The study of colloidal effects on retention, which is of considerable practical interest, is deemed to be outside the scope of this project and left open for other projects.

Two appendices are included in this report. Appendix I is a summary of the present state of knowledge concerning the collection of small particles by a uniform mat of cylindrical fibers at low flow rates by Brownian motion or diffusion. An approximate hydrodynamic theory for diffusional retention is developed and checked with the available experimental evidence. The agreement appears to be satisfactory. The relationship in the dimensionless form is

$$E = \alpha' f(\epsilon)\left(\frac{\rho d_f U}{\mu}\,\frac{\mu}{\rho D}\right)^{-2/3}$$

where α' is a constant for a given system including the factors governing adhesion of particles to fibers, $f(\epsilon)$ is an unknown porosity function which appears to be a very mild one from the evidence of other work at the Institute, $\rho \underline{d_f} \underline{U}/\mu$ is the Reynolds number, which is limited to about unity for the expression to be valid, and $\mu/\rho \underline{D}$ is the Schmidt number which is of the order of 10^{-5} for the experiments cited. ρ, μ, and $\underline{U}$ are the density, viscosity, and approach velocity of the fluid, respectively. $\underline{D}$ is the diffusivity of the particles in the fluid. Appendix II explains the statistical calculations of $\underline{E}$ and $\underline{p_s}'$ from filtration data for incompressible mats in this work.

INTRODUCTION

PARTICLE DYNAMICS

When small particles are suspended in a quiescent fluid, they are subjected to various forces which govern their motions relative to the fluid. The gravitational force tends to pull the particles downward and the buoyancy force of the fluid tends to move them upward. The net force acting on the particles is proportional to the difference between particle and fluid densities. As the particles are set in motion, they experience the resistance of the fluid. The acceleration of particles is proportional to the difference between the net gravitational force and the fluid resistance which is, in turn, proportional to the relative velocity of particles and fluid if the motion is slow.

Quite independent of gravitation, the suspended particles are under bombardment of fluid molecules, resulting in an erratic zigzag motion called Brownian movement. The statistical mean displacement in a given direction is proportional to the square root of particle diameter and independent of particle density. The algebraic average displacement of all particles, however, is zero at all times. On the basis of the kinetic theory, Brownian motion represents a diffusional characteristic of fine particles.

For spherical particles of density 1.6 g. per cc. suspended in water at 70°F., a comparison of the relative importance of diffusion versus sedimentation is indicated in Table I.

TABLE I

BROWNIAN MOTION AND SEDIMENTATION

Particle Diameter, microns	Displacement in 1 Second, microns	
	Due to Brownian Motion	Due to Gravitational Settling
0.1	2.36	0.003
0.5	1.05	0.083
1.0	0.745	0.332
5.0	0.334	8.31
10.0	0.236	33.2

In flow of a suspension, a particle will follow the motion of the fluid if its inertia is negligible, i.e., its center of mass will assume the same streamline in the field of flow. Brownian motion will be superimposed on the particle motion along the streamline. If the inertia of a particle is appreciable, the particle will execute a trajectory different from the streamline. The exact manner in which a particle moves is determined solely by the resultant force acting on the particle.

If solid objects are placed in a field of flow, the particles will collide with the objects because of diffusion, inertial impaction, or both. The frequency of collision may be determined from the concentrations, the flow patterns, and the collision mechanisms. Some details of the collection mechanisms, especially with regard to diffusion, are presented in Appendix I.

When a particle collides with a solid object, it may adhere or bounce. Once adhered to the object, it may be detached by the motion of the fluid or the impact of another particle. Adhesion and detachment are governed by the forces operating at short distances between the particles and the solid object, as well as by the fluid forces acting at the site of collision.

The adhesion of small particles to one another is a result of the Van der Waals-London attractive forces, which are dependent only on the molecular nature and the distance of separation. In the absence of repulsive forces the particles will tend to agglomerate or flocculate; the rate of agglomeration increases with increasing particle concentration due to the increasing frequency of collision.

In aqueous suspensions with which we are dealing, the dispersion of hydrophobic particles may be achieved by introducing certain ionic compounds to the solution. If the nature of the particles is such that certain anions tend to adsorb preferentially on the particles, a diffused layer of cations will be surrounding the negatively charged particles. The repulsive forces so created will lessen the tendency toward flocculation. In such suspensions the state of dispersion is a delicate balance between the attractive and repulsive forces in the critical range of ionic concentrations.

The adhesion of particles to fibers is not well understood, but probably follows the same physicochemical laws. Cellulose fibers have slight negative charges in distilled water. If the particles are also negatively charged in a colloidal environment, they may also exhibit repulsion from fibers. For the purpose of particle retention, the colloidal conditions may be altered to suppress the repulsive forces, but the state of particle dispersion may be maintained by sufficient dilution.

The attractive and repulsive forces alone are not sufficient to determine whether a particle will or will not adhere to a fiber on their close encounter. The particle inertial force and the fluid drag force should also be taken into consideration. For small particles the inertial as well as gravitational forces may be neglected, provided their motion in the neighborhood of the fibers is slow. The fluid drag forces which act on the fibers, however, may be appreciable, depending on

the geometry and rate of flow. At present we are unable to analyze the various forces operating at the sites of collision even in a simple case. We merely assume that the probability of particle retention exists in the a posteriori sense.

DESCRIPTION OF FINES

Upon hydromechanical treatment, discrete wood fibers will continue to shed fibrils and debris mainly from primary walls and partly from secondary walls. The fibrils generally retain the elongated form of fibers, but have smaller axis ratios and thinner cross sections. The debris may assume irregular shapes, mostly in platelike forms. Together with broken fibers, ray cells, and small vessel segments, these materials are called "fines."

A common practice in distinguishing fines from fibers is to use screen classification. The fraction of a pulp which passes through a screen of a certain mesh is arbitrarily designated as fines. As an actual example, the results of screening an unbeaten softwood sulfite pulp in a laboratory classifier are given in Table II.

TABLE II

CLASSIFICATION OF A SULFITE PULP

Apparatus: Bauer-McNett
Sample weight: 10 g.
Consistency: 0.5%
Flow rate: 3 g.p.m.

	Screen Mesh		Weight, %
Retained on	14		45.8
	28		29.0
	65		10.8
	150		4.4
Passed through	150	Balance:	10.0

The fibers retained on the screens were measured microscopically to have an average length of 2.2 mm., and a width of 36 microns, which give an axis ratio of 60. The fraction which passed through the 150-mesh screen contained largely detached fibrils, a few of which are shown in the electron micrograph of Fig. 1. The size distribution of this fraction was determined with a Coulter counter which measures, one at a time, the effective volume of particles suspended in a conductive solution flowing through an aperture, on which an electric field is imposed. The results of counting are cited in Table III.

TABLE III

SIZE DISTRIBUTION OF "FINES"

Apparatus: Coulter counter
Fines concentration: 2.12×10^{-4} g./cc.
NaCl concentration: 6.4×10^{-2} g./cc.

Size in Microns	Number of Particles
4-6	36,352
6-8	63,831
8-10	23,313
10-15	7,857
15-20	8,033
20-30	8,938
30-40	446
above 40	36

In this example of an unbeaten pulp, fines below 4 microns were not counted. It is apparent, however, that a larger number of small particles of the order of 1 micron would be present in the fines of a refined pulp.

Figure 1. Electron Micrograph of "Fines" Classified from Unbeaten Sulfite Pulp (70,000X)

FILTRATION PROCESS

The separation of particles from a fluid by passing the suspension through a filter medium is called filtration. In the sheet-forming process, the solid particles are discrete fibers and fines, as well as other small particles added to the suspension for various purposes.

The retention of fibers on a wire screen is accomplished by virtue of their elongated form so that they may be deposited initially on the screen and subsequently on the fiber mat itself simply by bridging across the openings of the wire or fiber structure. Obviously, the longer the fibers compared with the openings of the filtering structure, the higher is the retention. It is also clear that once a fiber is deposited, the chances for it to work its way out of the filtering structure are practically nil in the absence of disturbances.

As previously described, the so-called "fines" have a wide range of sizes and shapes. Relatively large broken fibers and long fibrils will be retained in a manner similar to discrete fibers. Very fine debris and short fibrils, on the other hand, will follow the passage of the permeating fluid in the void spaces of the fiber structure until they are caught in collisions with fibers. In the intermediate size range, fines may behave either as discrete fibers or as penetrating particles. In addition, they may be lodged in the openings of the fiber structure. The modes of retention are therefore dependent on the sizes and shapes of the fines with respect to those of the openings.

In this work we are concerned primarily with the retention of fine particles in the sheet-forming process. The pore sizes of a fiber mat are generally in the range of 1-100 microns. We may arbitrarily define the size of fines under consideration to be of the order of the pore size or smaller.

Since most fines retain an elongated form, we further describe the shape of fines by their axis ratios, and consider only those particles whose axis ratios are sufficiently low to be capable of moving with the fluid in the void spaces or pores. Under this crude classification, the fines to be studied will be of the order of 1 micron or less in width and several widths long at most.

ANALYSIS

THE ATTENUATION EQUATION

Consider a dilute suspension of small particles in a fluid flowing through a stationary fiber mat of a fixed mass. By virtue of their motion some particles will be collected by the fibers and others will penetrate through the mat. For a large number of particles the chances of their capture are statistically determinable.

It is reasonable to assume that the more particles there are approaching a layer of fibers, the more will be captured. In a precise statement, the rate of particle attenuation with respect to the distance x in the direction of flow is directly proportional to the particle concentration. If C is the number of particles per unit volume of fluid, then

$$-\frac{dC}{dx} = KC \qquad (1),$$

where K is the proportionality factor called attenuation coefficient.

If all factors influencing particle collection remain constant everywhere in the mat during permeation, K will be independent of x, and Equation (1) may be integrated to yield

$$C_L = C_o e^{-KL} \qquad (2),$$

or

$$\ln \frac{C_o}{C_L} = KL \qquad (3),$$

where C_o and C_L are the upstream and downstream concentrations, respectively, across a mat of thickness L. The resulting exponential function is a consequence

of the foregoing assumption which has been verified experimentally. In this derivation it is implied that the concentration is uniform as the particles approach a layer of fibers (see Appendix I).

In the field of aerosol filtration the attenuation coefficient K for a uniform mat of cylindrical fibers with porosity ϵ and fiber diameter d_f is expressed in terms of collection efficiency E,

$$K = \frac{4(1 - \epsilon)E}{\pi d_f} \qquad (4).$$

The definition of collection efficiency was initiated for a single cylinder and then extended to a mat of fibers (see Appendix I).

To preserve the original concept of collection efficiency we now attempt to develop, in a similar manner, a formula for a mat of noncylindrical fibers, particularly wood fibers. For the time being, a stationary mat of uniform porosity will be considered. In a unit volume of the mat composed of N_f fibers of length L_f, the total fiber length per unit mat volume is $N_f L_f$. Since wood fibers have roughly an elliptical cross-sectional shape, their most stable position in a mat formed by filtration from a dilute fiber suspension would be an alignment with the long axis (width) of their cross sections perpendicular to the direction of flow. Then the total projected area of fibers per unit mat volume is $N_f L_f D_f$, where D_f is the projected axis. Through this projected area a uniform stream of particles of concentration C is flowing at a superficial velocity U. The number of particles passing through the projected area is therefore $CUN_f L_f D_f$ per unit time per unit mat volume. If the aggregated fibers have a collection efficiency E, which represents the ratio of particles collected by the fibers to the total particles approaching the fibers, then

$ECUN_f L_f D_f$ will be the number of particles collected by the fibers per unit time per unit mat volume.

Across an infinitesimal layer Adx of the mat with the total cross-sectional area A, the particle concentration is attenuated from C by $-dC$. The number of particles approaching this layer per unit time is CUA. The ratio of the collected to the approaching particles must obviously be the same as the fraction of particles removed by the fibers in the layer, i.e.,

$$-\frac{dC}{C} = \frac{CUEN_f L_f D_f A dx}{CUA}$$

$$= EN_f L_f D_f dx \qquad (5).$$

If the collection efficiency remains constant throughout the thickness of the mat, Equation (5) may be integrated to yield

$$\ln \frac{C_o}{C_L} = EN_f L_f D_f L \qquad (6)$$

or more generally,

$$\ln \frac{C_o}{C_L} = E \frac{A_f}{V_f} (1 - \epsilon) L \qquad (7),$$

where A_f/V_f is the projected area per unit volume of fibers.

Since wood fibers have an internal porous structure, the total porosity of a wood fiber mat consists of both interfiber and intrafiber voids. In permeation the fluid in the intrafiber voids is considered to be stagnant, and therefore contributes no frictional losses. By the same reasoning the particles

are supposed to be collected only on the external surfaces of the fully swollen fibers. Thus, only interfiber porosity is pertinent in the calculation of collection efficiency:

$$1 - \epsilon = \frac{Wv}{AL} \tag{8}$$

where v is the hydrodynamic specific swollen volume or the volume of wet fibers (V_f) including the immobile water per unit mass of dry fibers, and W/A is the mat basis weight.

In Equation (6) the number of fibers per unit mass of dry fibers, n_f, which is directly measurable,

$$N_f = \frac{n_f W}{AL} \tag{9}.$$

Thus, the collection efficiency for a uniform mat of wood fibers may be expressed in terms of experimental quantities:

$$E = \frac{\ln (C_o/C_L)}{n_f L_f D_f (W/A)} = \frac{v \ln (C_o/C_L)}{n_f L_f D_f (1 - \epsilon) L} \tag{10}.$$

Comparing with the attenuation equation (3), it is seen that

$$K = \frac{n_f L_f D_f (1 - \epsilon)}{v} E$$

$$= \frac{A_f}{V_f} (1 - \epsilon) E \tag{11}.$$

For cylindrical fibers Equation (11) reduces to Equation (4).

THE CONTINUITY EQUATION

We proceed to consider an aqueous suspension of discrete fibers and small particles of negligible volume flowing downward through a wire screen or septum on which a mat of fibers is formed. The co-ordinates of the filtration system in one-dimensional flow are shown below in Fig. 2.

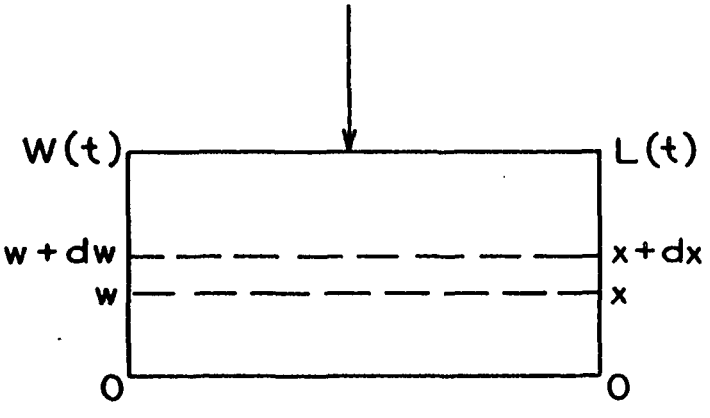

Figure 2. Filtration Co-ordinates

Lacking detailed knowledge of the velocity distribution in the pores of the mat, we define an internal superficial fluid velocity U to be the volumetric flow rate divided by the total mat area. The particles suspended in the fluid are called free particles. If C, as before, is the number concentration (per unit volume of fluid), then UC is the average free particle flux at the x-plane. The particles attached to the fibers are designated as bound particles. If the fibers may also be treated as a continuum, the average bound particle flux is $U_f C'$, U_f being the internal superficial velocity of fibers and C' the bound particle concentration expressed in number of particles per unit volume of fibers.

In a stationary volume element $\underline{A}d\underline{x}$ of the mat with the local porosity ϵ, the free particle concentration is $\epsilon \underline{C}$ and the bound particle concentration is $(1 - \epsilon)\underline{C}'$. These concentrations being expressed in numbers of particles per unit mat volume, are therefore additive. The rate of accumulation of particles in the element is

$$\frac{\partial}{\partial t}[\epsilon C + (1 - \epsilon)C']Adx .$$

The rate of particle net input across the two faces of the element is

$$(UC + U_f C')A - [(UC + U_f C')A + \frac{\partial}{\partial x}(UC + U_f C')Adx] .$$

By the principle of mass conservation, the two rates must be equal. The equation of particle continuity, therefore, is

$$\frac{\partial}{\partial t}[\epsilon C + (1 - \epsilon)C'] = -\frac{\partial}{\partial x}[UC + U_f C'] \qquad (12) .$$

INCOMPRESSIBLE MATS

In a filtration process, as fibers are deposited on a mat face, water and free particles permeate the mat structure already formed. During their passage some of the free particles will be caught by the fibers. For an incompressible mat of uniform porosity, the attenuation of free particles in the direction opposite to the $\underline{x}$ co-ordinate should follow Equation (1):

$$-\frac{dC}{d(L - x)} = KC \qquad (13) .$$

Integrating from 0 to $\underline{L}$ and setting the free particle concentration at the mat face to be $\underline{C_s}$ as the boundary condition, we have

$$C = C_s e^{-K(L-x)} \qquad (14),$$

which shows the instantaneous distribution of free particle concentration in a mat of thickness L, provided K remains constant with $(L - x)$.

Meanwhile, more fibers are deposited on the mat so that its thickness L increases at a velocity V. If filtration is carried out without any fiber loss at constant rate, the rate of growth of the mat will be constant at $V = L/t$. Under this simplified condition we may substitute Vt for L in Equation (14) and take partial differentiation of the equation with respect to the two independent variables t and x. The resulting rate equations are

$$\frac{\partial C}{\partial t} = -KVC_s e^{-K(Vt-x)} \qquad (15)$$

and

$$\frac{\partial C}{\partial x} = KC_s e^{-K(Vt-x)} \qquad (16).$$

Under the prescribed conditions (ϵ = constant, U = constant, and $U_f = 0$) the equation of particle continuity is reduced to

$$\epsilon \frac{\partial C}{\partial t} + (1 - \epsilon) \frac{\partial C'}{\partial t} = -U \frac{\partial C}{\partial x} \qquad (17).$$

Combining Equations (15) through (17), we obtain a single partial differential equation to describe the retention process:

$$\frac{\partial C'}{\partial t} = KC_s \frac{\epsilon V - U}{1 - \epsilon} e^{-K(Vt-x)} \qquad (18).$$

This equation may be integrated with respect to t at constant x to give

$$C' = -C_s \frac{\epsilon V - U}{V(1 - \epsilon)} e^{-K(Vt-x)} + f(x) \qquad (19),$$

where $f(\underline{x})$ is an integration constant. The boundary condition may be specified:

$$\text{at} \quad x = L = Vt, \qquad C' = C_s',$$

where $\underline{C_s}'$ is the bound particle concentration in the approaching suspension.

The integration constant is then evaluated to be

$$f(x) = C_s' + C_s \frac{\epsilon V - U}{V(1 - \epsilon)} \tag{20},$$

and the final solution is

$$C' - C_s' = C_s \frac{U - \epsilon V}{V(1 - \epsilon)} \left[e^{-K(L-x)} - 1\right] \tag{21}.$$

It should be reiterated that the free particle concentration $\underline{C}$ and the bound particle concentration $\underline{C}'$, as previously defined, are based on fluid volume and fiber volume, respectively.

Experimentally, it is more convenient to measure masses rather than volumes. The basis weight of a fiber mat is

$$\frac{W}{A} = \rho_f(1 - \epsilon)L \tag{22}$$

and similarly, for a layer of fibers from the septum,

$$\frac{W}{A} = \rho_f(1 - \epsilon)x \tag{23},$$

where ρ_f is the density of solid fibers. Introducing $\underline{p}$ and $\underline{p}'$ as the masses of free and bound particles per unit mass of fluid and fiber, respectively, their relations to $\underline{C}$ and $\underline{C}'$ are

$$p = \frac{m_p C \epsilon}{\rho_f (1 - \epsilon)} \tag{24}$$

and

$$p' = \frac{m_p C'}{\rho_f} \tag{25},$$

where m_p is the mass per particle.

At the mat face $(x = L)$ the particle concentrations C_s and C_s' are assumed to be those in the approaching suspension; then

$$p_s = \frac{m_p C_s \epsilon_s}{\rho_f (1 - \epsilon_s)} \tag{26}$$

and

$$p_s' = \frac{m_p C_s'}{\rho_f} \tag{27},$$

where ϵ_s is the porosity or volume fraction of fluid in the suspension.

The relation between the superficial fluid velocity U and the mat face velocity V may be established by a fiber balance:

$$-\frac{1 - \epsilon_s}{\epsilon_s} U = (1 - \epsilon) V \tag{28},$$

the negative sign being used to account for the opposite directions of U and V. If the fiber suspension is dilute $(V << U)$,

$$\frac{U - \epsilon V}{V(1 - \epsilon)} \cong \frac{U}{V(1 - \epsilon)} = -\frac{\epsilon_s}{1 - \epsilon_s} \tag{29}.$$

Substituting Relations (22), (23), (25), (26), (27), and (29) into Equation (21), the result is

$$\frac{p' - p_s'}{p_s} = 1 - \exp\left[-\frac{K}{\rho_f(1 - \epsilon)}\left(\frac{W}{A}\right)\left(1 - \frac{w}{W}\right)\right] \qquad (30),$$

showing the distribution of bound particles in a uniform mat formed from a dilute fiber suspension at constant rate. Equation (30) may also be put in the form

$$-\ln\left(1 - \frac{p' - p_s'}{p_s}\right) = K'\left(1 - \frac{w}{W}\right) \qquad (31),$$

which reveals a linear relationship between the natural logarithmic term and $[1 - (w/W)]$ with the slope K'. For cylindrical fibers, it is recalled from Equation (4) that

$$K' = \frac{K(W/A)}{\rho_f(1 - \epsilon)} = \frac{4E(W/A)}{\pi d_f \rho_f} \qquad (32).$$

COMPRESSIBLE MATS*

In the analysis of the filtration process in a rather general manner, it has been shown (1) that the continuity equation for a system of fiber and water, both in motion, in the co-ordinates of Fig. 2 is

$$\frac{\partial \epsilon}{\partial t} = -\frac{\partial U}{\partial x} = \frac{\partial U_f}{\partial x} \qquad (33).$$

Combining this equation with the particle continuity equation (12), we obtain

$$\epsilon \frac{\partial C}{\partial t} + (1 - \epsilon)\frac{\partial C'}{\partial t} = -U\frac{\partial C}{\partial x} - U_f \frac{\partial C'}{\partial x} \qquad (34).$$

For compressible mats the attenuation equation (1) may be generalized to account for the effect of fiber motion. Suppose an observer is moving along

* A more rigorous and comprehensive treatment of this topic will be presented in another report of this project.

with a layer of fibers at the same velocity. Then the retention process in accordance with the previously introduced attenuation concept is described by the observer as

$$(1 - \epsilon) \frac{\partial C'}{\partial t} = K|U_r| C \qquad (35),$$

where $|\underline{U_r}|$ is the velocity of water relative to that of the layer of fibers or the observer, irrespective of the directions of the relative motion. In the filtration analysis it has also been demonstrated that $\underline{U_r}$ is related to the internal superficial velocities of water and fiber by

$$U_r = U - \frac{\epsilon}{1 - \epsilon} U_f \qquad (36),$$

in the case where water and fibers are moving in the same direction.

Now if the observer looks at a stationary volume element $\underline{A}d\underline{x}$ of Fig. 2, he also sees the motion of the fibers, and consequently the rate of increase of bound particles across the element. His description of the retention process would be

$$(1 - \epsilon) \frac{\partial C'}{\partial t} + U_f \frac{\partial C'}{\partial x} = K\left|U - \frac{\epsilon}{1 - \epsilon} U_f\right| C \qquad (37).$$

Combining with Equation (34), the resulting attenuation equation is

$$\epsilon \frac{\partial C}{\partial t} + U \frac{\partial C}{\partial x} = -K\left|U - \frac{\epsilon}{1 - \epsilon} U_f\right| C \qquad (38).$$

For the previous case of steady flow $(\partial \underline{C}/\partial \underline{t} = 0)$ through an incompressible mat $(\underline{U_f} = 0)$, Equation (38) reduces to

$$-\frac{dC}{dx} = KC \qquad (1).$$

The retention and attenuation equations, (37) and (38), are to be solved, in general, with the filtration equation (1),

$$-\frac{\partial \epsilon}{\partial t} = -\frac{\partial}{\partial x}\left[\frac{\epsilon}{1-\epsilon} U_f - \frac{K_D}{\mu}\frac{\partial P}{\partial x}\right] \qquad (39),$$

where K_D is Darcy's permeability coefficient and P is the fluid pressure. Furthermore, information concerning the mat compressibility, $\epsilon = f(\Delta P)$, and the dependence of K and K_D on ϵ will be needed. The mathematical difficulties involved in such solutions are obvious.

For experimental purposes, it is more convenient to use w (cumulative mass of dry fibers), rather than x, as an independent variable. The relation between w and x for a unit area of a compressible mat is

$$W = \rho_f \int_0^x (1 - \epsilon)dx \qquad (40).$$

To avoid the negative velocities with respect to x or w of Fig. 2 we may choose a new mass co-ordinate downward from the mat face in the same direction of flow,

$$w' = W - w \qquad (41),$$

where W is a function of time only. For clarity in the subsequent treatment, we also introduce a new time co-ordinate t' to replace the previous co-ordinate t,

$$t' = t \qquad (42).$$

The new independent variables, w' and t', are related to the original ones, x and t, by the rules of partial differentiation performed on Equations (40) through (42). These are

$$\frac{\partial}{\partial x} = \rho_f(1 - \epsilon)\frac{\partial}{\partial w} = -\rho_f(1 - \epsilon)\frac{\partial}{\partial w'} \qquad (43)$$

and $$\frac{\partial}{\partial t} = \frac{\partial w}{\partial t}\frac{\partial}{\partial w} + \frac{dW}{dt'}\frac{\partial}{\partial w'} + \frac{\partial}{\partial t'} \qquad (44).$$

since $$\frac{\partial w}{\partial t} = \rho_f \int_o^x -\frac{\partial \epsilon}{\partial t}\, dx \qquad (45),$$

and by integrating Equation (33), the result being

$$\int_o^x \frac{\partial \epsilon}{\partial t}\, dx = -\int_o^x \frac{\partial U}{\partial x}\, dx = \int_o^x \frac{\partial U_f}{\partial x}\, dx$$

$$= U(0,t) - U(x,t) = U_f(x,t) - U_f(0,t) \qquad (46),$$

where $\underline{U_f}(0,\underline{t})$ at the septum is necessarily zero, we arrive at

$$\frac{\partial w}{\partial t} = -\rho_f U_f \qquad (47).$$

Then Equation (44) becomes

$$\frac{\partial}{\partial t} = \rho_f U_f \frac{\partial}{\partial w'} + \frac{dW}{dt'}\frac{\partial}{\partial w'} + \frac{\partial}{\partial t'} \qquad (48).$$

Equations (43) and (48) may be used to transform Equations (37) and (38), respectively, into

$$(1 - \epsilon)\frac{\partial C'}{\partial t'} + (1 - \epsilon)\frac{dW}{dt'}\frac{\partial C'}{\partial w'} = K|U_r|C \qquad (49)$$

and $$\epsilon \frac{\partial C}{\partial t'} - [\rho_f(1 - \epsilon)U_r - \epsilon \frac{dW}{dt'}]\frac{\partial C}{\partial w'} = -K|U_r|C \qquad (50).$$

In this report we propose to deal with a rather oversimplified case of slow filtration at constant rate with a dilute suspension of fibers and small particles. When the suspension is dilute, the internal superficial velocity of water $\underline{U}$ would be practically constant. Furthermore, the term $\epsilon \underline{U}_f/(1 - \epsilon)$ in $\underline{U}_r$ will be negligibly small compared with $\underline{U}$. If the filtration is slow, we may assume that the mat is in successive equilibrium states during its build-up. Finally, under the equilibrium assumption, the change of both free and bound particles would be nearly independent of time at the same relative position of the growing mat.

Under these simplified conditions, Equations (49) and (50) reduce, respectively, to

$$\frac{\partial C'}{\partial w'} = - \frac{KUC}{(1 - \epsilon)(dW/dt')} \qquad (51)$$

and

$$\frac{\partial C}{\partial w'} = - \frac{KUC}{\rho_f(1 - \epsilon)U - \epsilon(dW/dt')} \qquad (52).$$

The negative sign has been inserted because $\underline{U}$ in $|\underline{U}_r|$ is inherently negative with respect to the original $\underline{x}$-co-ordinate.

The rate of growth of dry fibers in the mat for constant-rate filtration may be calculated by a fiber balance between the suspension and the mat:

$$\frac{dW}{dt'} = - \frac{1 - \epsilon_s}{\epsilon_s} \rho_f U \qquad (53),$$

and for a dilute suspension $(\epsilon_s \approx 1)$, its magnitude is negligible compared with $\rho_f(1 - \epsilon)\underline{U}$. Equation (52) then reduces to

$$\frac{\partial C}{\partial w'} = - \frac{KC}{\rho_f(1 - \epsilon)} \qquad (54).$$

The attenuation coefficient $\underline{K}$ may be, in general, expressed in terms of the collection efficiency $\underline{E}$, based on the concept of total projected area of fibers as discussed before,

$$K = \frac{A_f}{V_f}(1 - \epsilon)E \qquad (11).$$

Substituting this general definition of $\underline{K}$ into Equation (54), we have

$$\frac{\partial C}{\partial w'} = - \frac{A_f E C}{V_f \rho_f} \qquad (55).$$

Upon integration at constant time and $\underline{E}$, the result is

$$C = C_s \exp(- \frac{A_f E}{V_f \rho_f} w') \qquad (56).$$

Substituting Equations (56), (11), and (53) into Equation (51), we obtain

$$\frac{\partial C'}{\partial w'} = - \frac{A_f E \epsilon_s C_s}{V_f \rho_f (1 - \epsilon_s)} \exp(- \frac{A_f E}{V_f \rho_f} w') \qquad (57).$$

Integrating again under the same conditions as before, we arrive at the final solution:

$$C' = C_s' + \frac{\epsilon_s C_s}{1 - \epsilon_s}[1 - \exp(- \frac{A_f E}{V_f \rho_f} w')] \qquad (58).$$

The concentrations may be expressed in terms of particle-fiber ratios by the definitions (25), (26), and (27):

$$\frac{p' - p_s'}{p_s} = 1 - \exp\left[-\frac{A_f E}{V_f \rho_f} w'\right] \qquad (59).$$

Returning to the $\underline{w}$ co-ordinate and Definition (11), Equation (59) becomes for a mat of total area $\underline{A}$,

$$\frac{p - p_s'}{p_s} = 1 - \exp\left[-\frac{K}{\rho_f(1 - \epsilon)} \left(\frac{W}{A}\right)\left(1 - \frac{w}{W}\right)\right] \qquad (30),$$

which turns out to be exactly the same as the incompressible case after all the rather involved mathematical manipulations.

There are probably two reasons for this rather perplexing result. First, the assumption of successive equilibrium states permits a compressible mat to behave like an incompressible mat so far as the retention process is concerned. Second, the assumption of constant collection efficiency means its independence of porosity. This latter assumption is partially justified by the experimental evidence in the air filtration work recently carried out at the Institute for diffusional retention at a mat porosity smaller than 0.9.

In the case of wood fibers, replacing $\rho_{\underline{f}}$ by the reciprocal of $\underline{v}$, Equation (59) becomes

$$\frac{p' - p_s'}{p_s} = 1 - \exp\left[-\frac{A_f v E}{V_f} w'\right] \qquad (60).$$

Proceeding as before, the final solution is

$$-\ln\left(1 - \frac{p' - p_s'}{p_s}\right) = n_f L_f D_f E \left(\frac{W}{A}\right)\left(1 - \frac{w}{W}\right) \qquad (61)$$

or

$$-\ln\left(1 - \frac{p' - p_s'}{p_s}\right) = K'\left(1 - \frac{w}{W}\right) \qquad (62).$$

EXPERIMENTS

FIBERS

Three-denier dacron fibers (Du Pont) of high modulus of elasticity were used in forming incompressible mats. These fibers are cylindrical in shape and uniform along their lengths. The density of dacron fibers, which do not swell appreciably in water, is 1.41 g. per cc. The surface treatment of these macroscopically smooth fibers is not known. The dimensions of the fibers were measured microscopically in a dehydrated state. The results are shown in Table IV.

TABLE IV

DIMENSIONS OF DACRON FIBERS

Frequency, %	Diameter, $\underline{d}_f$, microns	Frequency, %	Length, $\underline{L}_f$, mm.
1	10.53	0.9	1.25
1	11.70	2.2	2.20
2	12.87	7.1	3.16
3	14.04	28.8	4.30
7	15.21	35.8	5.21
24	16.38	19.0	6.21
55	17.55	4.9	7.18
4	18.72	1.3	8.50
2	19.89	arithmetic av. =	5.03
1	23.40		
arithmetic av. =	16.9		

Classified wood fibers were used in forming compressible mats. Dry laps of a bleached sulfite pulp (Weyerhaeuser) were soaked in water for 24 hours. The wet pulp was slushed in a Valley beater for five minutes without application of load on the bedplate. The slushed pulp was screened in a Bauer-McNett classifier with 20, 28, 48, and 65-mesh screens. The fibers retained on the screens were combined and designated as classified fibers. The arithmetic average fiber length, $\underline{L}_f$, and width, $\underline{D}_f$, were determined microscopically to be 2.11 and 0.039 mm., respectively. The specific volume, $\underline{v}$, was measured hydrodynamically to be 2.26 cc./g. The number of fibers per gram, $\underline{n}_f$, was determined by a special method to be 2.78×10^6. The density of dry fibers was taken from the literature to be 1.59 g./cc. The measurements of wood fibers will be discussed in another report of this project.

PARTICLES

In the initial experiments, titanium dioxide particles of a commercial grade (Glidden RG) which had been treated on their surfaces with sodium hexametaphosphate as a dispersing agent were mixed with distilled water to make a suspension of 73% solids. The suspension was stirred in a Waring Blendor until a minimum viscosity was reached (in about 20 minutes). The dispersed stock was diluted and kept in a slowly rotating vessel to prevent the particles from settling. The stock contained 0.1096 g. of titanium dioxide per cc.

The titanium dioxide particles were roughly spherical in shape. Their sizes were measured by the sedimentation technique with a special centrifuge. According to a previous determination the number average diameter was 0.15 micron. The density of titanium dioxide particles is approximately 3.9 g./cc.

Fines of sizes suitable for the experimental purposes were prepared from the same sulfite pulp used for obtaining classified fibers. Several grams of dry lap were ground in a Wiley mill. The fibrous materials which passed through an 80-mesh screen were subjected to wet grinding in a pebble mill for 48 hours. The fines so obtained were in a size range of 0.5 to 2 microns as estimated from the electron micrographs, one of which is shown in Fig. 3. The stock contained 4.3 mg. of fines per cc.

The fines were tagged with radioactive silver-110 for the purpose of quantitative identification. The isotope was supplied as a solution of silver nitrate in 1.08N nitric acid. The specific activity was 1,038 millicuries per g. of silver. Silver-110 decays with emission of betas 0.1, 0.5, 2.1, and 2.9 m.e.v., and gammas 0.7, 0.9, and 1.4 m.e.v. Its half life is 270 days. The original solution was diluted with 0.5N nitric acid to yield a stock of 0.2 millicurie per cc. of solution.

To 300 cc. of the fines stock, 1 cc. of the radioactive silver stock was added. The mixture was heated gradually to 90°C. with continuous stirring. A solution of 0.1N sodium hydroxide was then introduced, drop by drop, to the hot mixture until a pH value of 9 was reached. The radioactive fines stock was transferred to a bottle which was kept in rotation to prevent the particles from settling. The radioactive chemical was fixed on the fines as precipitated silver. Under the specified conditions, practically all the silver in the solution was transferred to the fines. The filtrate as well as the washings showed little radioactivity in a test.

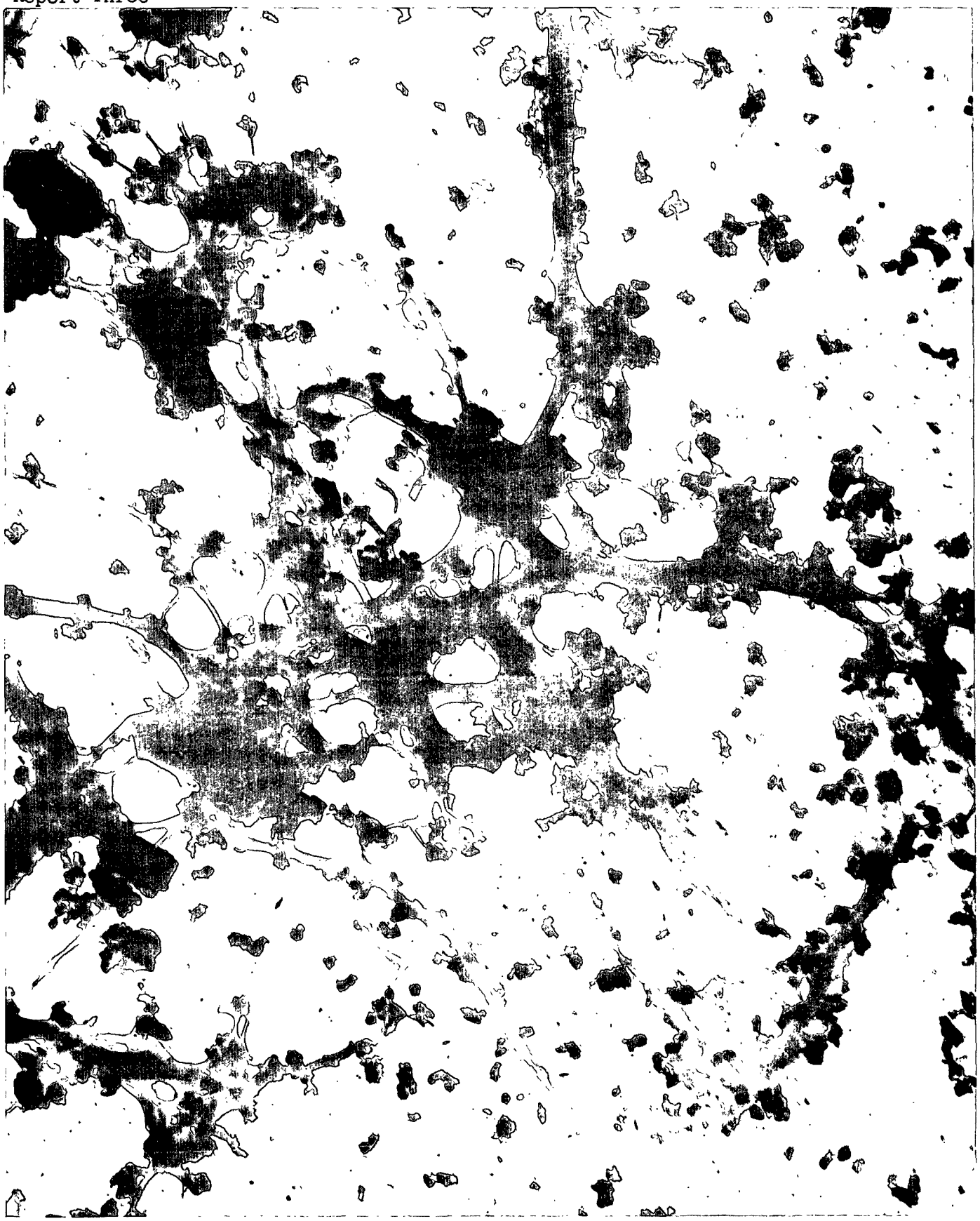

Figure 3. Electron Micrograph of Fines from Wet-Ground Sulfite Pulp
(ca. 29,000X)

APPARATUS

The filtration apparatus is shown schematically in Fig. 4. It consists of two feed tanks, a filtration tube, a filtrate pump, a water leveling bottle, and accessories.

The stainless steel feed tanks are equipped with agitators for the dispersion of suspensions. The Lucite filtration tube is 3 inches in diameter (A = 45.6 sq. cm.). Its top section has a concentric outer chamber from which the suspension overflows evenly into the tube. A septum is inserted between two sections of the tube and sealed by an O-ring. The septum is a perforated brass plate covered with a 150-mesh wire screen.

The bottom section of the tube is connected with a positive displacement metering pump with a variable-speed drive. A rotameter is placed in the discharge line of the pump to indicate the flow rate. The leveling bottle is incorporated with the bottom section for the purpose of setting the water level in the tube before and after a filtration run. A water manometer is located on the bottom section to indicate the pressure drop across the mat and septum. The pressure drop may also be sensed by a bellows-type pressure transmitter and recorded on the strip chart of a potentiometer-type recorder.

SUSPENSIONS

Very dilute particle suspensions used in the retention experiments were prepared from the previously described titanium dioxide and fines stock. In the case of a titanium dioxide suspension, in order that the particles would be retained to a measurable extent in a fiber mat, the dispersing action of the phosphate ions adsorbed on the particle surfaces was partly counteracted by

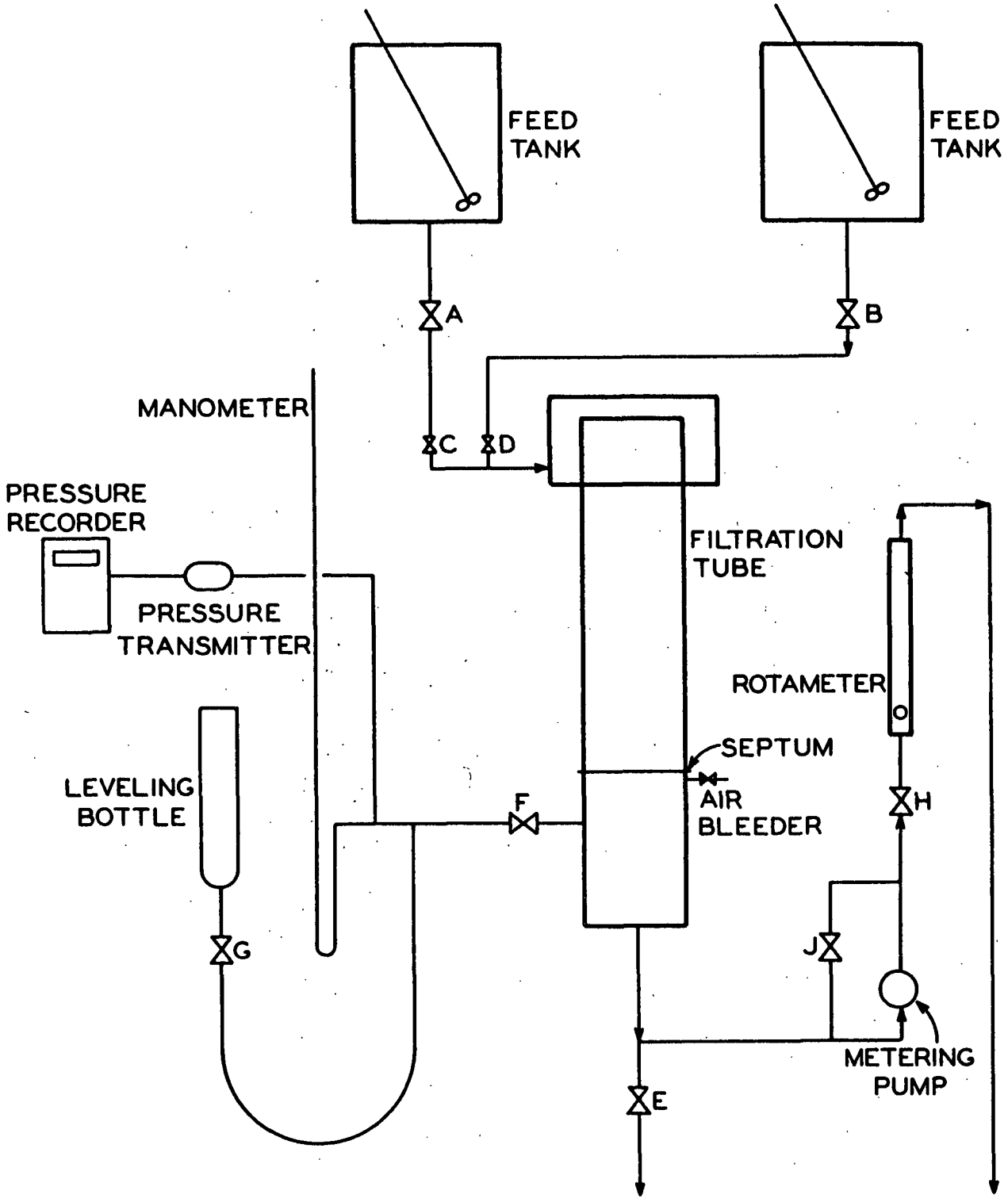

Figure 4. Schematic Diagram of Filtration Apparatus

introducing to the suspension certain ionic compounds, the ions of which do not adsorb on the particles. Calcium, sodium, and hydrogen chlorides were found to be effective for this purpose.

A known amount of the stock was dispersed in a feed tank filled with distilled water containing calcium chloride. The pH of the suspension was adjusted with concentrated hydrochloric acid to the strongly acidic side. The dilute suspension was kept in a dispersed state under agitation.

When a suspension of fines was prepared merely by dilution, it was found by preliminary experiments that the retention of fines in a fiber mat was not sufficient for precise measurements. By providing calcium and hydrogen chloride ions as in the case of titanium dioxide suspensions, retention was considerably improved, but at a low pH there occurred serious leaching of radioactivity to the solution. The final procedure was to add only calcium chloride dihydrate or sodium chloride to the fines suspension without the use of hydrochloric acid. The leaching test will be described later.

Fiber suspensions were prepared from the dry fibers in the case of dacron and from the classified wet fiber stock in the case of sulfite pulp. In all cases the fibers were dispersed in distilled water and deaerated in a flask under prolonged vacuum. The deaerated fibers were further dispersed in a large amount of distilled water, and the suspension adjusted to the same ionic conditions as in the particle suspension. In the initial experiments of the retention of titanium dioxide in dacron fiber mats, the particle and fiber suspensions were kept in two separate feed tanks and mixed on their way to the filtration tube. In the subsequent experiments with fines a single suspension of fibers and fines prepared in one feed tank was used.

PERMEATION

In a permeation run a mat was first formed from a suspension of fibers and the formed mat was then permeated with a particle suspension for a certain duration under known conditions. Prior to the run a clean, dry septum was inserted in the filtration tube. Distilled and deaerated water was fed into the bottom section of the tube by means of the leveling bottle. The water flowed slowly upward through the septum until it reached the top of the tube. In this way trapping of air bubbles at the septum was avoided. The line connecting the tube with the feed tanks which had been filled previously with water was opened for a short while to let the water overflow into the tube and drain through the tube under the action of the metering pump. When the desired flow rate was reached by adjusting the feed valve (C or D in Fig. 4) and the discharge valves (H and J), the pump was stopped, and, simultaneously, the tank valve (A or B) was shut off, leaving the feed valve undisturbed. If both feed tanks were to be used, this procedure was repeated.

With the system ready for operation and the fiber and particle suspensions prepared in the feed tanks as previously described, the mat-forming process was initiated by starting the pump and opening the feed line of the fiber suspension tank. With some minor adjustments of the feed and discharge valves, the filtration rate quickly reached the predetermined setting. The operation was continued until a rather thick mat was formed.

At the known flow rate and final pressure drop the feed line was now switched to the particle suspension. The permeation process was carried on until a measurable quantity of particles was retained in the mat without an excessive increase in pressure drop. After the pump had been stopped, the remaining water

in the tube was drained slowly through the leveling bottle. The mat together with the septum was then removed from the tube.

For a permeation run the volumes of the fiber and particle suspensions were determined from the levels in the tanks before and after the run. The thickness of the mat was measured with a ruler under the permeating condition near the end of the run. The total retention in the mat was determined by methods to be explained later.

FILTRATION

In filtration runs a suspension of fibers and particles, prepared either in a single tank or by mixing two feed streams from two separate tanks, was pumped through the septum, on which the fibers were retained to form a mat with simultaneous collection of particles by the fibers. The procedure of a filtration run was the same as described before.

At the end of the run the water in the tube was drained away through the mat. It was suspected that some retained particles might be removed in this draining procedure. To minimize the loss of particles in the later filtration experiments the water in the upper part of the tube was drained slowly through the mat until it reached the mat face, and the water below the septum was drained by bleeding air at a point slightly below the septum.

After its removal from the tube, the mat was sectioned or split by hand into several layers. The layers were dried in an oven at 220°F. and the mass of fibers in each layer was weighed.

PARTICLE MEASUREMENTS

For the determination of titanium dioxide particles the dried layers placed in crucibles were ashed in an electric furnace. The temperature was rapidly raised to 600°F., then slowly to 900°F., kept at 900°F. for one hour and finally at 1200°F. for two hours. After the crucibles had been cooled to room temperature, 2 g. of ammonium sulfate and 5 cc. of concentrated sulfuric acid were introduced to each of them. Each crucible was then heated with a burner until the ash was completely dissolved. The cooled contents were transferred to a 25-ml. volumetric flask and diluted to the mark with distilled water.

From each flask two 10-ml. samples were pipetted to two 100-ml. flasks. To one flask was added 10% sulfuric acid to make up the specified volume. To the other flask 5 ml. of 3% hydrogen peroxide solution was added, and the remaining volume was made up with 10% sulfuric acid. Peroxide forms a complex with titanium ions, resulting in a stable color which can be measured with a spectrophotometer (Coleman Model 14). By measuring light transmission of the peroxide solution against the solution without peroxide as a reference at the same temperature, the result in percentage transmission was converted to the titanium dioxide concentration in g./cc. by the use of a calibration curve which was checked from time to time against known solutions.

In the case of tagged fines, ashing was done in planchets with the addition of sulfuric acid so that silver was converted to the stable sulfate form. In the ashing procedure the temperature of the furnace was brought up slowly to 500°F. Then a few drops of concentrated sulfuric acid were added to the charred contents. The furnace temperature was raised to 950°F. and kept there for one hour. After the planchets had cooled to room temperature several drops of water were used to form a suspension uniformly spread in the planchets. The contents

in each planchet were then evaporated to dryness. The radioactivity of the dry substance in the planchet was measured under a fixed geometry with a Geiger-Müller counter (Nuclear-Chicago Radiation Counter Type D-34). The counting result was read from a scaler (Berkeley Model 2000) in counts per minute (c.p.m.), corrected for background radioactivity. No calibration of radioactivity with the quantity of fines was attempted. The counting results were significant only on a relative basis.

RESULTS

PERMEATION RUNS

The purpose of permeation runs was to obtain data from which the attenuation coefficient and collection efficiency could be determined for a given particle-fiber system under a specific set of conditions. In the case of the titanium dioxide-dacron system the experimental results for a single run are summarized as follows:

Particles:	TiO_2	$\underline{C}_o = 1.42 \times 10^{-4}$ g./cc., $\underline{C}_L = 1.14 \times 10^{-4}$ g./cc.
Fibers:	dacron	$\underline{d}_f = 1.71 \times 10^{-2}$ cm., $\rho_f = 1.41$ g./cc.
Fiber mat:		$\underline{W} = 4.695$ g., $\underline{A} = 45.6$ sq. cm., $\underline{L} = 4$ cm.
Flow conditions:		$\underline{U} = 1.0$ cm./sec., $\Delta p \cong 2$ cm. H_2O
Ionic conditions:		pH = 3.5, $CaCl_2$ concn. = 1.9×10^{-5} g.-moles/cc.
Temperature:		23°C.

The attenuation coefficient is evaluated to be:

$$K = \frac{1}{L} \ln \frac{C_o}{C_L} = 5.5 \times 10^{-2} \text{ cm.}^{-1}$$

The porosity of the mat is

$$\epsilon = 1 - \frac{W}{AL\rho_f} = 0.982$$

and the collection efficiency therefore is

$$E = \frac{\pi d_f K}{4(1 - \epsilon)} = 4.05 \times 10^{-3}$$

For the fines-sulfite system, three sets of duplicate runs were made. The experimental conditions and results of these permeation runs are summarized in Table V. The values of E are calculated from Equation (10).

TABLE V

PERMEATION RESULTS OF THE FINES-SULFITE SYSTEM

	Set I			Set II		Set III	
	Run 1	Run 2	Run 3	Run 4	Run 5	Run 6	Run 7
U, cm./sec.	0.987	0.987	0.987	0.987	0.987	0.987	0.987
pH	6.4	6.4	6.4	5.8	5.8	5.1	5.1
$CaCl_2$ concn., g.-moles/cc.	1.9×10^{-5}	1.9×10^{-5}	1.9×10^{-5}	--	--	--	--
NaCl concn., g.-moles/cc.	--	--	--	1.02×10^{-5}	1.02×10^{-5}	1.08×10^{-6}	1.08×10^{-6}
T, °C.	ca.23	ca.23	ca.23	21	21	21.5	21.5
ΔP (initial), cm. H_2O	16.2	15.6	16.2	7.00	7.75	6.70	7.40
ΔP (final), cm. H_2O	19.4	20.0	19.3	8.20	9.50	8.60	9.40
t, sec.	1352	1080	1034	998	1009	934	1005
L (final), cm.	1.8	1.8	1.8	1.4	1.4	1.4	1.4
W, g.	5.088	5.006	4.978	2.943	3.001	3.102	3.173
C_o, c.p.m.	13,173	6,824	7,629	40,423	40,151	24,906	24,028
C_L, c.p.m.	117	52.2	60.6	26,902	26,545	21,654	20,845
$\ln (C_o/C_L)$	4.73	4.86	4.83	0.407	0.414	0.140	0.142
W/A, g./sq. cm.	0.112	0.110	0.109	0.0645	0.0658	0.0680	0.0696
$E \times 10^3$	18.5	19.4	19.3	2.75	2.74	0.899	0.895
Average $E \times 10^3$		19.1		2.75		0.897	

FILTRATION RUNS

In filtration runs the retention of small particles follows that of fibers. Because long fibers and a fine-mesh wire screen were used in the experiments, the fiber retention was considered to be complete. The dimension of the square openings of the 150-mesh screen was about 0.01 cm. The sulfite fibers have an average length of 0.211 cm. The ratio of the dimension of the screen to the fiber length being 0.05, the initial fiber retention would be complete in accordance with the fiber retention theory (2), as shown in Fig. 5.

Two runs were made with the titanium dioxide-dacron system. In these runs the particle and fiber suspensions were kept in two separate feed tanks. The two feed streams were mixed shortly before the entrance of the filtration tube. This was done in the hope that the particles would not adhere to the fibers prior to the mat formation. As will be shown later, this hope was not realized.

The experimental conditions were identical with those in the permeation runs for the same system. Where any differences existed, they will be specified. The data of these two filtration runs are tabulated in Table VI.

The mat was sectioned into eight layers. The measses of particles and fibers in each layer were determined. Each data point in Table VI represents the cumulative amount in successive layers beginning from the layer at the septum. The data points of the two duplicate runs are plotted separately in Fig. 6 and 7. It is seen that each set of data may be represented by a smooth curve. The slope of the curve at any point is the local bound particle content, p', defined as the mass of particles per unit mass of fibers. Obviously, the reliability of the values of p' improves with the increasing number of layers, increasing precision in the mass measurements, and increasing accuracy in determining the slopes.

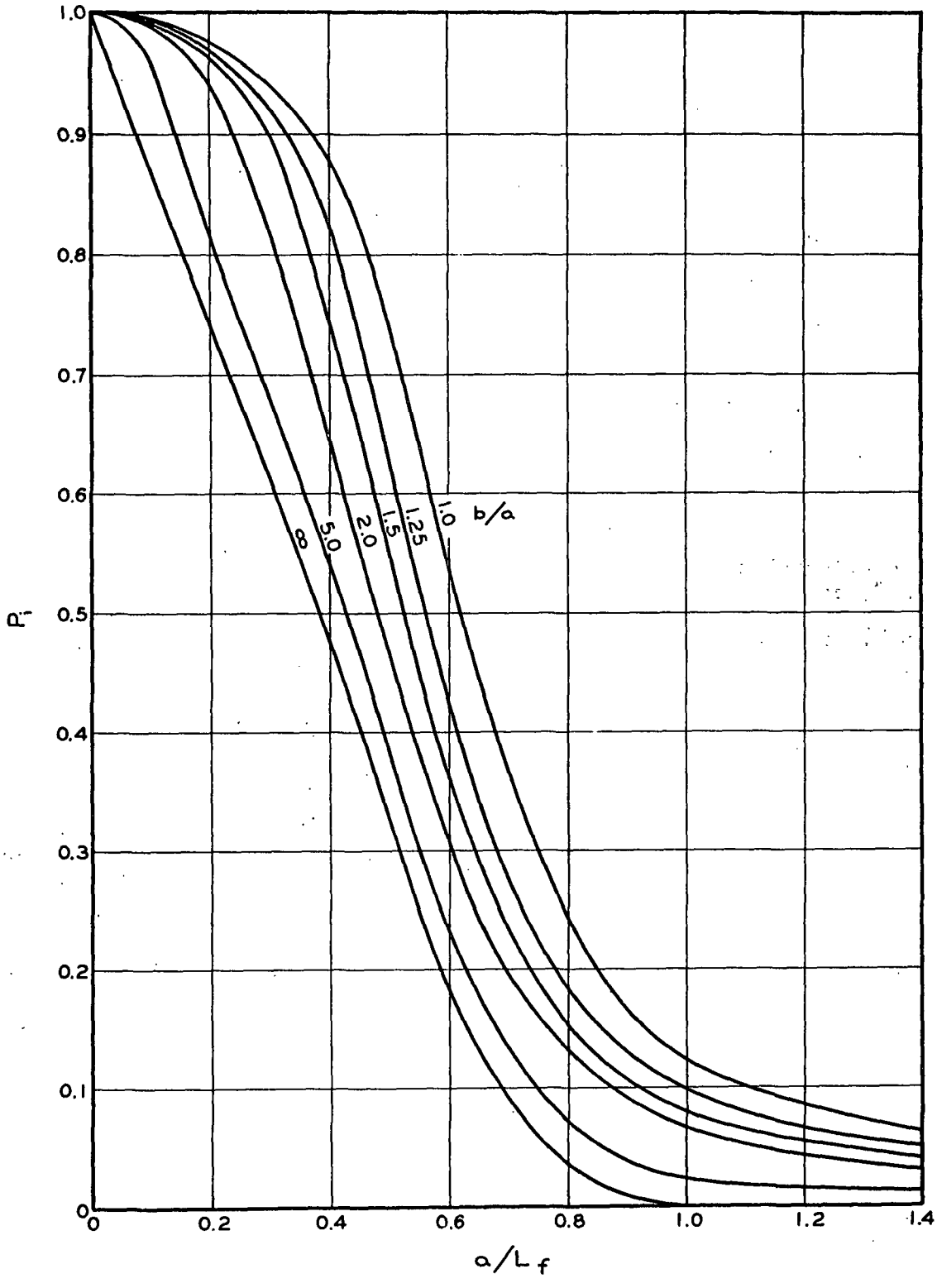

Figure 5. Initial Retention Probability of Fibers on Wire Screens

TABLE VI

FILTRATION DATA FOR THE TITANIUM DIOXIDE-DACRON SYSTEM

	Run 1	Run 2
TiO_2 concn. x 10^6, g./cc.	2.31	2.31
Fiber concn. x 10^5, g./cc.	6.84	6.84
pH	3.6	3.6
Particle suspension volume used x 10^{-4}, cc.	6.11	6.22
ΔP (final), cm. H_2O	1.9	1.9

w, g.	m', g.	w, g.	m', g.
0.545	0.0041	0.545	0.0040
1.045	0.0074	0.985	0.0070
1.607	0.0109	1.714	0.0116
2.175	0.0143	2.276	0.0149
2.560	0.0163	2.910	0.0181
3.194	0.0191	3.445	0.0206
4.016	0.0230	4.083	0.0232
4.698	0.0253	4.773	0.0254

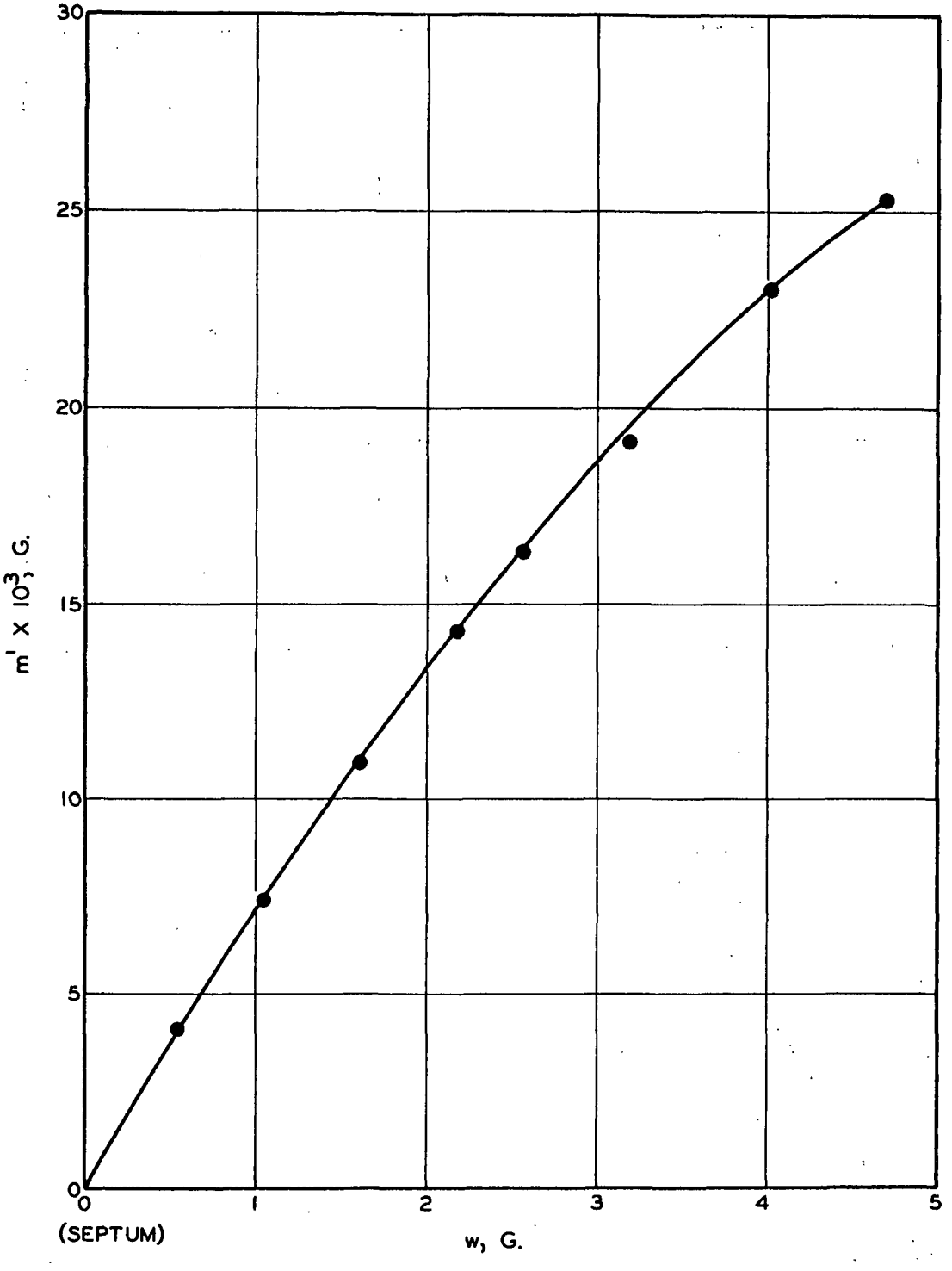

Figure 6. Filtration Data for the Titanium Dioxide-Dacron System, Run 1

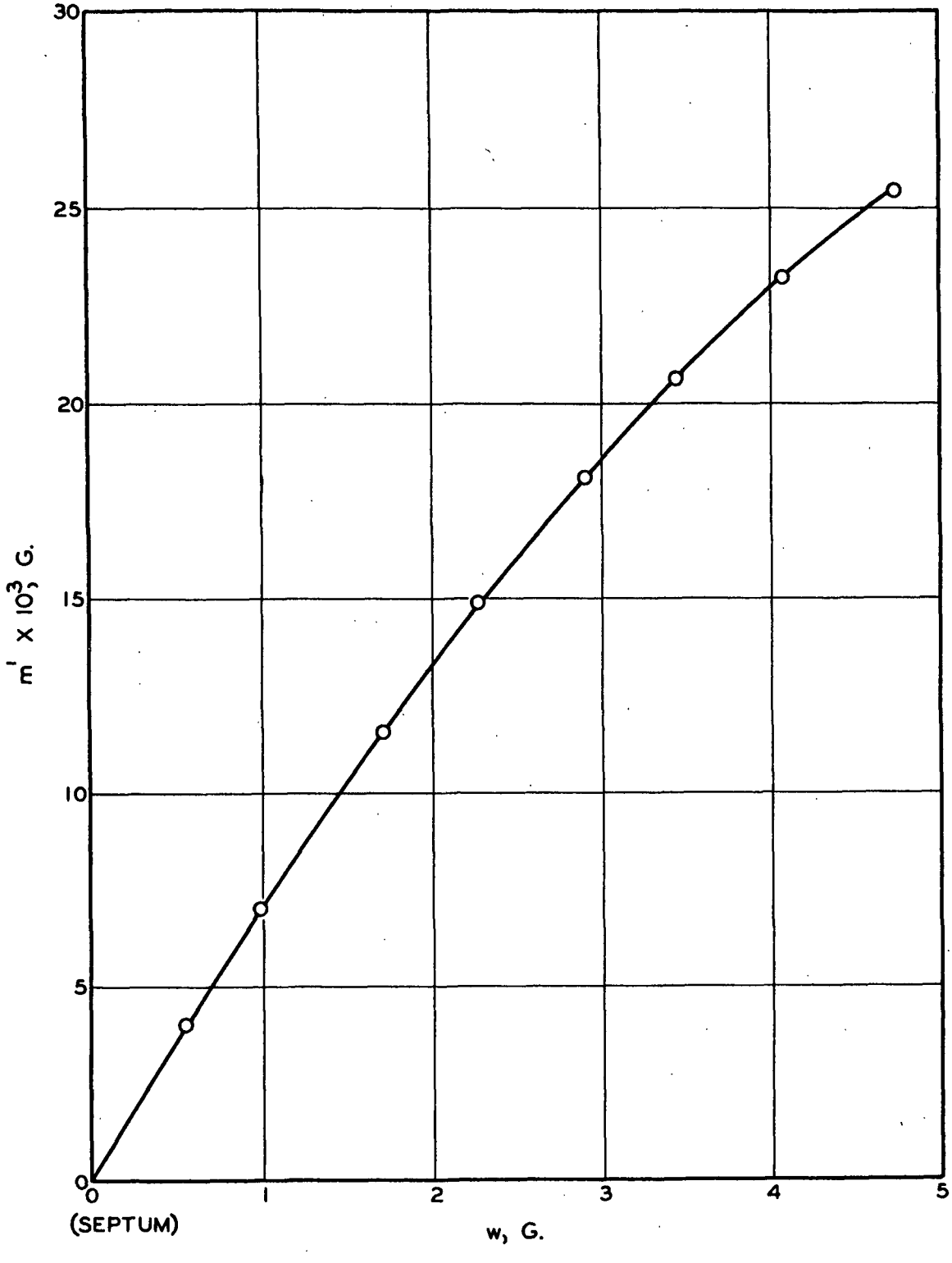

Figure 7. Filtration Data for the Titanium Dioxide-Dacron System, Run 2

The simplest way of obtaining p' is by direct graphical determination of slopes on the smooth curve. The results of such determination are shown in Table VII.

TABLE VII

GRAPHICAL DETERMINATION OF p'

Run 1		Run 2	
w/W, g./g.	$p' \times 10^3$, g./g.	w/W, g./g.	$p' \times 10^3$, g./g.
0.116	7.12	0.114	7.05
0.223	6.59	0.206	6.58
0.342	6.13	0.359	6.01
0.463	5.58	0.477	5.51
0.545	5.11	0.607	4.86
0.680	4.63	0.722	4.44
0.855	3.82	0.856	3.76
1.00	p_s' 2.92	1.00	p_s' 3.00

A somewhat more elaborate graphical method would be to plot the ratio of $(m' - m_n')/(w - w_n)$ vs. $(w - w_n)$, where the subscript n represents the layer concerned, and to draw a smooth curve through these points. The intercept of this curve at $w - w_n = 0$ is p'. Both graphical methods are more or less subject to bias and uncertainty, especially with regard to p_s'.

From the previous analysis of particle retention in an incompressible mat of cylindrical fibers formed at constant-rate filtration from a dilute suspension, the resulting expression for particle distribution in the mat is shown to be

$$-\ln\left(1 - \frac{p' - p_s'}{p_s}\right) = K'\left(1 - \frac{w}{W}\right) \qquad (31),$$

where
$$K' = \frac{K(W/A)}{\rho_f(1 - \epsilon)} = \frac{4E(W/A)}{\pi d_f \rho_f} \qquad (32).$$

The mass of free particles per unit mass of fibers in the suspension, $\underline{p_s}$, can be determined easily from the difference between the experimentally known value for the total mass of particles (free and bound) per unit mass of fibers, $(\underline{p} + \underline{p}')_{\underline{s}}$, and the graphically determined $\underline{p_s}'$. The value of $\underline{p_s}$ for both runs was found to be 2.71×10^{-2} g./g.

Having established the correspondence of $\underline{p}'$ and $\underline{w/W}$ in Table VII and evaluated $\underline{p_s}'$ and $\underline{p_s}$, the data may now be converted to $-\ln [1 - (\underline{p}' - \underline{p_s}')/\underline{p_s}]$ and $(1 - \underline{w/W})$, respectively, and plotted thus in Fig. 8 and 9. A linear relationship is evident in these figures. The slopes of the lines are $\underline{K}'$. The collection efficiencies are calculated from Equation (32) to be 3.53×10^{-3} and 3.32×10^{-3}, respectively, for Run 1 and Run 2.

In the above calculations by the graphical method the most uncertain as well as sensitive quantity is $\underline{p_s}'$. For this reason a statistical computation method was devised to obtain the best values of $\underline{p_s}'$ and $\underline{E}$ with the aid of a computer (IBM 1620) as follows:

From the previous definitions:

$$dm' = p'dw \qquad (63),$$

$$m_s' = p_s' \qquad (64),$$

and
$$m_s = p_s W \qquad (65).$$

Then, accepting the retention equation to be valid, the cumulative mass of particles in any given layer of the formed mat from the septum is

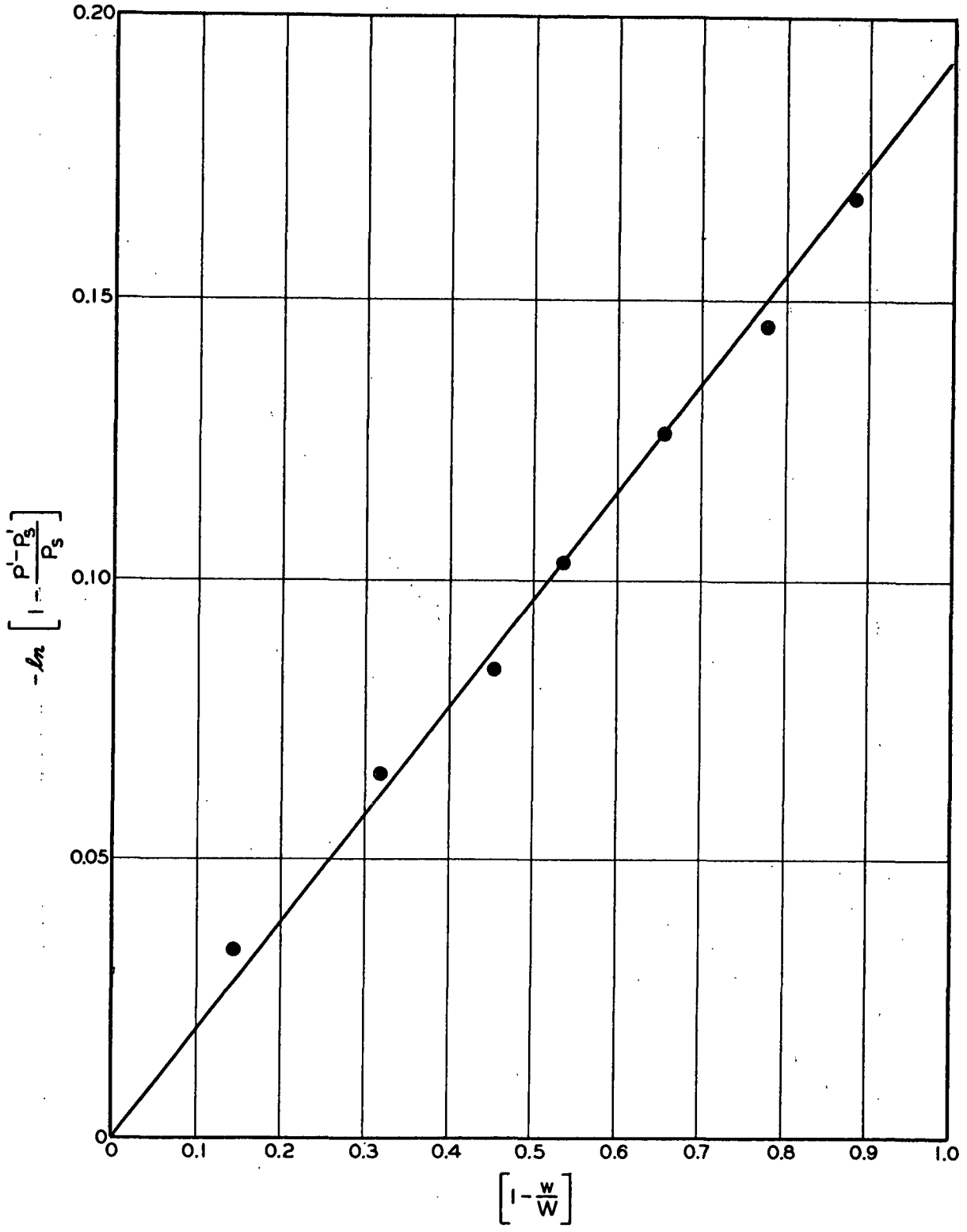

Figure 8. Distribution of Titanium Dioxide in Dacron Mat, Run 1

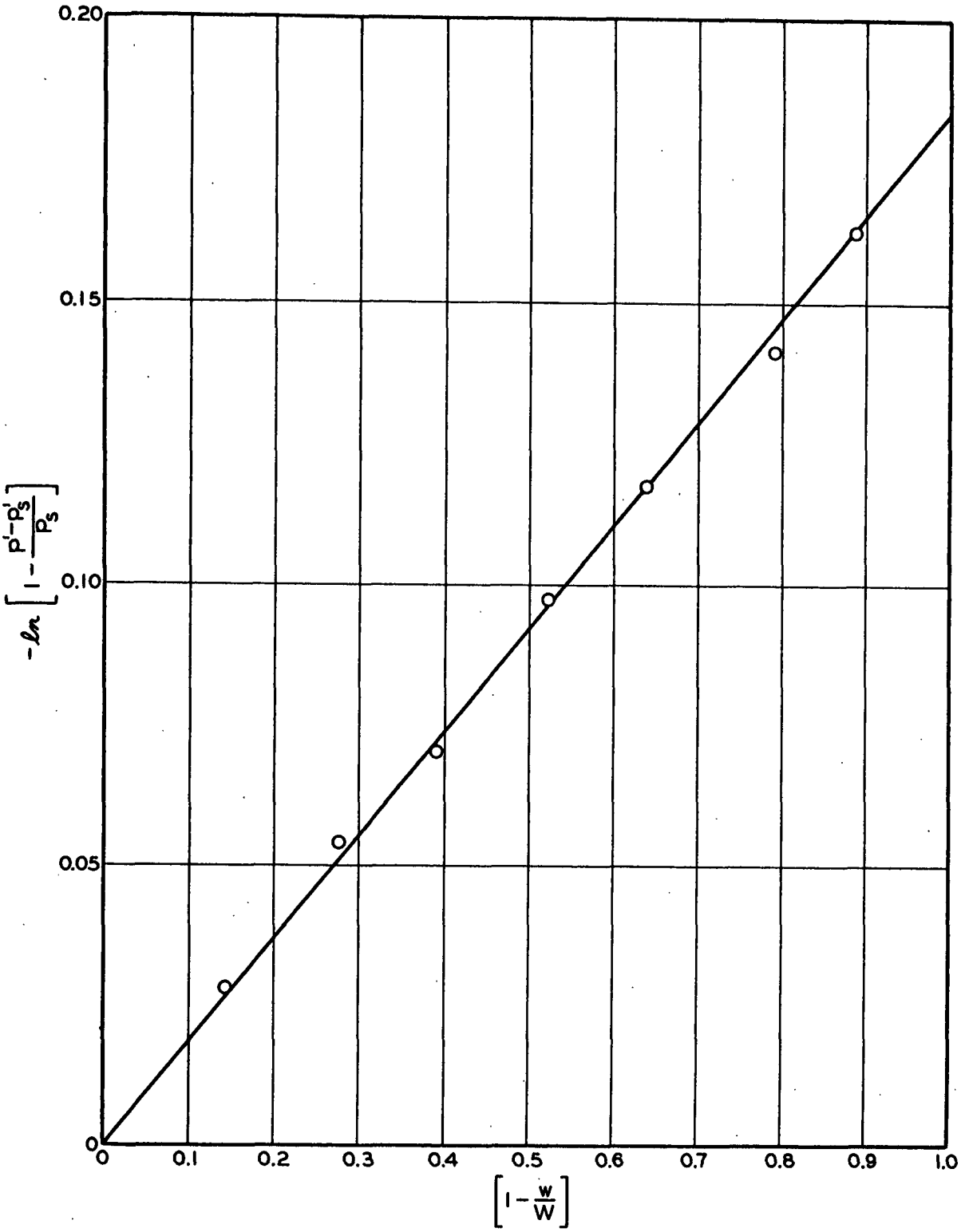

Figure 9. Distribution of Titanium Dioxide in Dacron Mat, Run 2

$$m' = \int_0^w p'dw = -\int_1^{1-(w/W)} [m_s' + m_s(1 - e^{-K'(1-\frac{w}{W})})]d(1 - \frac{w}{W})$$

$$= (m_s + m_s')(\frac{w}{W}) + \frac{m_s}{K'}[e^{-K'} - e^{-K'(1-\frac{w}{W})}]$$

$$= (m + m')_s(\frac{w}{W}) - \frac{(m + m')_s - m_s'}{K'}[e^{-K'(1-\frac{w}{W})} - e^{-K'}] \quad (66).$$

The term $(\underline{m} + \underline{m}')_{\underline{s}}(\underline{w}/\underline{W})$ is the total mass of free and bound particles in the approaching suspension during the portion of the filtration time to form a layer of $\underline{w}$ g. of fibers. The next term represents the mass of free particles which have penetrated through the layer. Their difference is the mass of bound particles in the layer.

By solving the integrated equation (66), and using the graphically determined values of $\underline{m}_{\underline{s}}'$ and $\underline{K}'$ in an initial trial, a calculated value for $\underline{m}'$ is obtained for each value of $(\underline{w}/\underline{W})$ from the original data. The discrepancy between the calculated and experimental values of $\underline{m}'$ is minimized by the least squares method, and the best values for $\underline{p}_{\underline{s}}'$ and $\underline{E}$ are obtained for the complete set of data. The process of computation is described in Appendix II. The results of computation are as follows:

Run	$\underline{m}_{\underline{s}}' \times 10^2$	$\underline{K}' \times 10$	$\underline{p}_{\underline{s}}' \times 10^3$	$\underline{E} \times 10^3$
1	1.487	1.739	3.16	3.20
2	1.426	1.844	2.98	3.34

The subsequent experiments are concerned with the retention of fines. Two runs (3 and 4) were made for the fines-dacron system, the data and results of

which are reported in Table VIII and shown in Fig. 10 and 11. The values for p_s' and E were evaluated graphically.

It should be mentioned at this point that these preliminary experimental results with fines are not very reliable because of the leaching of radioactivity to the solution in which the fines and fibers are suspended under the prescribed ionic conditions. The leaching is due primarily to the low pH at which the deposited silver in the form of metallic silver or possibly silver oxide resulting from incidental oxidation has appreciable solubility in acidic aqueous solutions. The remedy would appear to be an increase in pH to such a value that the leaching is minimized while the dispersion of the particles is maintained by sufficient dilution, and the retention of particles by fibers is kept to a measurable extent with the aid of calcium chloride.

A leaching test was therefore carried out as follows: Two solutions were prepared at a calcium chloride concentration of ca. 2 g.-moles per liter, but different pH values (ca. 3.5 and 6.5). Ten cc. of the tagged fines from a suspension were introduced to each of three centrifuge tubes. The first tube was centrifuged for 20 minutes, and the supernatant was decanted. The residue was transferred with distilled water to a planchet. The two other tubes were centrifuged and decanted in a similar manner, but refilled with 10 cc. of each of the two solutions at different pH values. The process was repeated five times. The final residues were transferred to separate planchets. All three planchets were dried at 220°F. overnight, and their radioactivities measured at room temperature. Six tests were made, and the results are shown in Table IX.

TABLE VIII

FILTRATION DATA FOR THE FINES-DACRON SYSTEM

	Run 3			Run 4		
Fines concn., c.p.m./cc.	22.3			20.4		
Fiber concn. x 10^5, g./cc.	6.84			6.84		
$CaCl_2$ concn. x 10^5, g.-moles/cc.	1.9			1.9		
pH	3.5			3.6		
$\underline{T}$, °C.	25			26		
$\underline{U}$, cm./sec.	1.0			1.0		
$\Delta\underline{P}$ (final), cm. H_2O	1.9			1.9		
$\underline{L}$ (final), cm.	4.0			4.0		
	$\underline{w}$, g.	$\underline{m}'$, c.p.m.	$\underline{p}'$ x 10^{-3}, c.p.m./g.	$\underline{w}$, g.	$\underline{m}'$, c.p.m.	$\underline{p}'$ x 10^{-3} c.p.m./g.
	0.824	2744	2.88	0.792	3653	3.06
	1.576	4710	2.29	1.299	5120	2.63
	2.101	5749	2.00	2.112	6824	2.14
	2.785	6840	1.42	2.595	8459	1.52
	3.270	7363	1.15	3.550	9333	1.21
	3.711	7733	0.88	4.064	9904	0.91
	4.359	8059	0.55	4.604	10242	0.53
	4.998	8168	0.15	5.227	10450	0.12
$\underline{p}_s$ x 10^{-5}, c.p.m./g.	3.36			3.24		
$\underline{K}'$ x 10^2	0.92			1.04		
$\underline{E}$ x 10^4	1.59			1.79		

Av. $\underline{E}$ = 1.7 x 10^{-4}

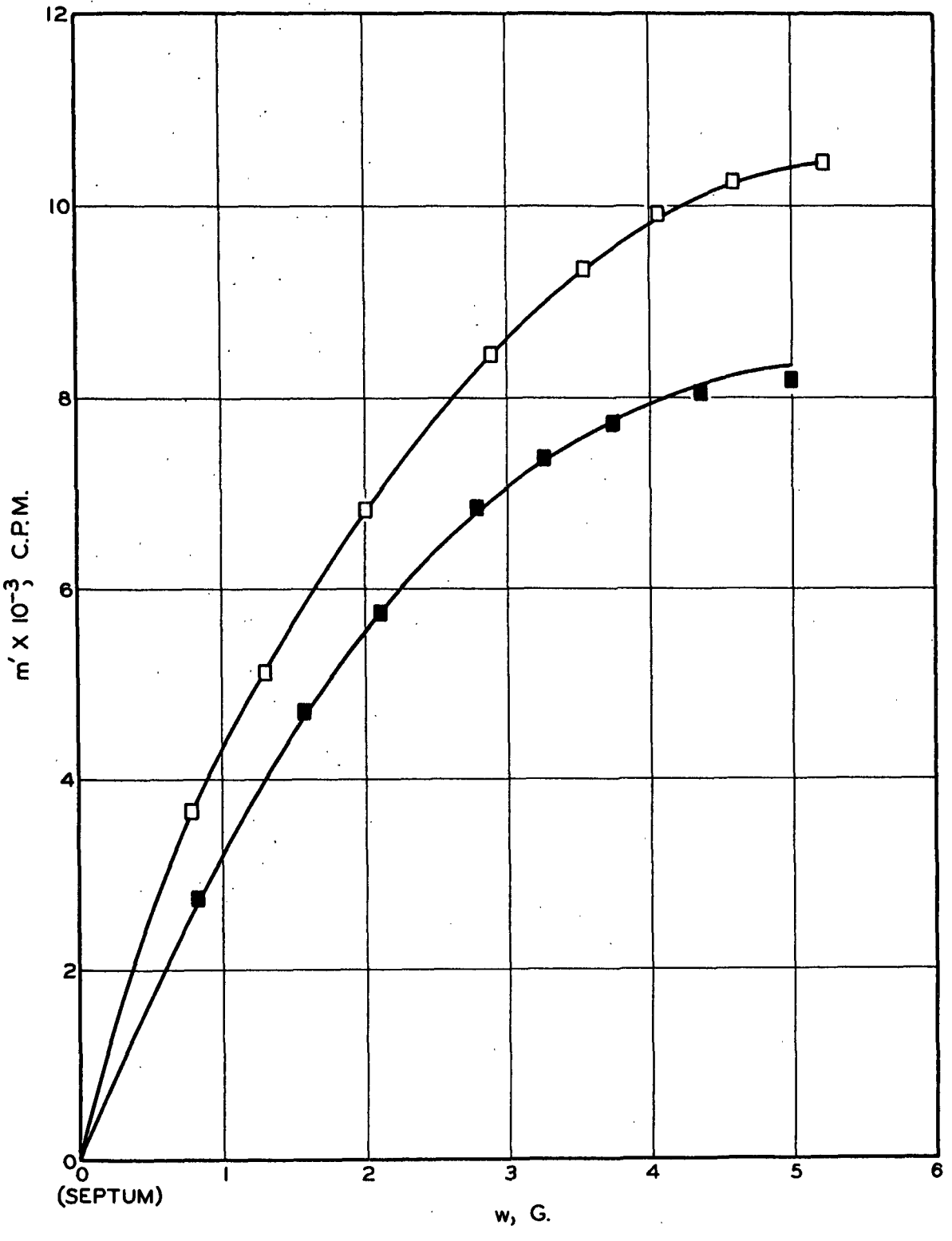

Figure 10. Filtration Data for the Fines-Dacron System, Run 3 (Lower Curve) and Run 4 (Upper Curve)

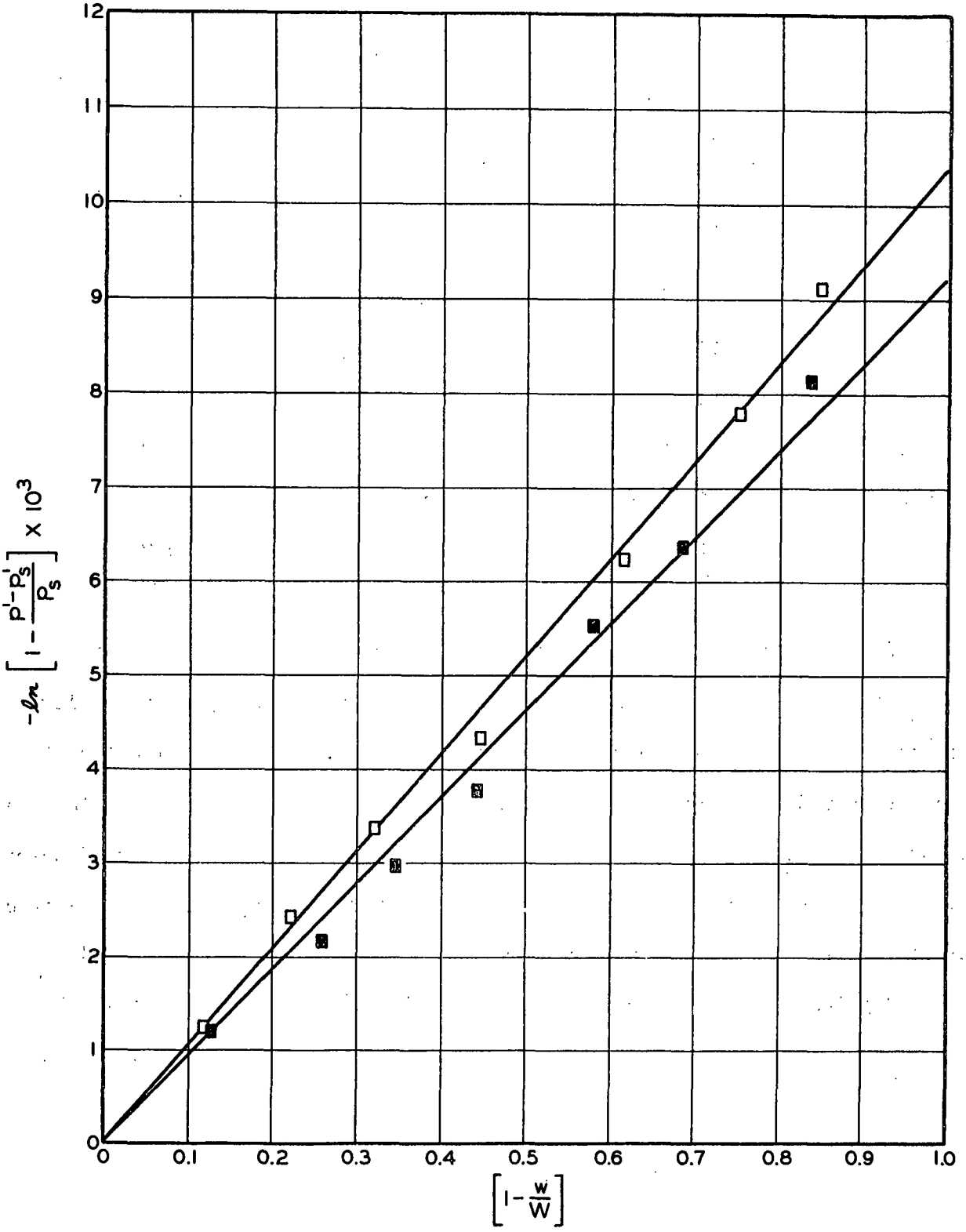

Figure 11. Distribution of Fines in Dacron Mats, Run 3 (Lower Line) and Run 4 (Upper Line)

TABLE IX

RADIOACTIVITY LEACHING TEST

Solution pH	Radioactivity Without Leaching, c.p.m.	Radioactivity With Leaching, c.p.m.	Loss of Radioactivity, %
3.6	25,200	21,600	14.3
3.8	31,200	24,400	21.8
3.8	31,200	26,200	16.0
6.5	27,400	26,100	5.0
6.5	27,400	26,000	5.3
6.5	25,200	23,500	6.7

Based on these results the subsequent experiments with fines were conducted at the higher pH value, ca. 6.5, for which no addition of hydrochloric acid to the suspension was required. Four runs (Set I) were made with the fines-sulfite system under the revised conditions. The data are summarized in Table X and shown in Fig. 12-14. After analyzing the results with the guidance of theory and discovering the apparent anomalies, a special experiment (Run 9) was designed to demonstrate the extreme case of uniform retention, and two more sets (II and III) of normal duplicate runs were conducted under modified ionic conditions in the direction of reduced retention. These results are also presented in the same table.

TABLE X

FILTRATION DATA FOR THE FINES-SULFITE SYSTEM

Set I

	Run 5	Run 6
Fines concn., c.p.m./cc.	0.460	0.460
Fiber concn. x 10^5, g./cc.	6.84	6.84
$CaCl_2$ concn. x 10^5, g.-moles/cc.	1.9	1.9
pH	6.4	6.4
$\underline{T}$, °C. (ca.)	23	23
$\underline{U}$, cm./sec.	0.987	0.987
$\Delta\underline{P}$ (final), cm. H_2O	4.1	24.2
$\underline{L}$ (final), cm.	0.8	2.25

Run 5			Run 6		
$\underline{w}$, g.	$\underline{m}'$, c.p.m.	$\underline{p}' \times 10^{-3}$, c.p.m./g.	$\underline{w}$, g.	$\underline{m}'$, c.p.m.	$\underline{p}' \times 10^{-3}$, c.p.m./g.
0.166	584	3.65	0.402	1508	4.00
0.436	1603	3.65	0.672	2630	4.00
0.775	2831	3.65	1.059	4138	4.00
1.245	4385	2.85	1.416	5620	4.00
1.645	5415	1.88	1.651	6592	4.00
2.039	5986	0.55	2.045	8249	4.00
$\underline{p}_s$ = 6.08 x 10^3 c.p.m./g.			2.496	10050	4.00
			3.075	12347	4.00
			3.578	14233	3.73
			3.708	14679	3.71
			4.030	15807	3.41
			4.625	17525	2.92
			5.174	18944	2.44
			5.822	19902	0.77
			$\underline{p}_s$ = 5.86 x 10^3 c.p.m./g.		

TABLE X (Contd.)

Set I

	Run 7			Run 8		
Fines concn., c.p.m./cc.	0.214			0.214		
Fiber concn. x 10^5, g./cc.	6.79			6.79		
$CaCl_2$ concn. x 10^5, g.-moles/cc.	1.9			1.9		
pH	6.4			6.4		
$\underline{T}$, °C. (ca.)	23			23		
$\underline{U}$, cm./sec.	0.987			0.987		
$\Delta\underline{P}$ (final), cm. H_2O	20.2			19.2		
$\underline{t}$, sec.	1596			1578		
$\underline{L}$ (final), cm.	1.8			1.8		
	$\underline{w}$, g.	$\underline{m}'$, c.p.m.	$\underline{p}' \times 10^{-3}$, c.p.m./g.	$\underline{w}$, g.	$\underline{m}'$, c.p.m.	$\underline{p}' \times 10^{-3}$, c.p.m./g.
	0.812	2168	2.69	0.649	1764	2.69
	1.280	3397	2.69	1.149	3120	2.69
	1.888	5098	2.69	1.791	4840	2.69
	2.278	6142	2.69	2.442	6599	2.69
	2.890	7747	2.69	3.117	8395	2.69
	3.428	9164	2.69	3.623	9745	2.69
	4.221	11206	2.52	4.019	10762	2.37
	4.835	12636	1.96	4.589	12142	2.29
	5.247	13157	0.90	5.151	13063	1.10
	$\underline{p}_s$ = 2.25 x 10^3 c.p.m./g.			$\underline{p}_s$ = 2.25 x 10^3 c.p.m./g.		

TABLE X (Contd.)

	Run 9
Fines concn. in beaker x 10^{2}, c.p.m./cc.	1.87
Fines concn. in feed tank , c.p.m./cc.	1.87
Fiber concn. in beaker x 10^{3}, g./cc.	6.79
Fiber concn. in feed tank x 10^{5}, g./cc.	6.79
$CaCl_2$ concn. x 10^{5}, g.-moles/cc.	1.9
pH	6.4
$\underline{T}$, $^{o}C.$	22
$\underline{U}$, cm./sec.	0.987
$\Delta\underline{P}$ (final), cm. H_2O	46.4
$\underline{t}$, sec.	2114
$\underline{L}$ (final), cm.	2.1

$\underline{w}$, g.	$\underline{m}'$, c.p.m.	$\underline{p}'$ x 10^{-3}, c.p.m./g.
1.353	4185	3.07
2.254	6966	3.07
3.086	9499	3.07
4.689	14239	2.91
5.420	16351	2.76

$\underline{p}_s \cong 0$ c.p.m./g.

TABLE X (Contd.)

Set II

	Run 10			Run 11		
Fines concn., c.p.m./cc.	0.900			0.900		
Fiber concn. x 10^5, g./cc.	6.79			6.79		
NaCl concn. x 10^5, g.-moles/cc.	1.02			1.02		
pH	5.8			5.8		
$\underline{T}$, °C.	21			21		
$\underline{U}$, cm./sec.	0.987			0.987		
$\Delta\underline{P}$ (final), cm. H_2O	8.3			8.2		
$\underline{t}$, sec.	1021			1020		
$\underline{L}$ (final), cm.	1.4			1.4		
	$\underline{w}$, g.	$\underline{m}'$, c.p.m.	$\underline{p}'$ x 10^{-3} c.p.m./g.	$\underline{w}$, g.	$\underline{m}'$, c.p.m.	$\underline{p}'$ x 10^{-3} c.p.m./g.
	0.532	2240	4.09	0.771	3056	3.94
	1.243	4791	3.43	1.340	5387	3.38
	1.791	6736	2.97	1.700	6350	3.06
	2.541	8720	2.00	2.440	8340	2.23
	3.045	9524	1.43	3.075	9440	1.37
	$\underline{p}_s$ = 1.18 x 10^4 c.p.m./g.			$\underline{p}_s$ = 1.18 x 10^4 c.p.m./g.		

TABLE X (Contd.)

Set III

	Run 12	Run 13
Fines concn., c.p.m./cc.	0.549	0.549
Fiber concn. x 10^5, g./cc.	6.79	6.79
NaCl concn. x 10^6, g.-moles/cc.	1.08	1.08
pH	5.1	5.1
$\underline{T}$, $^{o}C.$	21.5	21.5
$\underline{U}$, cm./sec.	0.987	0.987
$\Delta\underline{P}$ (final), cm. H_2O	8.0	8.1
$\underline{t}$, sec.	1011	1008
$\underline{L}$ (final), cm.	1.4	1.4

Run 12			Run 13		
$\underline{w}$, g.	$\underline{m}'$, c.p.m.	$\underline{p}'$ x 10^{-2} c.p.m./g.	$\underline{w}$, g.	$\underline{m}'$, c.p.m.	$\underline{p}'$ x 10^{-2} c.p.m./g.
0.719	698	9.09	0.645	627	9.29
1.434	1283	7.44	1.335	1240	7.71
1.990	1692	6.29	1.898	1627	6.43
2.455	1947	5.01	2.383	1930	5.66
3.102	2210	2.73	2.989	2221	2.94

$p_{\underline{s}}$ = 7.81 x 10^3 c.p.m./g. $p_{\underline{s}}$ = 7.81 x 10^3 c.p.m./g.

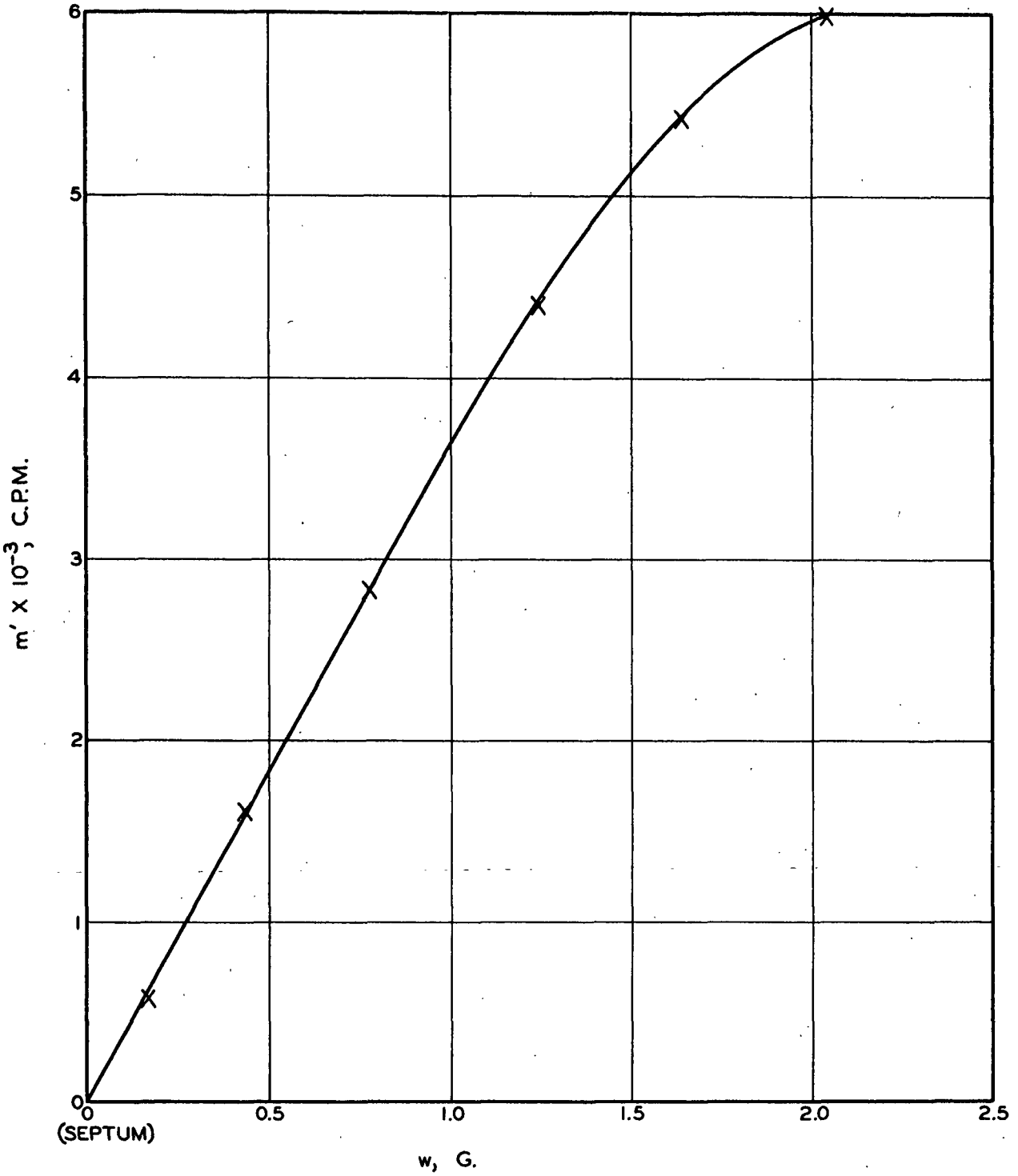

Figure 12. Filtration Data for the Fines-Sulfite System, Run 5

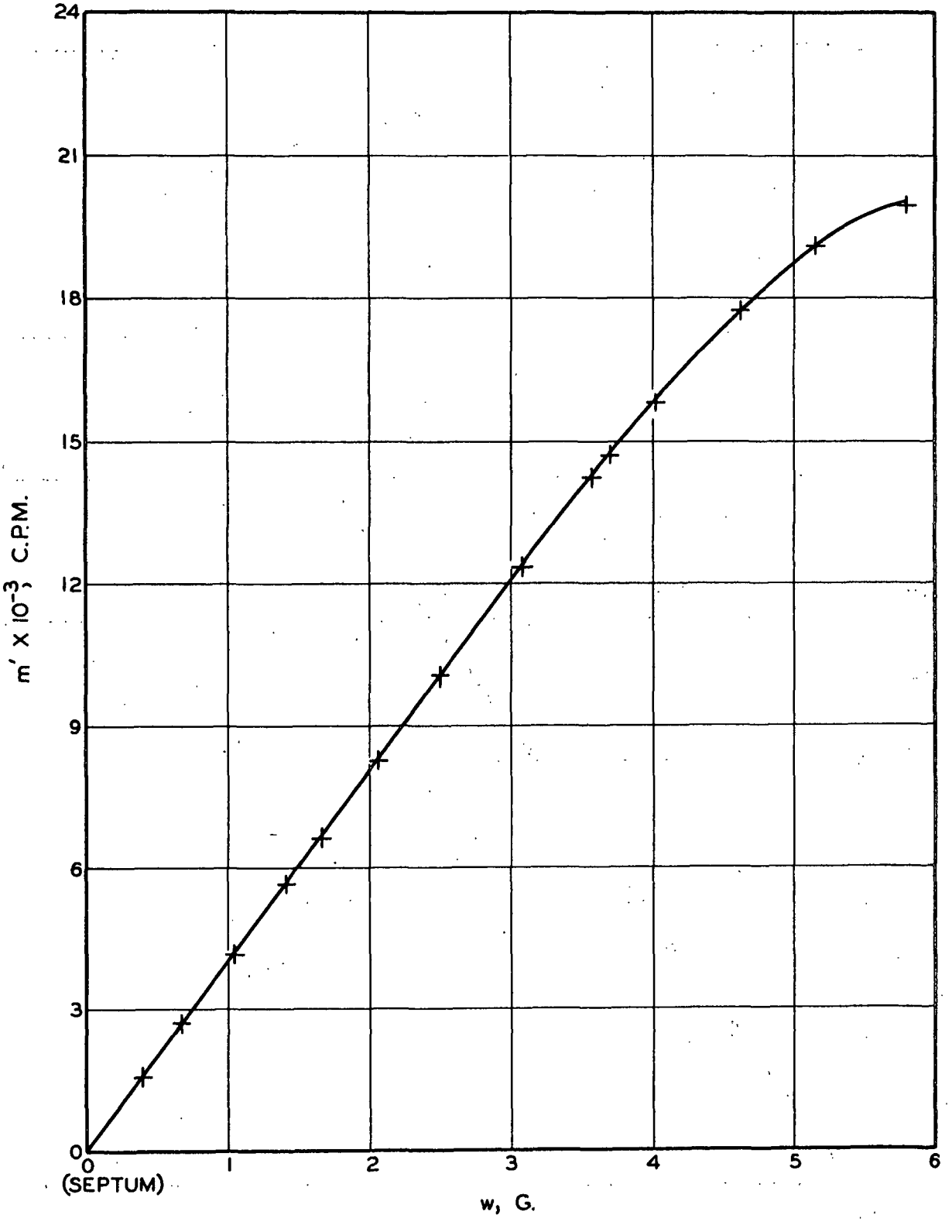

Figure 13. Filtration Data for the Fines-Sulfite System, Run 6

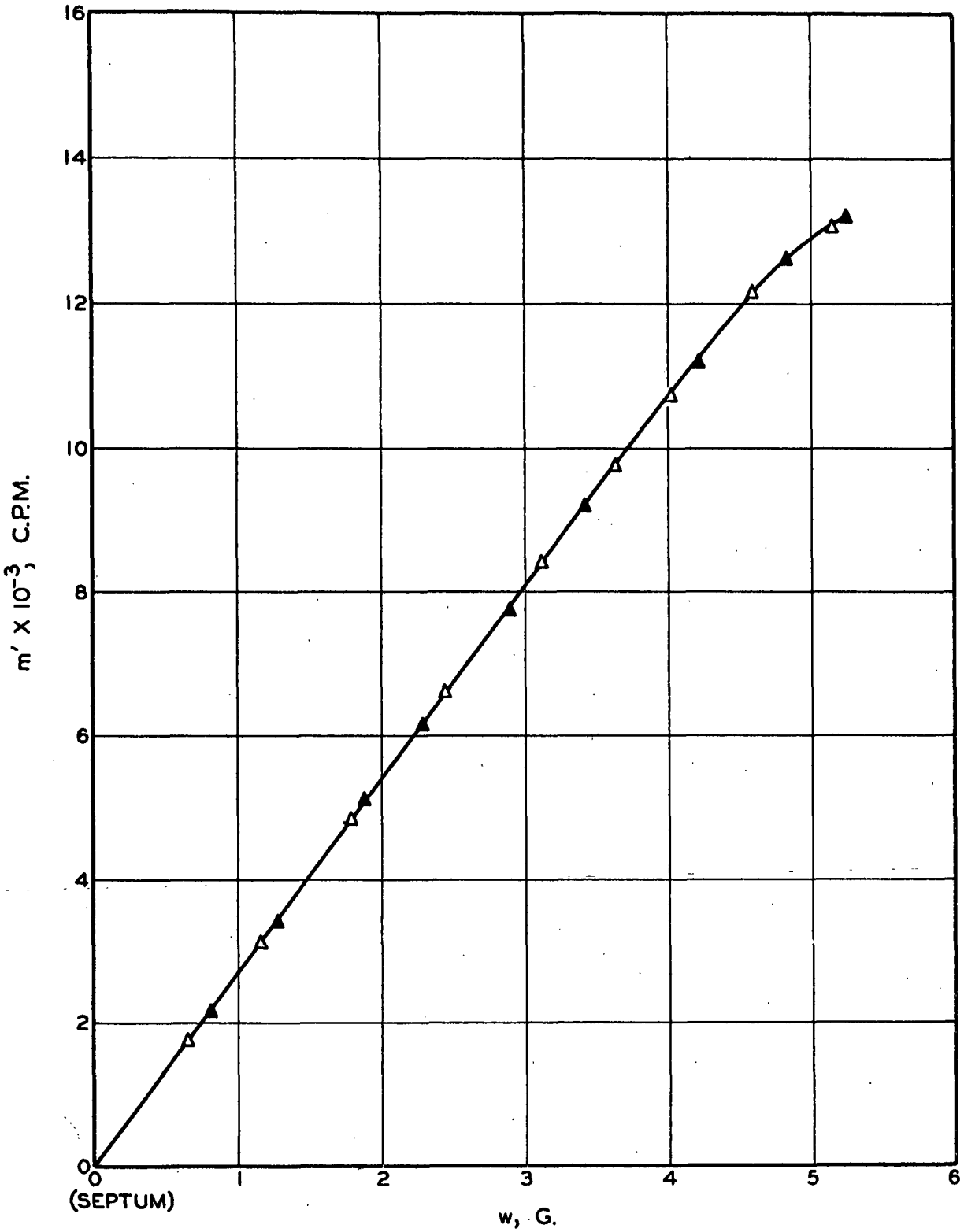

Figure 14. Filtration Data for the Fines-Sulfite System, Run 7 (Dark Triangles) and Run 8 (Triangles)

DISCUSSION

INCOMPRESSIBLE MATS

In the introduction to the retention problem we briefly described its complexity, especially with regard to the ill-defined fines. Subsequently, in the analysis of the retention process, we dealt initially with the simplest case of the retention of fine particles in an incompressible mat of cylindrical fibers formed from a dilute suspension in constant-rate filtration. The result of analysis under the simplified conditions is expressed by the retention equation:

$$-\ln\left(1 - \frac{p' - p_s'}{p_s}\right) = \frac{4E(W/A)}{\pi\rho_f d_f}\left(1 - \frac{w}{W}\right) \qquad (31\text{-}32),$$

showing the distribution of particles bound to fibers in a mat as a result of the attenuation of free particles during filtration.

By carefully examining the retention equation it is seen that the distribution is essentially of an exponential nature with most particles located at the bottom of the mat $(\underline{w} = 0)$ and fewest particles at the mat face $(\underline{w} = \underline{W})$. In theory, very little retention takes place at the top of the mat; the particles found there $(\underline{p_s}')$ have already become attached to the fibers in the suspension, and are simply deposited along with the fibers on the mat face. This mode of particle distribution is not very difficult to visualize if one accepts the attenuation concept that the longer a layer of fibers is subjected to collisions with free particles, owing to any causes whatsoever, the more will the fibers capture some of these particles.

The original concept of the attenuation process, based on the steady permeation of a fiber mat with a uniform particle suspension, was that the more

particles approaching a layer of fibers, the more they will be collected, thus resulting in an exponential decrease of bound particles in the direction of flow. The only modification incorporated in the retention equation is the necessary feature that as the fluid permeates through the mat already formed, its free particle concentration decreases continuously in accordance with the experimentally verified attenuation law. As the mat builds up, fewer and fewer free particles approach a particular layer, and therefore fewer and fewer particles are being collected there timewise.

The experimental verification of the retention equation is desirable in view of the assumptions involved and in anticipation of the subsequent development for more complicated cases. We begin our discussion with the titanium dioxide-dacron system. The choice of dacron fibers was dictated by their rigidity to satisfy the condition of an incompressible mat. Glass fibers would have been even more suitable for this purpose, but for the experimental difficulties in dispersing the fibers and forming a uniform mat. The use of titanium dioxide particles was adopted for the practical reason that a concentrated and dispersed stock of a commercial grade of characterized particles was available at the Institute.

In evaluation of the original data presented in Table VI, we mentioned the bias and uncertainty involved in the graphical determination of $\underline{p}'$, especially $\underline{p}_s'$, which is the slope of the smoothed curve at the last data point ($\underline{w} = \underline{W}$). If these values for $\underline{p}'$ are accepted, the results of the two duplicate runs in Fig. 8 and 9 show a linear relationship. This serves to indicate the validity of the retention equation in form, if not in substance.

The slopes of Fig. 8 and 9 are $\underline{K}'$ from which the collection efficiencies were calculated in accordance with Equation (32). The discrepancy between

the duplicate runs was only 6%, which was probably within the experimental precision, and the average value of 3.4×10^{-3} was fairly well established.

The subsequent numerical computation of the best values of $\underline{p_s}'$ and $\underline{E}$ by the least squares method was based on the contention that the retention equation is essentially correct. The results of the graphical evaluation and the statistical computation are compared as follows:

	$\underline{p_s}' \times 10^3$		$\underline{E} \times 10^3$		
	Run 1	Run 2	Run 1	Run 2	Av.
Graphical	2.92	3.00	3.53	3.32	3.4
Statistical	3.16	2.98	3.20	3.34	3.3

The final test of the retention equation is to check $\underline{E}$ from the filtration runs against that from the permeation experiment under apparently identical conditions of retention. The latter value has been reported to be 4.0×10^{-3}. The discrepancy between the filtration and permeation results is about 15%.

We are inclined to attribute this rather large discrepancy to the experimental errors. The major error probably occurred in the particle measurement. In the case of permeation, a single measurement of the particles retained in the mat was sufficient for the evaluation of $\underline{E}$. For filtration, however, the involved colorimetric analysis of titanium dioxide was performed on each of the eight layers of a mat. In any single analysis the sample had to be ashed, chemically treated, and transferred. All these manipulations entailed some losses of the particles. The cumulative losses in eight samples could conceivably account for the smaller value of $\underline{E}$ from filtration experiments.

It is also desirable to look into the meaning of the collection efficiency as evaluated from these experiments. In the derivation of the attenuation equation, $\underline{E}$ is assumed to be independent of the approaching particle concentration and the thickness of a uniform mat. These facts have been amply demonstrated in the field of aerosol filtration. In order that $\underline{E}$ may be constant, all factors which influence retention must remain unchanged as the particle suspension permeates a mat.

For slow flow with small particles, retention is controlled by diffusion. It is shown in Appendix I that the known hydrodynamic factors governing diffusional retention may be correlated by

$$E = \alpha \left(\frac{\rho d_f U}{\mu}\right)^{-2/3} \left(\frac{\mu}{\rho D}\right)^{-2/3} = \alpha \left(\frac{D}{d_f U}\right)^{2/3} \qquad (67),$$

provided the Reynolds number $(\rho \underline{d_f} \underline{U}/\mu)$ is less than one or the diffusion number $(\underline{D}/\underline{d_f}\underline{U})$ is less than 2×10^{-5}. The diffusion coefficient of titanium dioxide particles in water may be estimated from Einstein's equation to be

$$D = \frac{kT}{3\pi\mu d_p} = \frac{(1.38 \times 10^{-16})(296)}{(3\pi)(0.936 \times 10^{-2})(0.15 \times 10^{-4})}$$

$$= 3.1 \times 10^{-8} \text{ cm.}^2/\text{sec.} \qquad (68),$$

and therefore for the experimental system,

$$\frac{\rho d_f U}{\mu} = \frac{(1)(1.7 \times 10^{-3})(1)}{(0.936 \times 10^{-2})} = 0.18$$

and

$$\frac{D}{d_f U} = \frac{(3.1 \times 10^{-8})}{(1.7 \times 10^{-3})(1)} = 1.8 \times 10^{-5}.$$

Both number are within the known limits for a similar system of titanium dioxide and nylon fibers (Appendix I).

Accepting the correlation (67), its coefficient is calculated to be

$$\alpha = \frac{E}{(\frac{D}{d_f U})^{2/3}} = \frac{(3.3 \times 10^{-3})}{(1.8 \times 10^{-5})^{2/3}} = 4.8 .$$

It is interesting to compare the value 4.8 obtained from this work with the value 11 from the cited system, which is about two times larger. Quite obviously, the retention coefficient includes all factors other than those represented by the diffusion number. The major factors would be those which govern adhesion of particles to fibers, the porosity factor being a minor one. The ionic conditions which balance the dispersion and the retention of particles in the two systems are compared as follows:

	Temp., °C.	pH	$CaCl_2$ Concn., g.-moles/cc.	α
TiO_2-dacron	23	3.5	2×10^{-5}	4.8
TiO_2-nylon	25	4	5×10^{-6}	11

It has been mentioned before that calcium, sodium, and hydrogen chlorides were added to the suspension, singly or in combination, to increase particle retention. The behavior of these ionic compounds has been found to be quite similar in a manner that retention remains unchanged at very low ionic concentrations, rises rapidly above a certain concentration, and levels off again after a very narrow critical concentration range. Polyvalent ions are generally more effective than monovalent ions. Comparing the two systems, it is seen that the titanium dioxide-dacron system of this work exhibits much lower retention at much

higher ionic concentrations than the titanium dioxide-nylon system. Apparently, the effects of the same ionic compounds on different particle-fiber systems could vary considerably. In the light of the previous crude discussion of adhesion, the single dominant factor would seem to be the surface nature and treatment of the particles and fibers. This important aspect of the retention process is beyond the scope of this project, and should be studied elsewhere.

In view of the importance of ionic conditions in retention, a part of the discrepancy between the results of permeation and filtration for the present system could also be accounted for by slight variations in ionic concentrations if they happened to be in the critical range. At present, we reiterate that the discrepancy would be attributed rather to the cumulative, uncontrolled experimental errors, whatever they may be.

The retention experiments with fines in incompressible mats of dacron fibers were conducted primarily to test whether the fines as prepared would behave in a manner similar to the titanium dioxide particles. Unlike titanium dioxide particles, fines of wood fibers are not hydrophobic, and the colloidal conditions which govern their dispersion and adhesion are not well known. An initial experiment with dyed fines suspended in distilled water indicated very slight retention in a dacron fiber mat. When similar ionic conditions were introduced to the suspension as in the case of titanium dioxide retention was much improved, but, as mentioned before, the leaching of radioactivity was quite serious at low pH values. This leaching complication threw some doubt on the reliability of these runs.

However, the original data of Runs 3 and 4 plotted in Fig. 10 appear to be very similar to the previous titanium dioxide-dacron curves. Upon analyzing the data graphically as before, the results in Fig. 11 indicate again a linear

relationship in agreement with the retention equation. These two duplicate runs reveal somewhat different slopes which yield collection efficiencies of 1.59×10^{-4} and 1.79×10^{-4}, averaging 1.7×10^{-4}. This value for $\underline{E}$ must be lower than the actual value because of the loss of radioactivity. Furthermore, it appears that the rate of leaching is probably constant, independent of filtration time.

We may now conclude that the retention equation for an incompressible mat formed from a dilute suspension at constant rate is correct in substance, if not in every detail. This conclusion reflects the theoretical analysis to be on a sound basis and amenable to further generalization.

COMPRESSIBLE MATS

In the retention analysis for compressible mats under simplified conditions of slow filtration at constant rate with a dilute suspension, we were somewhat perturbed by the final solution being the same as the incompressible case. In this sense experimental verification of the analytical conclusion was of great interest and necessity.

The cumulative mass data of the first four runs (5-8) for the fines-sulfite system as plotted in Fig. 12-14 reveal apparent differences from those for the incompressible case. A part of the curve beginning at the septum ($\underline{w} = 0$) appears to be linear, and the linear part occupies different proportions of the curves for varied conditions. This anomalous appearance is obviously in disagreement with the foregoing conclusion of analysis.

When the relationship between $\underline{m}'$ and $\underline{w}$ is linear, it simply indicates $\underline{p}'$ to be constant, which also means a uniform particle distribution in the mat. This is possible only when the fibers have taken up all the free particles prior

to filtration, or the prevailing conditions are such that no net retention occurs during filtration.

The first situation may be created by imposing highly favorable colloidal and hydrodynamic conditions in the fiber-particle suspension such that almost all particles become bound to the fibers in the suspension. The test described below will demonstrate this point.

Tagged fines and fibers were dispersed in a 4-l. beaker, and the suspension was kept in intermittent agitation for 25 hr. in order to increase the chances of particle-fiber binding. A filtration run (9) was then made according to the usual procedure, and the radioactivities of the layers of the mat were measured. The results are recorded in Table X and shown in Fig. 15. The uniform particle distribution in the mat except in the neighborhood of the mat face is clearly demonstrated. In this run, $\underline{p_s}$ is practically zero.

An example of the second situation has been mentioned, concerning the crude experiment with dyed fines and dacron fibers dispersed in distilled water. After the filtration run few dyed particles were observed visually in the mat, indicating very little retention under the circumstances.

Runs 5-8 do not completely fit these extreme situations. By similar reasoning, however, there are other possible variations. One possibility is that the free particles in the suspension have become so attenuated, when they reach a certain depth of the mat, that further retention becomes negligible. In such a case there will still be a gradation of bound particles in the lower part of the mat. If the bound particle concentration in the suspension happens to be so high that the attenuation process near the end of filtration is effective only

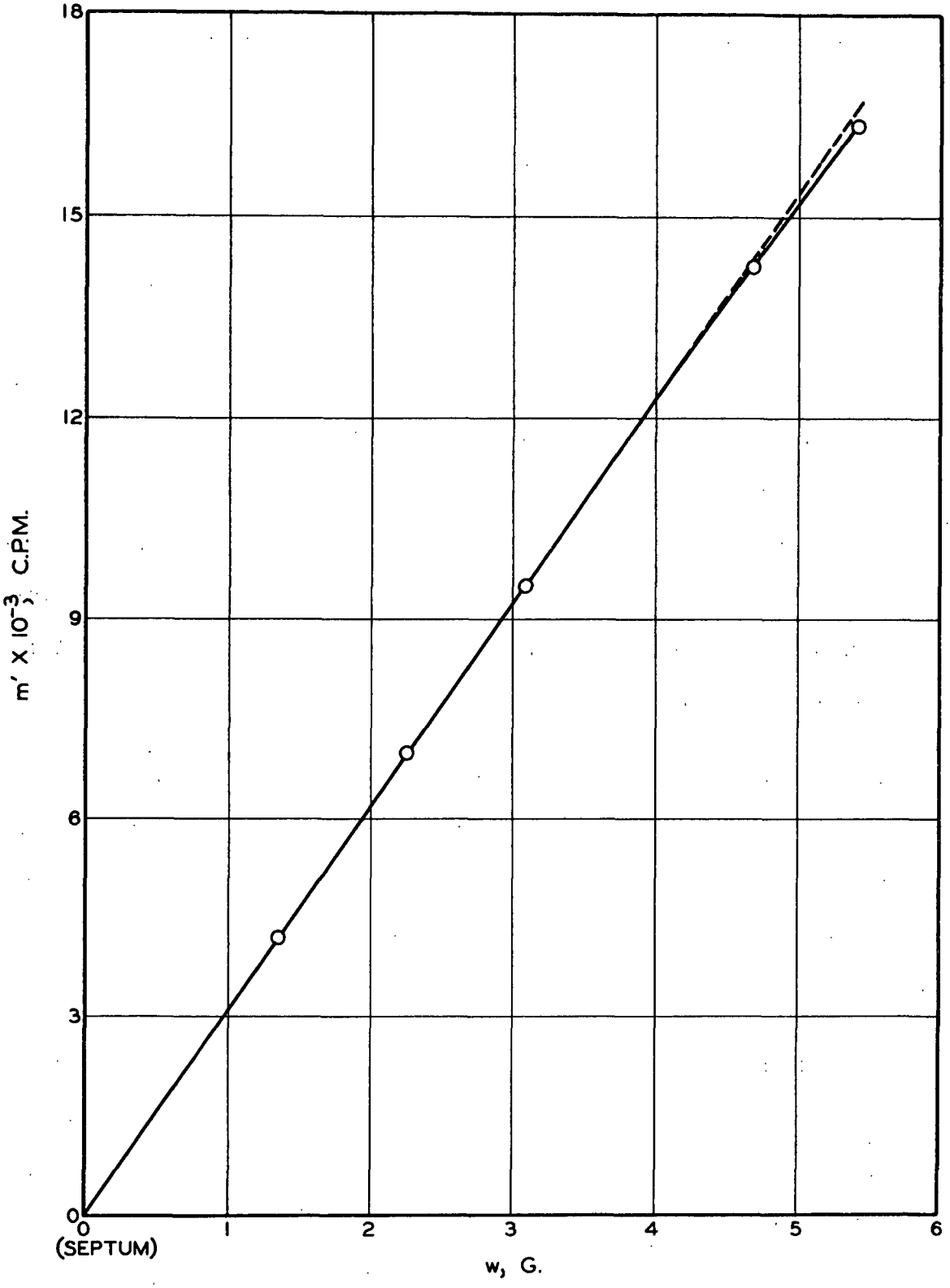

Figure 15. Filtration Data for the Fines-Sulfite System, Run 9

in the upper part of the mat, such a situation would explain the curved, but not the linear, part of the data.

A second variation of the same theme is concerned with the possibility of fibers in a mat becoming saturated with bound particles. By saturation is meant either in the static sense that no more particles can adhere to the fibers or in the dynamic sense that in the collision of particles with fibers assumed in the attenuation process, a state of equilibrium between adhesion and detachment is reached, resulting in no net retention. It is difficult to conceive the static condition which implies a complete coverage of the fibers or at least all the active sites of adhesion on the fibers. The alternative dynamic interpretation seems to be more tenable in that the forces operating at the sites of collision become more or less balanced so that particle adhesion is as likely as detachment under a given set of conditions.

In the light of the last-mentioned possibility the bottom layer at the septum would become saturated first, and the hypothetical phenomenon of saturation would spread gradually against the direction of flow. The saturated part of the mat would exhibit a uniform distribution of particles while the unsaturated part would show a distribution as predicted by the theoretical analysis.

To test this interpretation experimentally, it is necessary to reduce retention by modifying the ionic conditions and decreasing the mat weight, keeping the hydrodynamic conditions unchanged. Since retention is less favorable with monovalent than polyvalent ions, the subsequent runs (10-13) were carried out, using lower and lower concentrations of sodium chloride. Meanwhile, the radioactivity of the tagged fines was strengthened in order to measure retention with sufficient precision. These data have already been presented in Table X, and are further shown in Fig. 16 (Runs 10-11) and Fig. 17 (Runs 12-13). Permeation

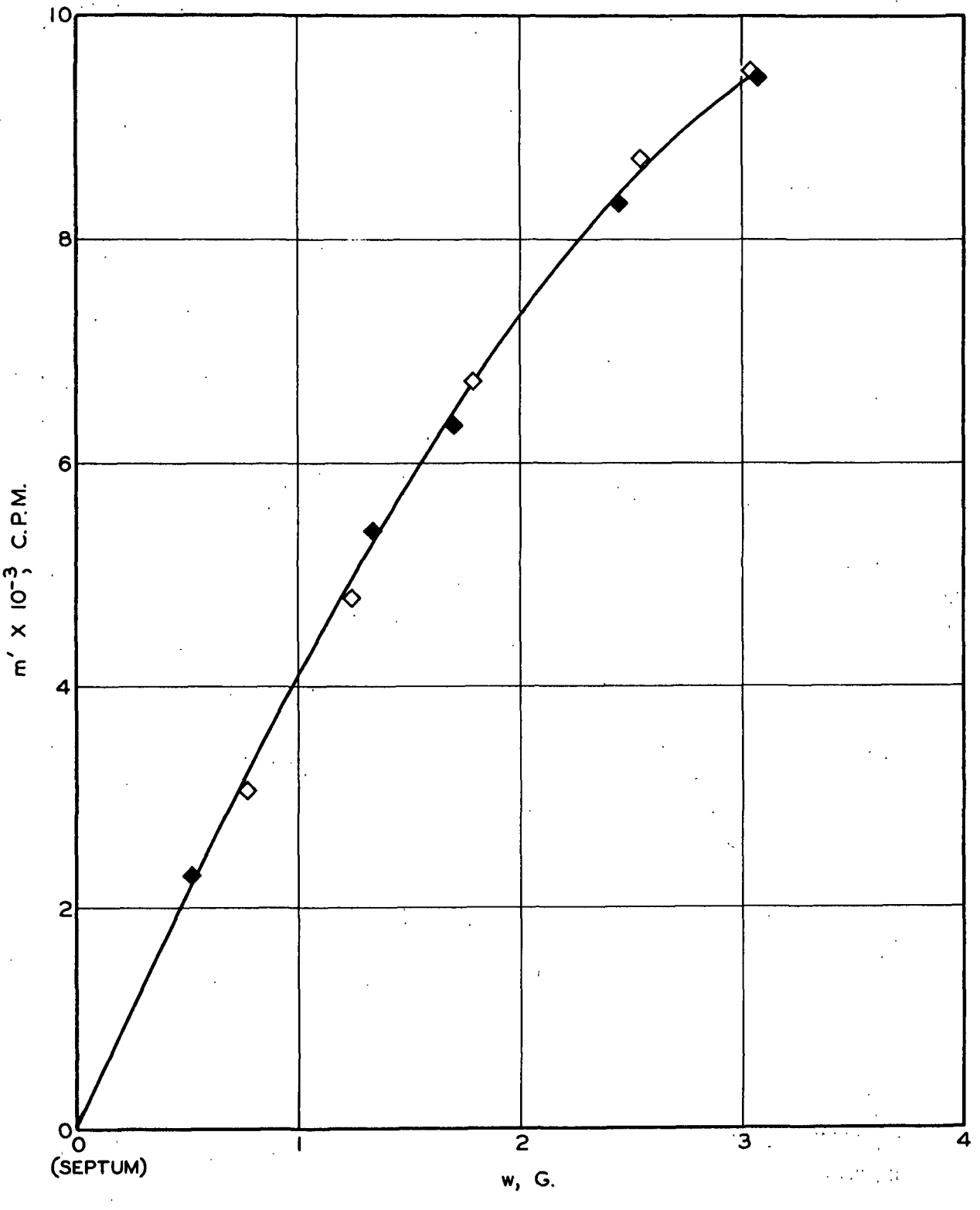

Figure 16. Filtration Data for the Fines-Sulfite System, Run 11 (Black Squares) and Run 10 (Squares)

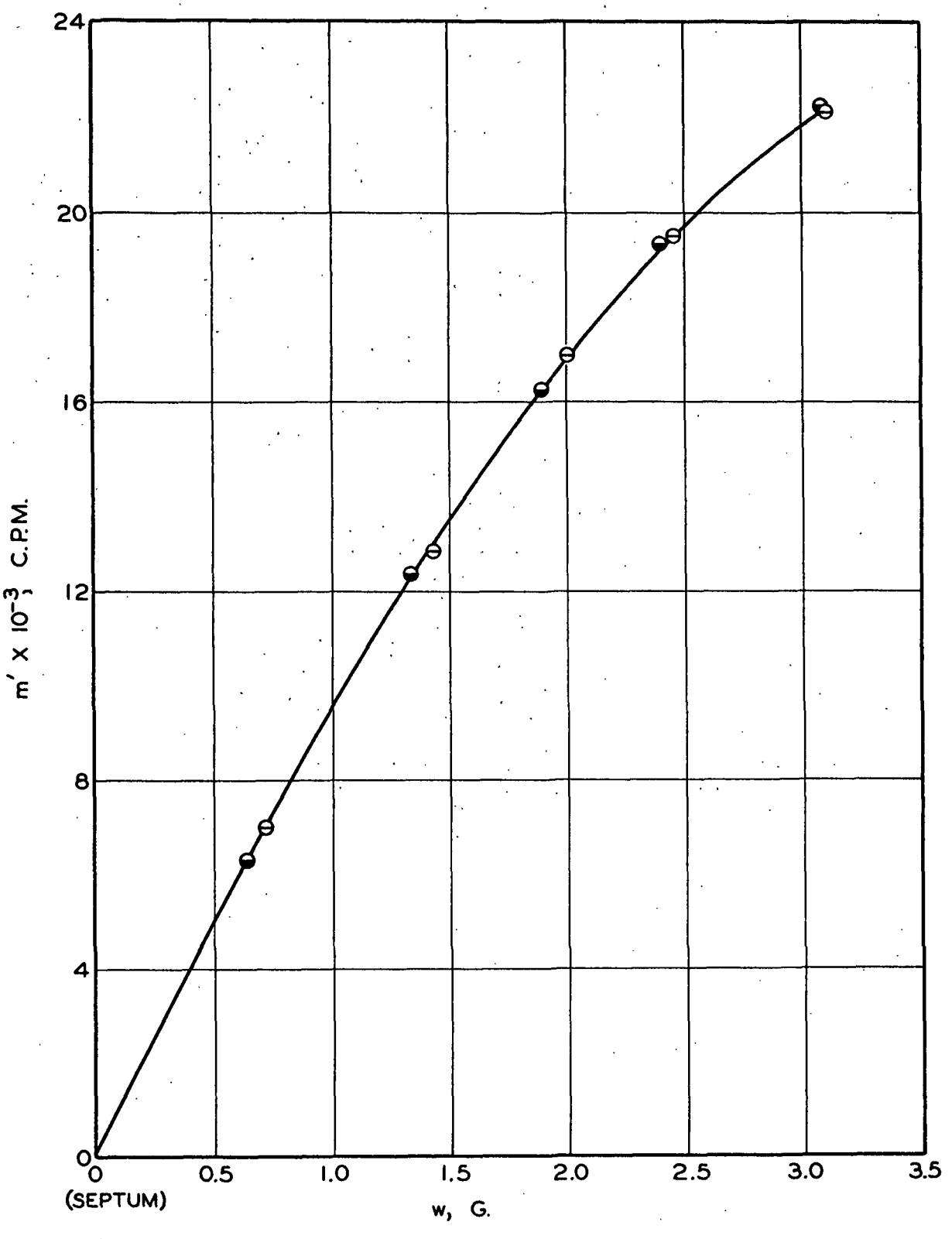

Figure 17. Filtration Data for the Fines-Sulfite System, Run 13 (Half Black Circles) and Run 12 (Circles)

experiments were also repeated under the same conditions of filtration and have been included in Table V.

The curves of Fig. 16 and 17. look more like those of incompressible cases, but still retain a minor part of the features of those previous ones (Runs 5-8). For the purpose of further analysis all runs are compared with the retention equation (62) applicable to wood fibers. This comparison is shown in Fig. 18. The three solid lines represent the equation at known average values of $\underline{E}$ from permeation experiments, Sets I, II, and III. The dashed curves are constructed from the smoothed data of duplicate Runs 7-8 corresponding to Set I, Runs 10-11 to Set II, and Runs 12-13 to Set III. The preliminary runs 5 and 6 were carried out without corresponding permeation experiments, and are therefore excluded from the graph. In this graph the deviations of the experimental results from the theory become vivid at once.

When the three sets of curves are compared, the graph shows clearly that as retention or collection efficiency decreases, the agreement becomes better. If the method of smoothing the data is permissible, it is also seen that each of the dashed curves consists of three regions starting from the mat face: a top region represented by the portion near the origin being linear and having the same slope as the solid line, an intermediate region being curved, and a bottom region being a horizontal line all the way to the septum. The upper curve (Set I) of the figure shows these three regions distinctly while those (Sets II and III) in the lower part conform more or less to the same pattern.

Examining these three sets of curves in more detail, one finds that the positions at which the dashed curves start to deviate from the solid lines as drawn in Fig. 18 are uncertain. If the experimental errors are set at 15% based

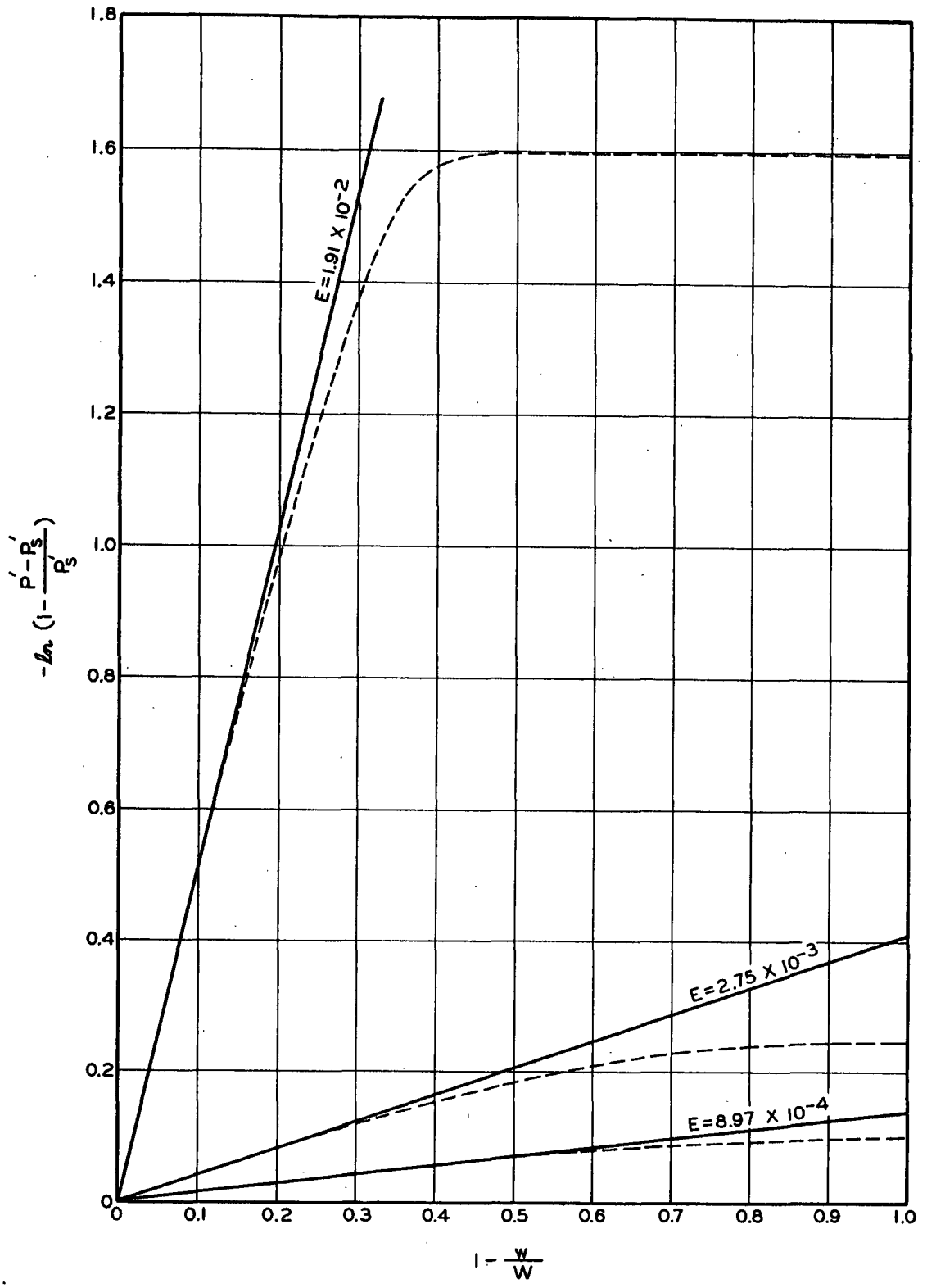

Figure 18. Comparison of Filtration Results with Theory, Runs 7 and 8 (Upper Curve), Runs 10 and 11 (Middle Curve), and Runs 12 and 13 (Lower Curve)

on the incompressible mats, the linear parts from the origin may be estimated to be roughly 30, 60, and 80% of the mats for Sets I, II, and III, respectively.

The intermediate region is more difficult to explain. The slope of the curve represents $\underline{K}'$, from which the collection efficiency, $\underline{E}$, may be evaluated. It is obvious that for each dashed curve $\underline{E}$ decreases continuously from the value derived from the permeation experiment until the last region is reached, in which the meaning of collection efficiency becomes vague. In conception, $\underline{E}$ represents the ratio of particles collected by the fibers to the total particles approaching the fibers. It could be either zero when the free particles are no longer collected by the fibers for whatever causes or indeterminate when there are no free particles left in the suspension to be collected. In the previous discussion we considered $\underline{E}$ in the flat region near the septum to be of the former meaning under the saturation hypothesis. This begets another question as to whether the fibers which are approaching the state of particle saturation alter their collection efficiency. Intuitively, the answer is affirmative. It seems likely for the fibers to change continuously from a finite value of collection efficiency when the bound particles are few, through a stage of decreasing collection efficiency when they are partially saturated, and finally to zero or negligible collection efficiency in the state of saturation. Such an interpretation would be in qualitative agreement with the existence of an intermediate range of retention, as depicted in Fig. 18.

If the hypothesis of saturation is valid, then the permeation experiments would show the same phenomena, as they were made under conditions identical to the filtration runs. The mat from permeation Run 1 of Set I was sectioned into six layers, and the fines content of each layer was measured in terms of its radioactivity. The data are shown in Table XI.

TABLE XI

RETENTION IN A PERMEATED MAT

(Run 1, Set I)

	w, g.	m', c.p.m.	p', c.p.m./g.
Mat face	0.918	4,396	5,760
	1.474	7,568	5,760
	2.303	11,727	3,100
	2.985	13,390	960
	3.956	13,575	220
Septum	5.088	13,749	38

The values of p' in the last column were obtained from smoothed data as explained before. The semilog plot of p' vs. w/W is shown in Fig. 19, which consists of a horizontal line and a sloping line joined together in an uncertain fashion represented by the dotted curve, corresponding, respectively, to the saturated, partially saturated, and unsaturated regions as hypothesized. The intermediate region, however, occupies only a small portion of the mat. This seems to indicate that for the particular experimental system, saturation could be attained rather quickly. But such a conjecture is somewhat at variance with the results of the corresponding filtration Runs 7 and 8 of Set I shown in Fig. 18. In permeation a constant stream of particles approaches the mat face while in filtration a diminishing number of particles reach the bottom of the mat as time proceeds. If the rate of approaching saturation is the same for both cases, then the state of saturation will spread in the mat under permeation farther than under filtration. This is not borne out by the smoothed data, the saturated region in permeation occupying about 40% of the mat as compared with 50% for filtration.

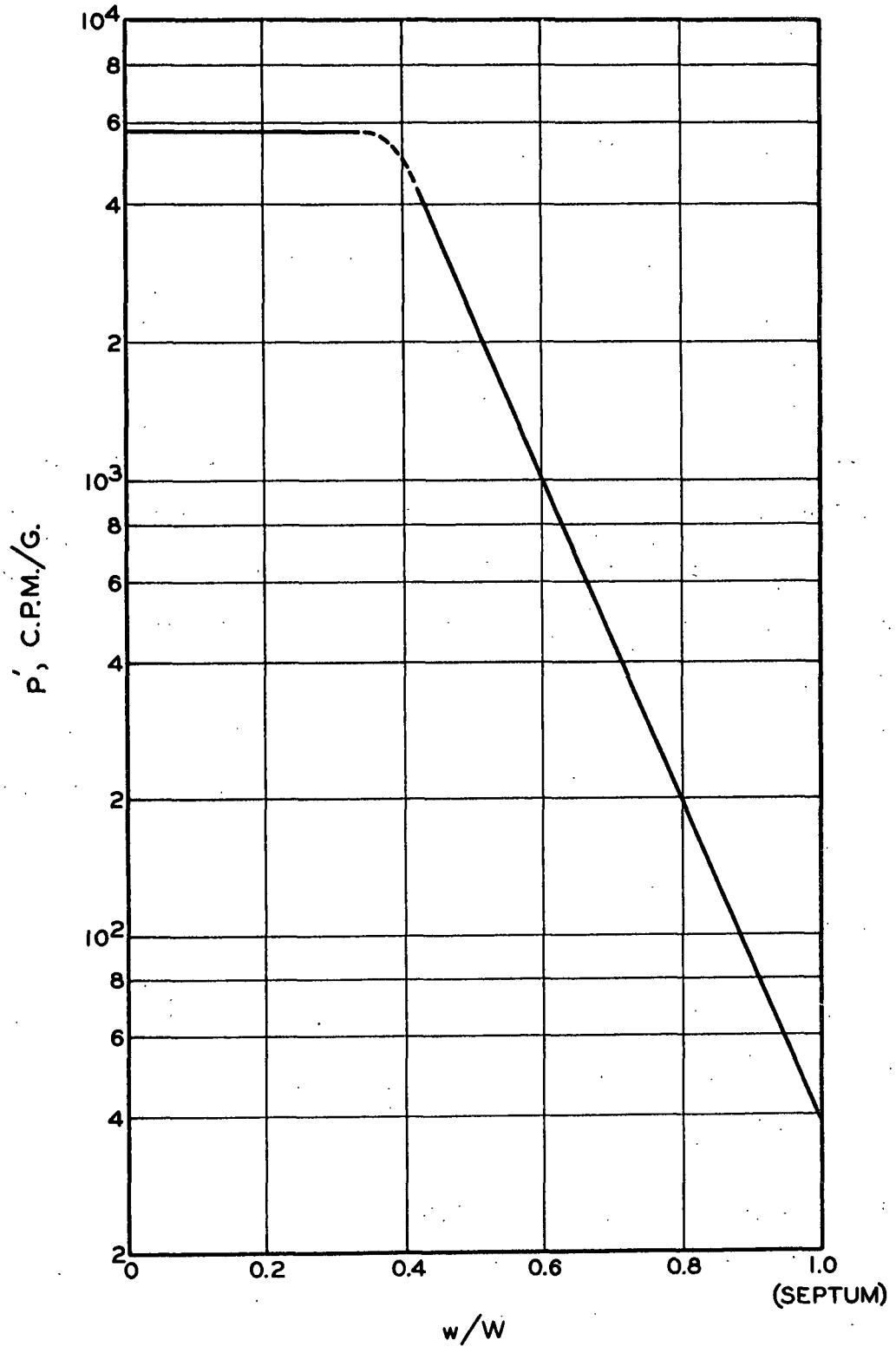

Figure 19. Retention in a Permeated Mat, Permeation Run 1

It should be mentioned with further reference to Fig. 19 that the correct collection efficiency is represented by the sloping part of the curve. The average collection efficiencies used in Fig. 18 were calculated with the ignorance of the possible existence of the saturated and partially saturated regions. Fortunately, the permeation and filtration experiments were carried out under closely identical conditions, and their comparison in Fig. 18 was justified so far as the qualitative aspects are concerned.

In conclusion, the divergence of the experimental evidence from the theoretical result for compressible mats can be explained by the hypothesis of fiber saturation with particles. To bring the theory and experiments into better agreement, either a more elaborate analysis is attempted or more simplified experimental conditions are constructed, or both. From the research viewpoint, the suggested line of attack is almost mandatory. On the other hand, an empirical exploration of the saturation hypothesis on the present foundation may yield more useful information, but possibly at the expense of a deeper insight into the problem of particle retention.

CONTINUING WORK

In the light of the results of investigation, certain avenues of further exploration may be suggested, the relative importance of which is dependent on different viewpoints and objectives.

1. Modified Experiments on Compressible Mats. The retention and distribution of fine particles in incompressible mats formed from a dilute fiber suspension at constant rate has been fairly well established, barring compensating factors yet undiscovered. The interpretation of the deviation of experimental data for compressible mats from the retention theory, which predicts the same

relationship as the incompressible case under the same conditions, is deemed plausible but inconclusive. The discovery of apparent fiber saturation, however, is of practical importance, and therefore needs to be confirmed.

Proceeing along the previous line of reasoning, the retention experiments should be extended to even lower collection efficiencies and thinner mats in order to make further check with theory. The splitting of a relatively thin mat into a large number of layers may be accomplished by the freezing device invented by Parker (3). The reduction of collection efficiency, however, may not be as easily achieved. Some orientation experiments on the colloidal conditions, such as ionic concentration and time of dispersion, will be called for to clarify their effects on retention although they are somewhat beyond the proposed objectives of the project.

2. Removal of Particles. If particles can be bound to fibers, they may also be removed. It is also possible for bound particles to migrate from one place to another by detachment and reattachment or by surface diffusion. To illustrate the possibility of particle removal, an experiment was performed as follows. A mat was formed as in the previous filtration runs for the fines-dacron system at about 1 cm. per second. The Geiger-Müller counter was mounted outside the filtration tube, directing toward the mat at an angle for the measurement of radioactivity. The remaining free suspension in the filtration tube was displaced with a solution of the same ionic concentration, which permeated through the formed mat at the same velocity. Meanwhile, the radioactivity was intermittently monitored. The results are shown in Table XII.

TABLE XII

FINES REMOVAL BY PERMEATION

Filtration--Suspension	
Dacron fiber concentration	6.84×10^{-5} g./cc.
Tagged fines concentration	4.71 c.p.m./cc.
NaCl concentration	1.02×10^{-5} g.-moles/cc.
pH	6.4
T	22°C.
U	0.987 cm./sec.
Permeation--Ionic Solution	
NaCl concentration	1.02×10^{-5} g.-moles/cc.
pH	6.4
T	22°C.
U	0.987 cm./sec.
Radioactivity	
Before displacement	63,795 c.p.m.
At 1/2 min.	55,543 c.p.m.
At 1 min.	48,630 c.p.m.
At 1-1/2 min.	46,614 c.p.m.
From 2-1/2 to 6 min.	44,720 c.p.m.
From 6-1/2 to 15 min.	43,111 c.p.m.

Obviously, the decrease in radioactivity in the filtration tube during permeation could be due to the removal of free or bound fines, or both. The volume of the suspension left in the tube after the mat had been formed was found to be 1970 cc. Assuming plug flow, this volume of suspension would require

44 sec. to be completely displaced by water. After that time, very little free fines would be left in the tube. Further permeation would remove only the bound fines. Assuming the bound fines to be roughly 55,000 c.p.m. at the end of displacement, then their removal would amount to about 22%.

However, the data also indicate that the rate of fines removal drops sharply in the first 2-1/2 min. and after that time slows down almost to a negligible extent, resembling again an exponential function. From this observation, it might be inferred that the particles bound to fibers have different degrees of adhesion. Their affinity is highest for the initial layer of particles directly attached to the fiber surfaces at the most active sites, and decreases as the layers build up or the sites of adhesion become weaker in a manner more or less similar to the adsorption of moisture on fibers. These are purely speculations, but have some bearing on the hypothesis of fiber saturation with particles and the possibility of particle migration, especially on the fiber surfaces.

The crude experiment just described may be considered as the reverse case of particle collection by a mat of bare fibers. It need not be construed to be a contradiction to the assumption of constant collection efficiency. For collection efficiency to remain constant, one only has to assume that a constant fraction of the free particles is collected upon collisions with fibers.

A refined continuous monitoring device during filtration or permeation together with the observation and measurement of particle distribution in the final mat will be very helpful in clarifying these dynamic phenomena concerned.

3. Effect of Fine Particles on Pressure Drop. It has been well established that fines in wood pulp greatly increase the resistance to flow because of their large specific surfaces. Fig. 20 illustrates this point clearly. The bottom curve shows the rise of pressure drop across the mat formed from the classified fibers for the subsequent permeation experiment (Run 1). The upper curve represents the corresponding filtration run (Run 7) with fines. At the final mat weight the pressure drop with fines is 1.2 times that without fines.

In order to study the quantitative effect of fines on drainage resistance, the state of agglomeration, the surface area of the fines, and their retention and distribution in the mat must be known. The present tagging technique, if refined and calibrated, will yield the information on the mass of fines retained. An appropriate description of fines attached to fibers, however, will be a formidable problem. Nevertheless, with the guidance of the filtration and retention theories, some useful information may be extracted from the data if they are judiciously carried out under varied conditions.

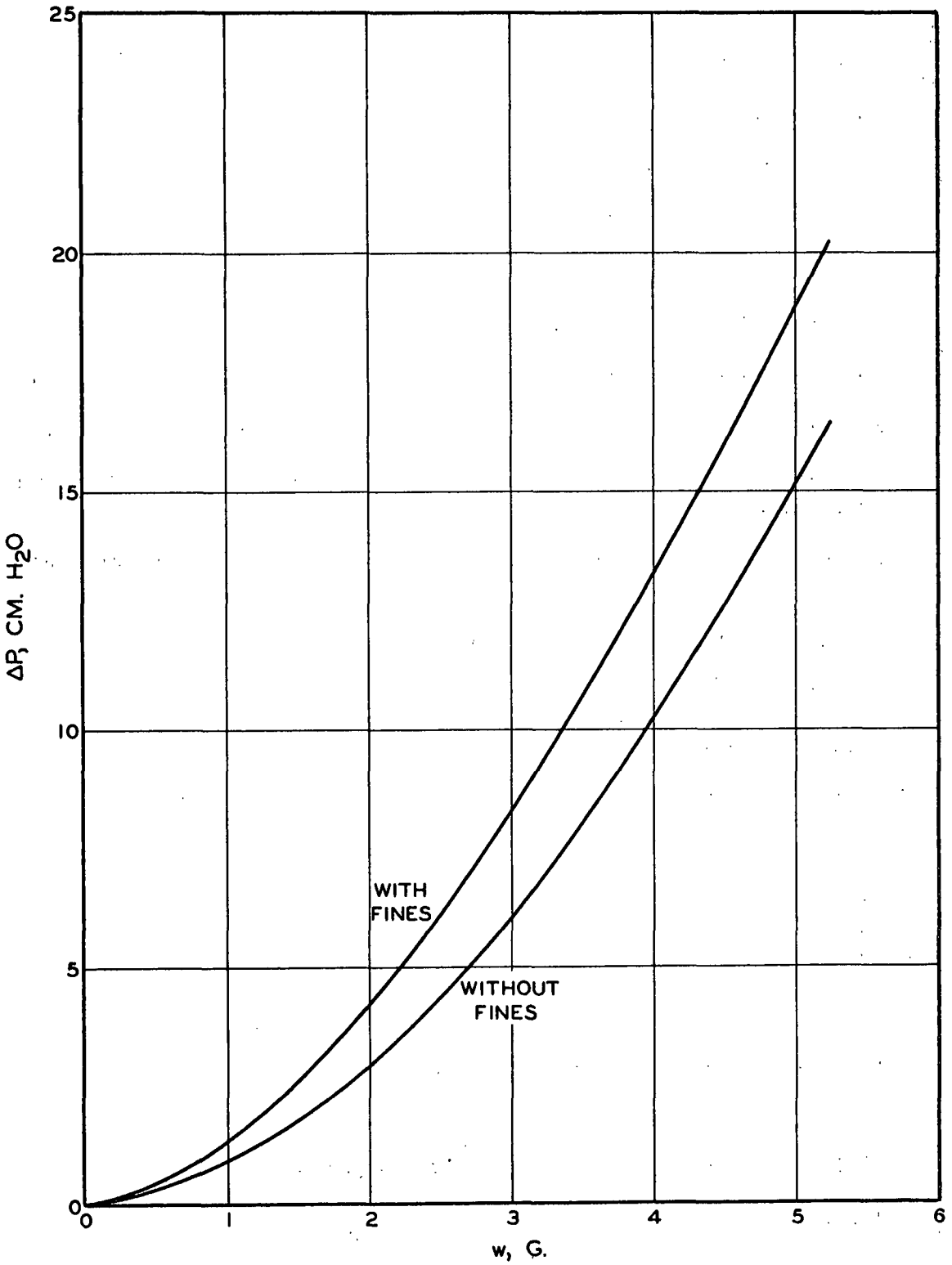

Figure 20. Comparison of Pressure Drops in Filtration

NOMENCLATURE

A = area of mat, sq. cm.

A_f = projected area of fibers, sq. cm.

a = width of screen openings, cm.

b = length of screen openings, cm.

C = free particle concentration, no. of particles/cc. of fluid

C' = bound particle concentration, no. of particles/cc. of fibers

C_L = free particle concentration downstream, no. of particles/cc. of fluid

C_o = free particle concentration upstream, no. of particles/cc. of fluid

C_s = free particle concentration in approaching suspension, no. of particles per cc. of fluid

C_s' = bound particle concentration in approaching suspension, no. of particles per cc. of fibers

D = diffusion coefficient, sq. cm./sec.

D_f = projected axis of fibers, cm.

d_f = diameter of cylindrical fibers, cm.

d_p = diameter of particles, cm.

E = collection efficiency, dimensionless

e = base of natural logarithm

exp = an exponential function of

f = a function of

K = attenuation coefficient, $cm.^{-1}$

K_D = Darcy's permeability coefficient, sq. cm.

K' = modified attenuation coefficient, dimensionless

k = Boltzmann's constant

L = thickness of mat, cm.

L_f = length of fibers, cm.

ln = natural logarithm

m_p = mass per particle, g.

m_s = mass of free particles in approaching suspension, g.

m' = mass of bound particles in a layer from the septum, g. or c.p.m.

m_n' = mass of bound particles in the nth layer, g.

m_s' = mass of bound particles in approaching suspension, g.

N_f = number of fibers per unit mat volume, 1/cc.

n_f = number of fibers per g. of dry fibers

P = pressure, dynes/sq. cm.

P_i = initial fiber retention probability, dimensionless

ΔP = pressure drop, dynes/sq. cm. or cm. H_2O

p = free particle-fiber ratio, g./g. or c.p.m./g.

p_s = free particle-fiber ratio in approaching suspension, g./g. or c.p.m./g.

p' = bound particle-fiber ratio, g./g. or c.p.m./g.

p_s' = bound particle-fiber ratio in approaching suspension, g./g. or c.p.m./g.

T = temperature, $^{o}C.$

t = time, sec.

t' = t

U = superficial velocity of fluid, cm./sec.

U_f = superficial velocity of fibers, cm./sec.

U_r = relative velocity of fluid and fibers, cm./sec.

V = velocity of mat growth, cm./sec.

V_f = volume of fibers, cc.

v = specific volume of swollen fibers, cc./g. of dry fibers

W = mass of dry fibers in a mat, g.

w = mass of dry fibers in a layer from the wire screen, g.

w_n = mass of dry fibers in the nth layer, g.

w' = $W - w$

$\underline{x}$ = distance from the origin, cm.

α = retention coefficient, dimensionless

α' = retention coefficient, dimensionless

ϵ = porosity of mat, cc./cc.

$\epsilon_{\underline{s}}$ = porosity of fiber suspension, cc./cc.

μ = viscosity of fluid, poises

ρ = density of fluid, g./cc.

$\rho_{\underline{f}}$ = density of solid fibers, g./cc.

ACKNOWLEDGMENT

The assistance of Miss Patricia Whitney in some of the experiments is gratefully acknowledged.

LITERATURE CITED

1. Draft chapter on Filtration, Project 2348.

2. Draft chapter on Retention, Project 2348.

3. Parker, J. D. Private communication.

THE INSTITUTE OF PAPER CHEMISTRY
Engineering and Technology Section

S. T. Han

S. T. Han

Nai L. Chang

N. L. Chang

APPENDIX I

COLLECTION OF SMALL PARTICLES BY FIBERS DUE TO DIFFUSION

INTRODUCTION

For small particles, let us assume perfect adhesion for the sake of simplicity. Their small sizes as compared with the diameters of the fibers diminish the chances of direct interception as they follow the motion of the fluid around the fibers. Provided their settling velocity is small in comparison with the fluid velocity, gravitational effects may be neglected. In the absence of electrostatic forces, the collection of small particles is controlled by diffusion (Brownian motion) at low fluid velocities and by inertial impaction (particle trajectory) at high velocities, if the flow is laminar. At still higher velocities turbulent or eddy diffusion becomes important. The difficulty in the study of collection lies in the separation of the different collecting mechanisms, flow patterns, and their interactions.

When the particles are very small, inertial impaction is inoperative even at relatively high fluid velocities. In this region diffusion controls collection. The longer the particles stay in the neighborhood of a fiber, the greater are the chances of their collision with the fiber due to Brownian motion. Particle collection by diffusion therefore increases with decreasing fluid velocities.

The mobility of particles in a fluid is characterized by diffusivity or diffusion coefficient. According to the kinetic theory of gases, diffusion coefficient increases with decreasing particle diameter and fluid viscosity, and with increasing temperature. The exact relation depends on the particle size relative to the mean free path of fluid molecules.

It is a well-known fact that diffusional collection is higher with fibers of smaller diameter. The reason for this is not easy to explain without going into a detailed discussion.

Retention in a fiber mat is complicated by the proximity of the fibers, which interfere with each other in relation to the flow pattern. Generally speaking, retention in the diffusion region is higher for a mat of fibers than that for isolated fibers. The effect of porosity, however, is complex.

COLLECTION EFFICIENCY

In the field of aerosol filtration, the term collection efficiency (1) was introduced early and has been widely accepted. It is based on the concept of fluid and particle dynamics applied to the ideal case of a single cylindrical fiber placed in a fluid stream moving in the direction perpendicular to the axis of the fiber. The collection efficiency of the fiber is defined as the ratio of the number of particles collected by the fiber to the total number of particles in the fluid stream approaching the fiber. If the concentration of particles is uniform at C_o and the fluid velocity is uniform at U_o, the total number of approaching particles per unit time which could possibly be intercepted by a cylinder of diameter d_f and length L_f is equal to $C_o U_o L_f d_f$, in which $L_f d_f$ is the projected area of the fiber. Since the fluid must spread around the fiber, only those particles passing through a cross-sectional area, $L_f b$, of the fluid stream per unit time will be captured by the fiber, where b is the width of the fluid stream far ahead of the fiber. Thus, in terms of flow geometry, the definition of collection efficiency becomes

$$E = \frac{C_o U_o L_f b}{C_o U_o L_f d_f} = \frac{b}{d_f} \qquad (A\text{-}1).$$

The collection efficiency of a fiber can be predicted theoretically for the simple case of "creeping" or very slow laminar flow around an infinitely long cylinder.

The concept of collection efficiency has been extended to the fibers in a mat. Let a fluid suspension of particles flow through a mat of fibers at a constant approach velocity U. Some particles will always penetrate the mat. The ratio of particles which pass through the mat to the total particles approaching the mat is called penetration, P. The fraction retained by the mat is obviously $1 - P$. If both upstream and downstream concentrations of particles are macroscopically uniform over the area of the mat, by the above definition,

$$P = \frac{C_L}{C_o} \qquad (A\text{-}2).$$

If the fiber mat of area A and thickness L is uniform, its porosity or void fraction is simply

$$\epsilon = 1 - \frac{W}{AL\rho_f} \qquad (A\text{-}3),$$

where W/A, in papermaking terminology, is the basis weight of the mat, and ρ_f is the density of the fibers. The solid fraction is $1 - \epsilon$.

If a unit volume of the mat is composed of N_f cylindrical fibers of diameter d_f and length L_f, the solid fraction is $\pi d_f^2 L_f N_f / 4$, or the total fiber length per unit mat volume is

$$N_f L_f = \frac{4(1 - \epsilon)}{\pi d_f^2} \qquad (A\text{-}4).$$

Across an infinitesimal layer of the mat, the particle concentration of the fluid stream is reduced from C by $-dC$. The volume of this infinitesimal layer is Adx, in which the total fiber length is $N_f L_f A dx$ and the total projected area in the direction of flow is $N_f L_f d_f A dx$. If we assume the fibers in the mat to behave similarly as an isolated fiber with a collection efficiency E, then the number of particles collected by the fibers in the differential layer would be $CUEN_f L_f d_f A dx$, according to the definition of the collection efficiency of a single fiber. The total number of particles approaching this layer is CUA. The ratio of the particles collected by the fibers to the total approaching particles must obviously be the same as the fraction of particles removed by the differential layer, or

$$-\frac{dC}{C} = \frac{CUEN_f L_f d_f A dx}{CUA}$$

$$= E \frac{4(1 - \epsilon)dx}{\pi d_f} \qquad \text{(A-5)}.$$

For a mat of constant porosity, if the collection efficiency remains constant throughout the thickness of the mat, this differential equation is integrated to yield an over-all relationship for penetration:

$$-\ln \frac{C_L}{C_o} = E \frac{4(1 - \epsilon)L}{\pi d_f} \qquad \text{(A-6)},$$

or

$$P = \frac{C_L}{C_o} = \exp[-E \frac{4(1 - \epsilon)L}{\pi d_f} \qquad \text{(A-7)},$$

where C_o and C_L are, respectively, the upstream and downstream particle concentrations. This equation, introduced by a number of workers in the field, is useful in comparing penetration or retention in similar mats of different thicknesses.

DIMENSIONAL ANALYSIS

The measurable variables to be considered in the retention of small particles by uniform fiber mats may be classified as follows:

Penetration	P, or collection efficiency E
Particles	d_p, ρ_p
Fluid	μ, ρ, U, Δp, T
Fiber	d_f, L_f, ρ_f
Mat	L, ϵ

If we choose collection efficiency as the dependent variable instead of penetration, the thickness of mat, L, is eliminated by Equation (A-6). In diffusional retention the density of particles, ρ_p, has very little effect. Introducing the diffusion coefficient D, we automatically include the full effects of particle diameter, d_p, and temperature, T, as well as the partial effect of fluid viscosity, μ. In laminar flow, the pressure drop, Δp, across the mat is directly proportional to the approach velocity, U, and the fluid density, ρ, has no effect on flow at all. The length of individual fibers, L_f, is unimportant in a closely packed mat. The density of fibers, ρ_f, has already been included in the porosity, ϵ, by its definition in Equation (A-3), and exerts no additional effect on retention.

For such a simple case we wish to investigate

$$E = f(D, \mu, U, d_f, \epsilon) \qquad (A\text{-}8).$$

Since E and ϵ are dimensionless quantities, the remaining four variables should form one or more dimensionless groups in order that the function sought will be dimensionally homogeneous. The fundamental dimensions involved in these variables are mass, length, and time. Upon inspection, the dimension of mass appears only in μ. Consequently, μ cannot enter into any dimensionless combination with other variables and must be eliminated.

Now we have five variables and two dimensions. According to Buckingham's theorem, there should be three dimensionless groups. Taking E and ϵ as two of them, the third group is $D/d_f U$, usually called the diffusion number. Thus, by dimensional analysis we conclude

$$E = f\left(\frac{D}{d_f U}, \epsilon\right) \qquad (A\text{-}9).$$

While the specific function must be theoretically developed or experimentally deduced, some elementary inference may be drawn from the yet undetermined dimensionless function. For instance, since the collection efficiency due to diffusion must increase with an increase in diffusivity of the particles, it must decrease with increasing velocities.

At higher fluid velocities we must take the fluid properties ρ and μ into account. This results in an additional dimensionless group, $\rho d_f U/\mu$, known as Reynolds number (Re_f), which describes crudely the flow pattern. We obtain

$$E = f\left(\frac{D}{d_f U}, \epsilon, \frac{\rho d_f U}{\mu}\right) \qquad \text{(A-10)}.$$

It is to be noted that the choice of dimensionless groups is arbitrary. Any combination of them will yield new groups of equal validity. For example, the combination of the reciprocals of the diffusion and Reynolds numbers yields

$$\left(\frac{d_f U}{D}\right)\left(\frac{\mu}{\rho d_f U}\right) = \frac{\mu}{\rho D} \qquad \text{(A-11)},$$

which group is called the Schmidt number (Sc).

For somewhat larger particles than are contemplated here, we should take the particle size into account and introduce a particle-fiber diameter ratio:

$$F = \frac{d_p}{d_f} \qquad \text{(A-12)}.$$

When inertial impaction is significant, another dimensionless parameter, called the impaction number, has been suggested as

$$I = \frac{(\rho_p - \rho) d_p^2 U}{18 \mu d_f} \qquad \text{(A-13)}.$$

Furthermore, if the gravitational effect is important, the settling parameter is usually defined as

$$S = \frac{(\rho_p - \rho) d_p^2 g}{18 \mu U} \qquad \text{(A-14)}.$$

Thus, a general correlation of particle retention in a fiber mat in the absence of electrostatic effects may be written as

$$E = f\left[\frac{D}{d_f U}, \epsilon, \frac{\rho d_f U}{\mu}, \frac{d_p}{d_f}, \frac{(\rho_p - \rho)d_p^2 U}{18\mu d_f}, \frac{(\rho_p - \rho)d_p^2 g}{18\mu U}\right] \qquad (A\text{-}15).$$

In the following discussion only the diffusion mechanism will be treated in detail.

DIFFUSION IN A CAPILLARY

The diffusion particles suspended in a fluid flowing through a capillary tube can be analyzed theoretically. Suppose a fluid suspension of uniform particle concentration C_o enters a tube of radius R in incompressible flow in the z-direction. Because of the collection of particles on the tube surfaces, the particle concentration C decreases along the z- and r-axes. This process of attenuation at a steady state may be represented by the following diffusion equation in cylindrical co-ordinates:

$$D\left(\frac{\partial^2 C}{\partial r^2} + \frac{1}{r}\frac{\partial C}{\partial r} + \frac{\partial^2 C}{\partial z^2}\right) - u\frac{\partial C}{\partial z} = 0 \qquad (A\text{-}16).$$

Neglecting the longitudinal diffusion term, $\partial^2 C/\partial z^2$, the equation is simplified to

$$D\frac{\partial^2 C}{\partial r^2} + \frac{D}{r}\frac{\partial C}{\partial r} - u\frac{\partial C}{\partial z} = 0 \qquad (A\text{-}17).$$

For laminar flow, the velocity distribution is parabolic:

$$u = u_o\left(1 - \frac{r^2}{R^2}\right) \qquad (A\text{-}18),$$

where u_o is the axial or maximum velocity. Substituting the laminar velocity function in the diffusion equation, we have

$$\frac{\partial^2 C}{\partial r^2} + \frac{1}{r}\frac{\partial C}{\partial r} - \frac{u_o}{D}\left[1 - \frac{r^2}{R^2}\right]\frac{\partial C}{\partial z} = 0 \qquad \text{(A-19)}.$$

The boundary conditions are:

$$\text{at } \underline{z} = 0, \ \underline{C} = \underline{C}_o,$$

and

$$\text{at } \underline{r} = \underline{R}, \ \underline{C} = 0.$$

The solution of the equation under these boundary conditions when $\underline{D}/\underline{R}\underline{u}_o << 1$ is:

$$\frac{\bar{C}}{C_o} = 0.8191e^{-7.314Z} + 0.097e^{-44.6Z} + 0.0325e^{-114Z} + \text{---} \qquad \text{(A-20)},$$

in which $\underline{Z} = \underline{z}D/\underline{R}^2\underline{u}_o$ and $\bar{C}$ is defined by

$$\bar{C} = \frac{\int_o^R Cu2\pi\, rdr}{\int_o^R u2\pi\, rdr} \qquad \text{(A-21)}.$$

Near the entrance region an approximation valid for small $\underline{Z}$ was given by Gormley and Kennedy (2) in the form of an asymptotic expansion:

$$\frac{\bar{C}}{C_o} = 1 - 4.07Z^{2/3} + 2.4Z + 0.446Z^{4/3} + \text{---} \qquad \text{(A-22)}.$$

DIFFUSION IN A FIBER MAT

If we could consider a fiber mat to consist of a number of parallel capillaries having length $\underline{z}$ equal to the mat thickness $\underline{L}$, then according to the first solution,

$$\frac{C_L}{C_o} \sim e^{(-D/R^2u_o)L} \qquad \text{(A-23)},$$

in which all other terms have been dropped.

Comparing with the penetration equation for a fiber mat,

$$\frac{C_L}{C_o} = \exp\left[-E\,\frac{4(1-\epsilon)L}{\pi d_f}\right] \qquad \text{(A-7)},$$

we would conclude that the collection efficiency $\underline{E}$ is proportional to the diffusion coefficient $\underline{D}$. This is in disagreement with the experimental evidence that $\underline{E}$ is nearly proportional to $\underline{D}^{2/3}$, which will be presented later.

It appears much more reasonable to conceive the porous structure of a fiber mat as a network of a very large number of interconnected capillaries of varying sizes and lengths. In such a model the attenuation process takes place only in the short capillaries between two interconnected points. Furthermore, at the intersections the mixing process takes place so that the approach concentration is uniform again before the next attenuation step. We assume that this process of alternating attenuation and mixing repeats itself many times as the fluid flows through the fiber mat.

For the attenuation step we apply the second solution of Gormley and Kennedy and further simplify it for an extremely short distance by dropping all the terms after the second. Thus,

$$\frac{\bar{C}}{C_o} = 1 - 4.07\left(\frac{zD}{R^2u_o}\right)^{2/3} \qquad \text{(A-24)},$$

or $$\frac{\Delta\bar{C}}{C_o} = \frac{\bar{C} - C_o}{C_o} = -4.07\left(\frac{zD}{R^2 u_o}\right)^{2/3} \qquad \text{(A-25)}.$$

If the process of attenuation is repeated always with the same very small segmental length, z_o, over a layer of mat thickness Δx, then the number of repeating times must be $\Delta x/z_o$. Since in each attenuation the approach concentration is C and the fraction attenuated is $\Delta C/C$, the total result in accordance with Equation (A-25) is

$$\frac{\Delta C}{C} = -4.07\left(\frac{z_o D}{R^2 u_o}\right)^{2/3} \frac{\Delta x}{z_o} \qquad \text{(A-26)}.$$

For an infinitesimal layer we may reduce Equation (A-26) to a differential form:

$$\frac{dC}{C} = -4.07\left(\frac{D}{R^2 u_o z_o^{1/2}}\right)^{2/3} dx \qquad \text{(A-27)}.$$

Integrating over the whole mat, we have

$$-\ln\frac{C_L}{C_o} = 4.07\left(\frac{D}{R^2 u_o z_o^{1/2}}\right)^{2/3} L \qquad \text{(A-28)}.$$

Upon comparison with the penetration equation, we find

$$E = \left[\frac{\pi d_f}{4(1 - \epsilon)}\right]\left[4.07\left(\frac{D}{R^2 u_o z_o^{1/2}}\right)^{2/3}\right] \qquad \text{(A-29)},$$

indicating that E is proportional to $D^{2/3}$ in the simple case of very slow flow.

POROUS PROPERTIES

The quantities $\underline{R}$, $\underline{u}_o$, and $\underline{z}_o$ may be examined in terms of the porous properties. In the simplest description of a mat composed of cylindrical fibers, only fiber diameter, $\underline{d}_f$, and porosity, ϵ, are needed. The axial velocity, $\underline{u}_o$, is approximately proportional to $\underline{U}/\epsilon$. On the dimensional ground we assume that the capillary radius, $\underline{R}$, and attenuation distance, $\underline{z}_o$, may be expressed in terms of $\underline{d}_f$ and a porosity function. Equation (A-29) may be thus transformed to

$$E = \alpha' f(\epsilon)\left(\frac{D}{d_f U}\right)^{2/3} \qquad \text{(A-30)},$$

in which all the proportionality factors are absorbed in the retention coefficient α'.

EXPERIMENTAL SUPPORT FOR THE DIFFUSION THEORY

Apparatus and Procedure

The thesis work of Johnson (3) on the removal of small particles from a liquid stream flowing through a fiber mat supplied the evidence for the diffusion theory just developed. Johnson's experimental study consisted of flowing a stream of water containing titanium dioxide particles through a fiber mat in a filtration apparatus and measuring the mass of particles retained in the mat. His apparatus and experimental system are shown in Fig. A-1 and A-2, respectively, which are self explanatory.

A commercial grade of titanium dioxide was dispersed in distilled water at a concentration of about 70% solids in a Waring Blendor with the aid of sodium hexametaphosphate and carbonate. The large agglomerates were removed by repeated

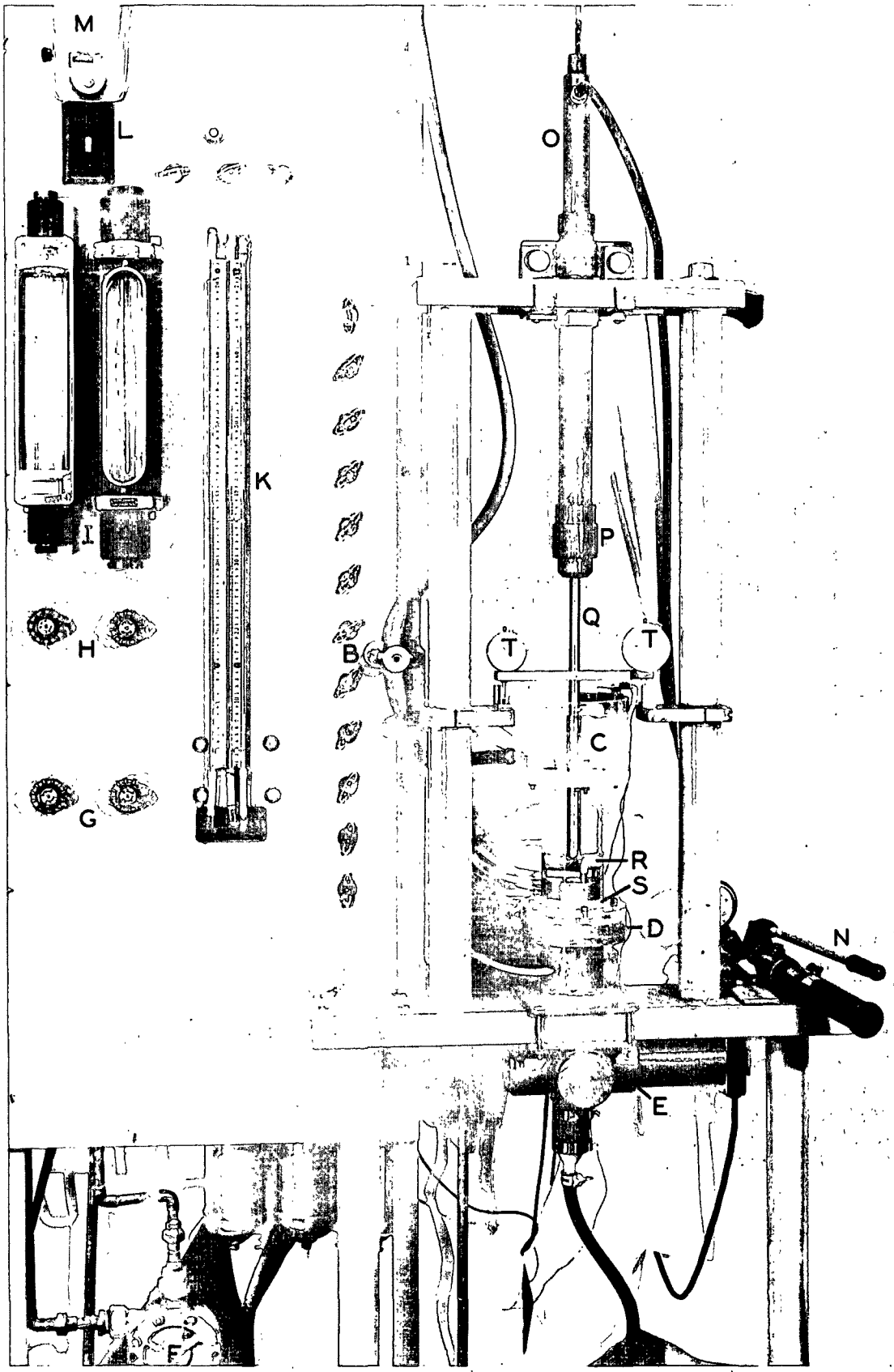

Figure A-1. Johnson's Filtration Apparatus

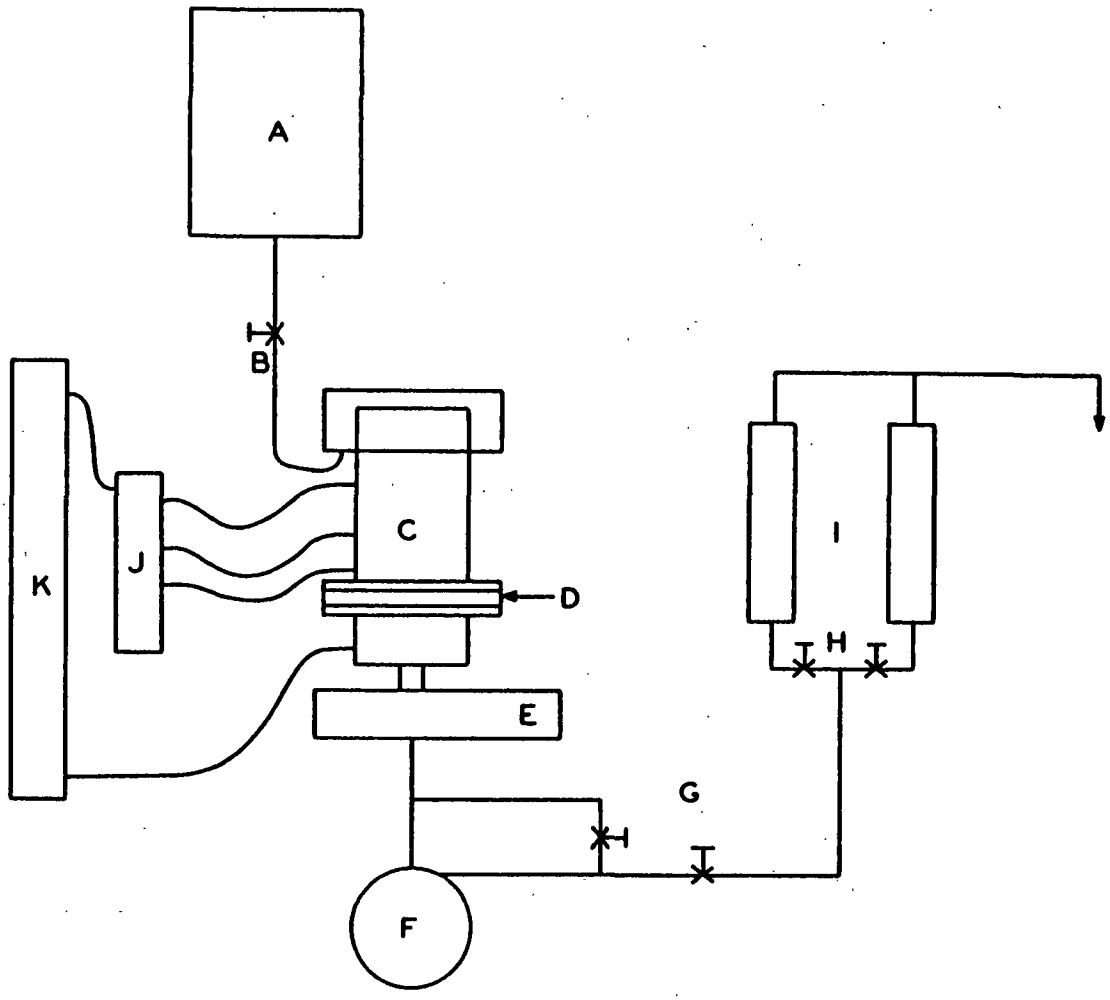

A STORAGE TANK
B INLET CONTROL VALVE
C FLOW TUBE
D SEPTUM
E LIGHT SCATTERING APPARATUS
F PUMP
G PUMP CONTROL VALVES
H ROTAMETER SELECTION VALVES
I ROTAMETERS
J MANOMETER MANIFOLD
K MANOMETER
L SWITCH
M ELECTRIC TIMER
N HYDRAULIC PUMP
O HYDRAULIC RAM
P JACOBS CHUCK
Q PISTON ROD
R PISTON
S MAT
T DIAL MICROMETERS

Figure A-2. Johnson's Experimental System

dilution and settling. The dispersed slurry was kept in a rotating jar to prevent further settling. This slurry was diluted with distilled water, acidified with hydrochloric acid to pH 4; a sufficient amount of calcium chloride was added to the suspension to establish a suitable colloidal condition for retention.

A mat was formed in the filtration apparatus from a dilute suspension of nylon fibers. The mat was kept at a uniform porosity under a permeable piston during the retention tests.

The dilute suspension of particles was drawn through the mat at a constant rate until a measurable amount of particles was retained in the mat. At the completion of the run the mat was removed from the apparatus and the retention of titanium dioxide was determined by a chemical analysis.

Particles

The particle size was originally measured on a slide under an optical microscope. The size range was stated to be from 0.2 to 2 microns, and the number average diameter was determined to be 0.96 micron. The electron micrograph of Fig. A-3 showed those particles having an over-all dimension of 1 micron to be agglomerates of a dozen or so smaller particles.

This elicited the question of whether or not the particle sizes Johnson observed under a microscope represented the actual state in his retention tests. It appeared that an independent method of particle size determination would be desirable to clarify this question. A sample of Johnson's original slurry kept in the rotating jar was recently analyzed by the centrifuge technique. The result indicated the number average diameter to be about 0.097 micron, which is about the size of the component particles observed by Johnson.

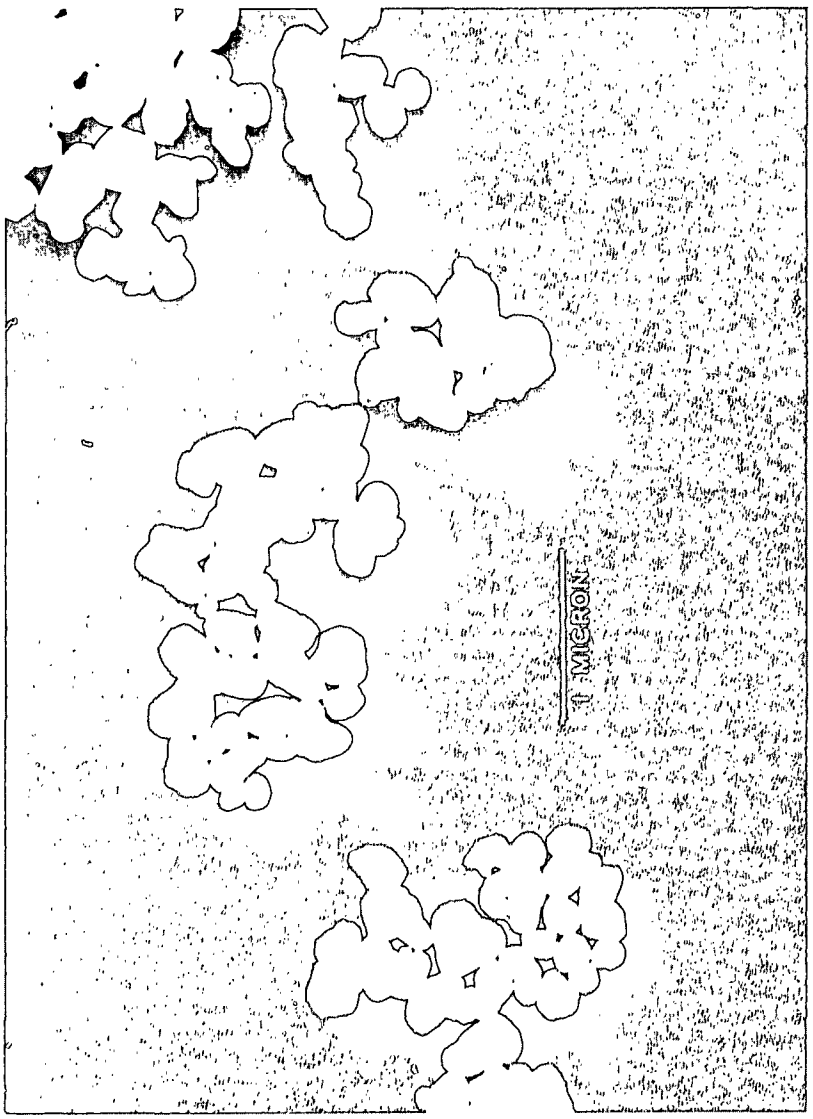

Figure A-3. Electron Micrograph of Titanium Dioxide Particles, Magnification 27,000X

The actual size distribution in suspension is dependent on dilution and dispersion, and therefore remains in doubt. In the light of the later discussion of the retention results, the small mean size appears to be more reasonably close to the true state than the large value. In this report the mean diameter is taken to be 0.1 micron.

The density of the titanium dioxide particles was estimated to be 4.3 g. per cc. The concentration of the dilute suspension was 1.085×10^{-5} by weight.

Fibers

Three sizes of nylon fibers were used. These fibers have very nearly circular cross sections which are rather uniform along their length. The density of the fibers in a water-swollen state is 1.14 g. per cc. The weighted average dimensions are given in Table A-I.

TABLE A-I

JOHNSON'S FIBER DIMENSIONS

Fiber Type	Denier	Average Diameter, microns	Average Length, in.
121	15	45.0	1/2
221	3	20.3	1/4
200	1.2	13.1	1/8

To form a mat in the filtration tube, the inside area of which was 45.3 sq. cm., 4.75 g. of fibers were used. The mat was compressed to a thickness of 0.61 cm., resulting in a porosity of 0.85.

Data

The retention results are expressed in penetration defined as the mass ratio of particles which have passed through a mat to the total particles approaching the mat.

$$P = \frac{C_L}{C_o} = \frac{W_L}{W_o} = \frac{W_o - W_r}{W_o} \qquad \text{(A-31)},$$

where the W's are the masses of the particles, with the subscripts o, L, and r denoting respectively upstream, downstream, and retained conditions.

Except for a few runs at porosities other than 0.85, the original data of Johnson are summarized in Table A-II as penetration (P) vs. approach velocity (U).

Particle Distribution in a Mat

The appearance of the deposits of titanium dioxide on fibers is shown in the photomicrographs of Fig. A-4. The nonuniform distribution of particles is rather striking. Some areas of the fibers have a coating many particles thick while some other areas are apparently bare. The bare areas, however, might not actually be void of particles, and could be covered with a layer of small particles not visible under the light microscope.

The patterns of the deposits in different layers of the mat are very similar, indicating that the retention process is a nearly random one. By this indication we would expect that the exponential distribution of particles in a mat previously discussed applies. Thus,

$$P = e^{-KL} \qquad \text{(A-32)},$$

TABLE A-II

RETENTION DATA OF JOHNSON (3)

Particle (TiO_2): $d_p = 10^{-5}$ cm., $\rho_p = 4.3$ g./cc.
Fluid (water): $\rho = 1$ g./cc.
Fiber (nylon): $\rho_f = 1.14$ g./cc.
Mat: $W = 4.75$ g., $A = 45.3$ sq. cm., $L = 0.61$ cm., $\epsilon = 0.85$

d_f, cm. x 10^3	U, cm./sec.	C_L/C_o	$d_f U/D$ x 10^{-4}	E, x 10^2	Re_f, $\rho d_f U/\mu$
$T = 25^oC.$, $\mu = 8.94 \times 10^{-3}$ poise, $D = 4.9 \times 10^{-8}$ sq. cm./sec.					
1.31	0.39	0.116	1.04	2.42	0.057
1.31	0.78	0.200	2.08	1.81	0.104
1.31	1.17	0.306	3.13	1.33	0.172
1.31	1.55	0.379	4.15	1.09	0.228
1.31	2.32	0.542	6.20	0.688	0.341
1.31	3.09	0.613	8.26	0.550	0.453
2.03	0.39	0.436	1.61	2.06	0.089
2.03	0.78	0.540	3.23	1.53	0.177
2.03	0.78	0.533	3.23	1.56	0.177
2.03	0.78	0.555	3.23	1.46	0.177
2.03	1.17	0.684	4.85	0.943	0.266
2.03	1.55	0.700	6.42	0.885	0.352
2.03	2.32	0.828	9.61	0.468	0.527
2.03	3.09	0.863	12.8	0.364	0.702
4.5	0.39	0.770	3.58	1.01	0.196
4.5	0.78	0.867	7.16	0.553	0.393
4.5	0.78	0.841	7.16	0.670	0.393
4.5	0.78	0.833	7.16	0.707	0.393
4.5	0.78	0.827	7.16	0.735	0.393
4.5	0.78	0.845	7.16	0.650	0.393
4.5	1.17	0.906	10.7	0.383	0.591
4.5	1.55	0.912	14.2	0.357	0.781
4.5	1.55	0.907	14.2	0.379	0.781
4.5	2.32	0.933	21.3	0.266	1.17
4.5	3.09	0.963	28.4	0.146	1.56
$T = 50^oC.$, $\mu = 5.49 \times 10^{-3}$ poise, $D = 8.6 \times 10^{-8}$ sq. cm./sec.					
1.31	1.55	0.268	2.36	1.48	0.371
4.5	0.78	0.768	4.08	1.02	0.639
4.5	1.55	0.857	8.11	0.595	1.27

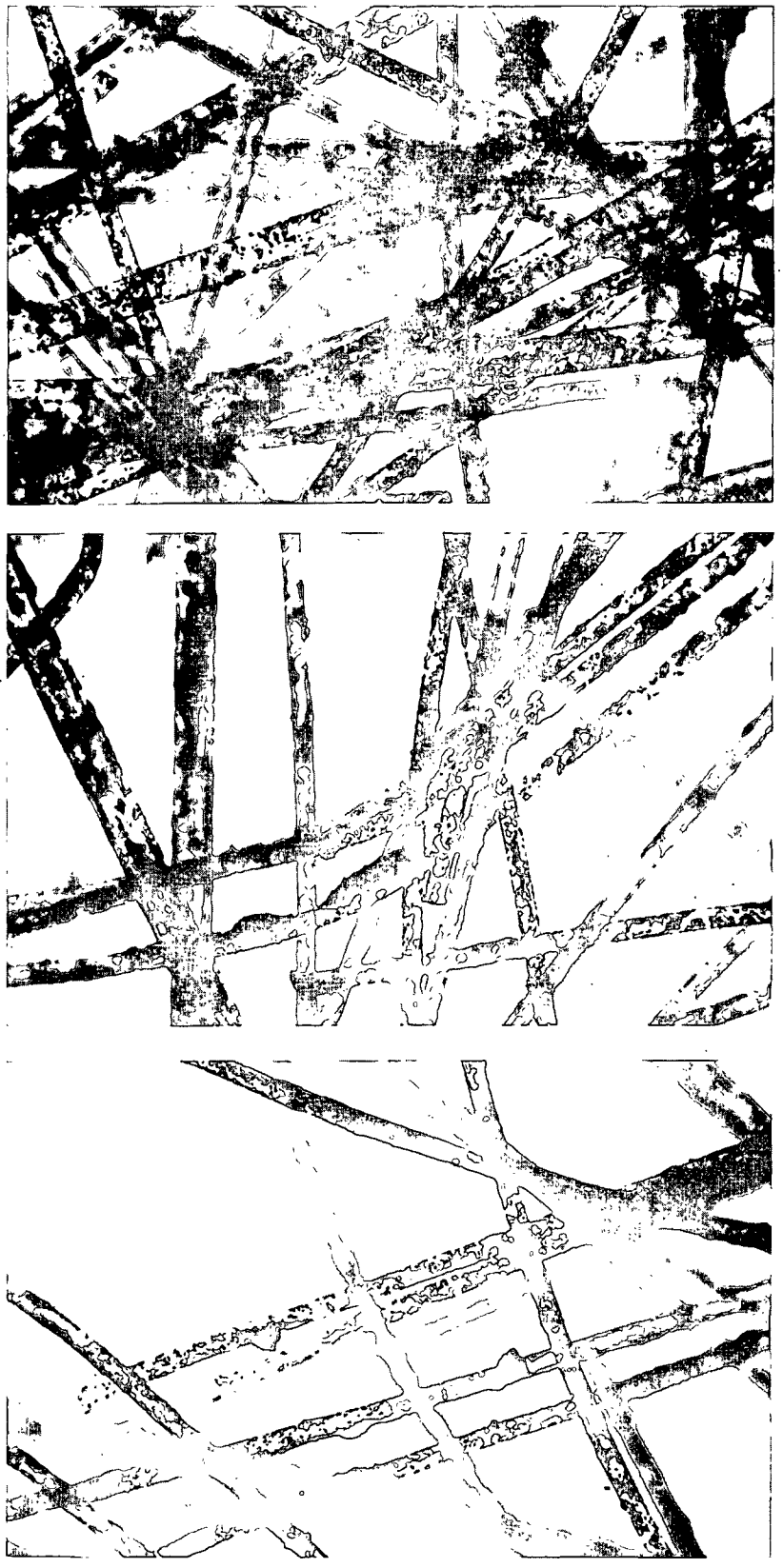

Bottom

Middle

Top

Figure A-4. Photomicrographs of Titanium Dioxide Deposits on Nylon Fibers in a Mat, Magnification 200X

or

$$-\log P \sim \frac{W}{A} \qquad \text{(A-33)}$$

where the basis weight, W/A, is directly proportional to the thickness, L, of the mat at uniform porosity.

Johnson sectioned the mat after the retention run and determined the amount of retention in each layer. In Fig. A-5, the negative common logarithm of penetration calculated from the cumulative retention in successive layers is plotted against the basis weight in accordance with Equation (A-33). It is seen that the assumed exponential distribution is in good agreement with the experimental data. We may conclude that the collection efficiency indeed remains constant from layer to layer in a mat of uniform porosity. Values of E are tabulated in Table A-II.

For collection efficiency to remain constant the approaching stream to each layer must have a random distribution of particles. This requirement necessitates a mixing process between layers. Since flow in the mats of Johnson's experiments is laminar ($Re_f < 1$), the question may be raised how a mixing process could take place. One explanation appears to be in the flow pattern around a cylinder. It has been shown by Tomotika and Soi (4) that even at Reynolds number (Re_f) as low as 0.05, eddies will be developed back of a cylinder. The backward movement of fluid into a pair of vortices in the wake of a cylinder constitutes a rather efficient mixing process. The interference of flow by the neighboring fibers in a mat would randomize this mixing pattern when eddies do exist. From another viewpoint a mat of fibers is considered to be a network of interconnected flow channels. At the intersections, mixing of flow could conceivably take place.

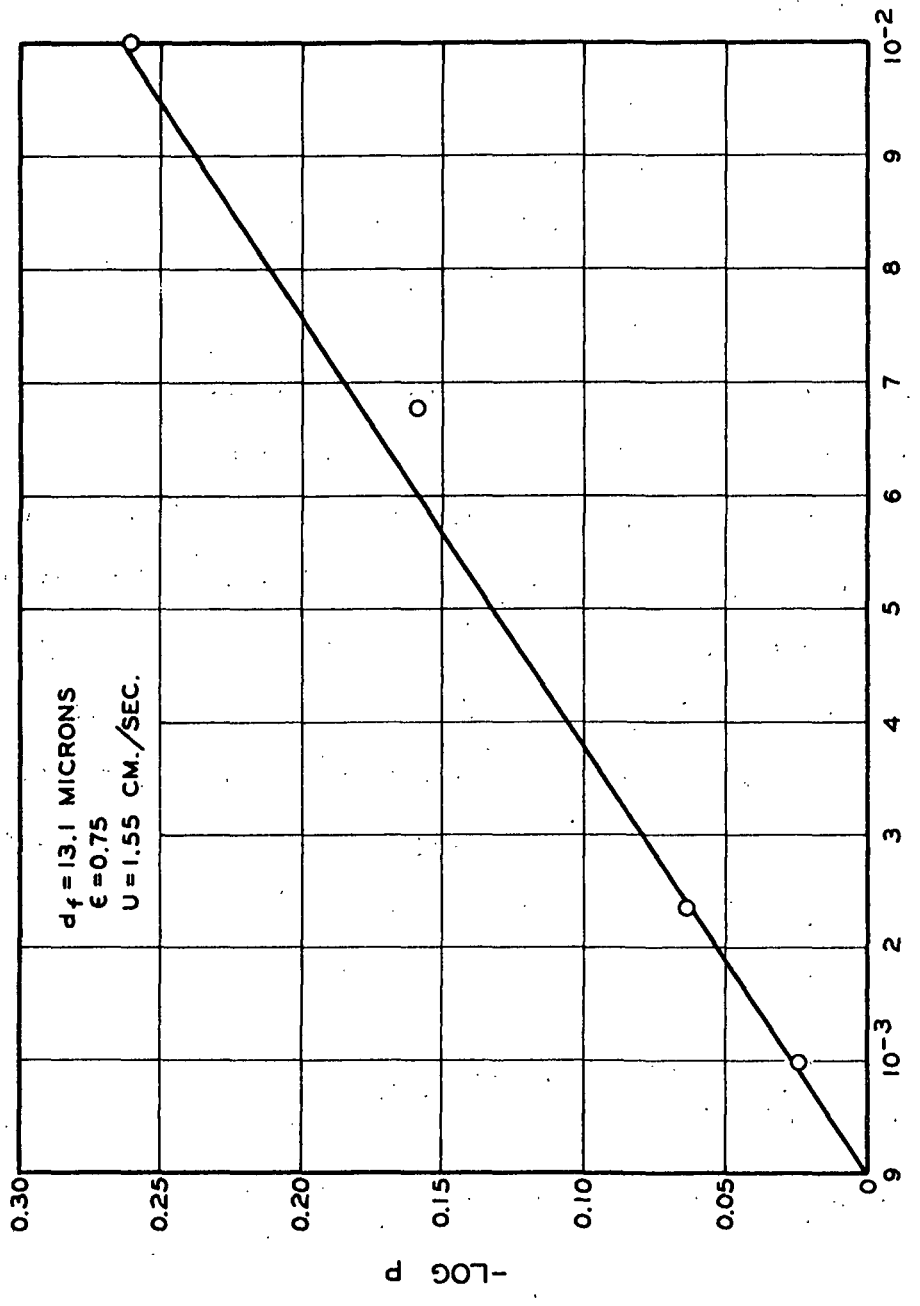

Figure A-5. Particle Distribution in a Mat

Diffusion Controlling

Johnson's experimental range may be summarized in terms of the pertinent dimensionless parameters:

$$\underline{Re}_f = 5 \times 10^{-2} - 1.5$$

$$\underline{F} = 2 \times 10^{-3} - 1 \times 10^{-2}$$

$$\underline{I} = 3 \times 10^{-7} - 6 \times 10^{-6}$$

$$\underline{S} = 6 \times 10^{-7} - 8 \times 10^{-6}$$

The majority of the runs were made at Reynolds numbers less than 1, indicating laminar flow in the mat. The small particle-fiber diameter ratio points to negligible retention due to direct interception. From the very small values of $\underline{I}$, inertial impaction may be considered absent. The critical impaction number has been suggested in the literature to be about 10^{-1}, below which impaction ceases to be effective. The small ratio of settling to approach velocities excludes the likelihood of significant retention by gravitational forces. All these considerations lead to the conclusion that diffusion is the controlling mechanism in Johnson's retention experiments, as far as the collision of particles with fibers is concerned.

The adhesion of particles to fibers or the cohesion of one particle to another is another matter. At first we were inclined to assumed that every collision results in the capture of a particle. In view of the extremely non-uniform deposition of particles on fibers such an assumption is doubtful. For the purpose of this analysis, however, we need only to assume that the factors governing adhesion and cohesion remain constant in all experiments. This is a reasonable assumption because the conditions controlling the colloidal behavior of the system were maintained constant throughout the experiment. Under the assumption we proceed to examine the hydrodynamic factors of retention.

Effect of Approach Velocity

Collection of small particles by diffusion increases with decreasing fluid velocity simply because the particles remain longer in the neighborhood of each fiber. According to the dimensional analysis, at constant T, ϵ, and d_f, E must be a unique function of U. Figure A-6 shows such a plot on logarithmic scales with d_f as the parameter.

It is apparent that the data can be represented quite well by three lines, except in the high velocity region. This indicates that a power function is suitable for correlation in a limited range. The slopes of these lines are nearly equal to -2/3, which value has some theoretical significance as previously discussed. If the few high-velocity data are emphasized, the lines would have a slope of about -4/5. We prefer the former value to the latter because the high-velocity data appear to be anomalous.

For diffusion of small particles in laminar flow over a single fiber, theoretical analyses by Langmuir (5) and Stairmand (6) indicate the dependence of E on -1/2 to -3/4th power of velocity. As the velocity is increased, inertial impaction sets in sooner or later. Since retention due to impaction increases with increasing velocity, the over-all collection efficiency due to both diffusion and impaction will exhibit a continuously decreasing slope in the region where diffusion still dominates. Johnson's high-velocity data indicate the opposite way, and consequently rule out impaction as a mechanism in his retention experiments. At present we have no adequate explanation for the anomalous behavior of his system at high velocities.

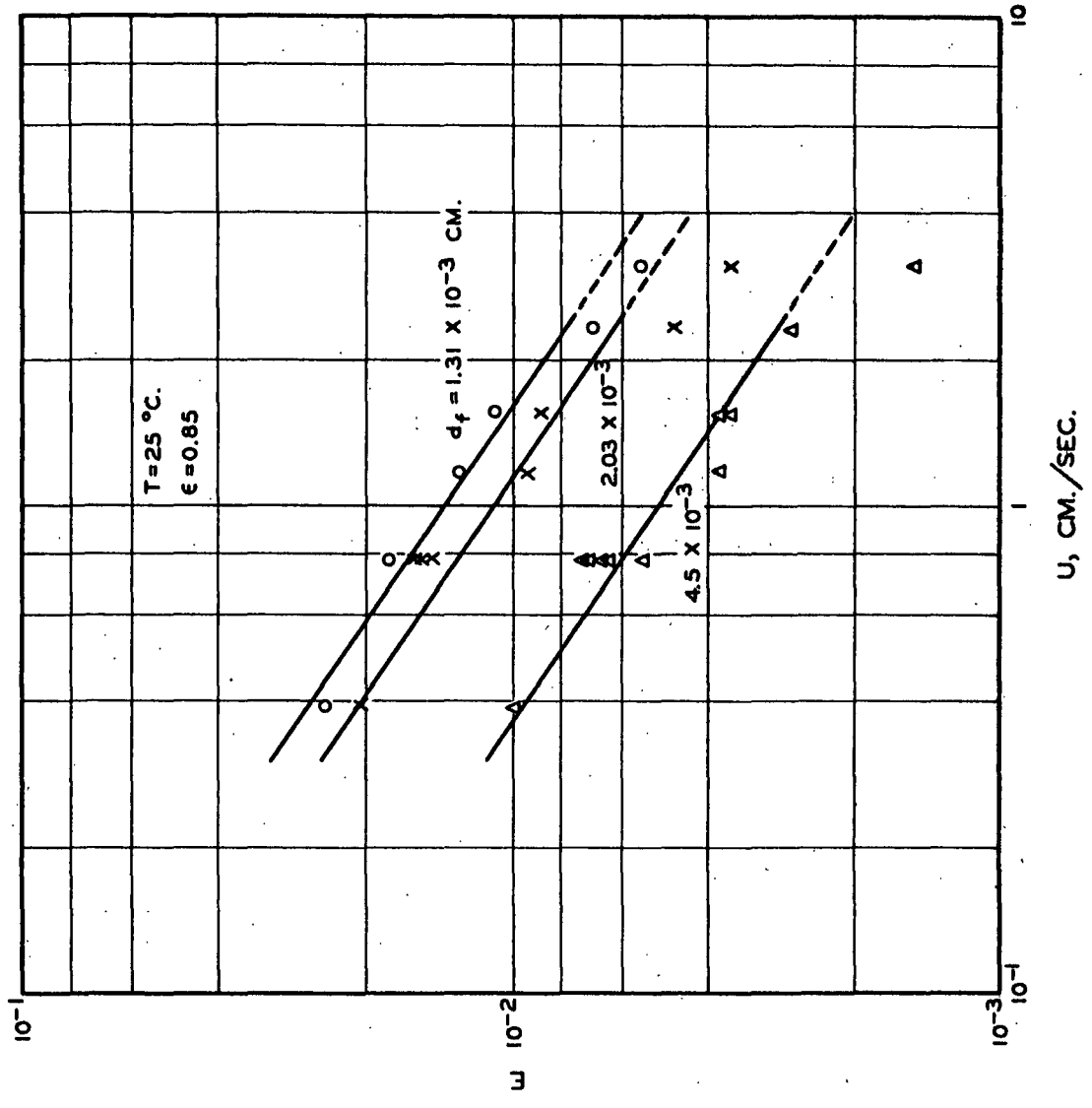

Figure A-6. Effect of Approach Velocity on Collection Efficiency

Influence of Fiber Diameter

It has been demonstrated early in the development of retention theories that retention should decrease with increasing fiber diameter. Figure A-6 shows clearly this effect.

If we assume that E is also a simple power function of d_f, then by the definition of E, we have

$$E = \frac{\pi d_f}{4(1 - \epsilon)L} (-\ln P) \sim U^{-2/3} d_f^{\,n} \qquad \text{(A-34)}.$$

At constant ϵ and L, $(-\ln P)U^{2/3}$ will be linear with d_f on a logarithmic plot, the slope of the line being $n-1$. The average values of $(-\ln P)U^{2/3}$ are plotted vs. d_f in Fig. A-7. If the line as shown could be justified by only three points, its slope may be evaluated to be $-5/3$, and n is therefore $-2/3$, same as the power of U.

At this point, recalling the indication of the dimensional analysis that E may be a function of Reynolds number for retention by diffusion, we may conclude that within the experimental range,

$$E \sim \left(\frac{\rho d_f U}{\mu}\right)^{-2/3} \qquad \text{(A-35)}.$$

This correlation is shown by the bottom line in Fig. A-8 for all data at 25°C. and 0.85 porosity.

Diffusivity

Retention by diffusion obviously increases with increasing diffusion coefficient. According to Einstein's original analysis of Brownian motion of

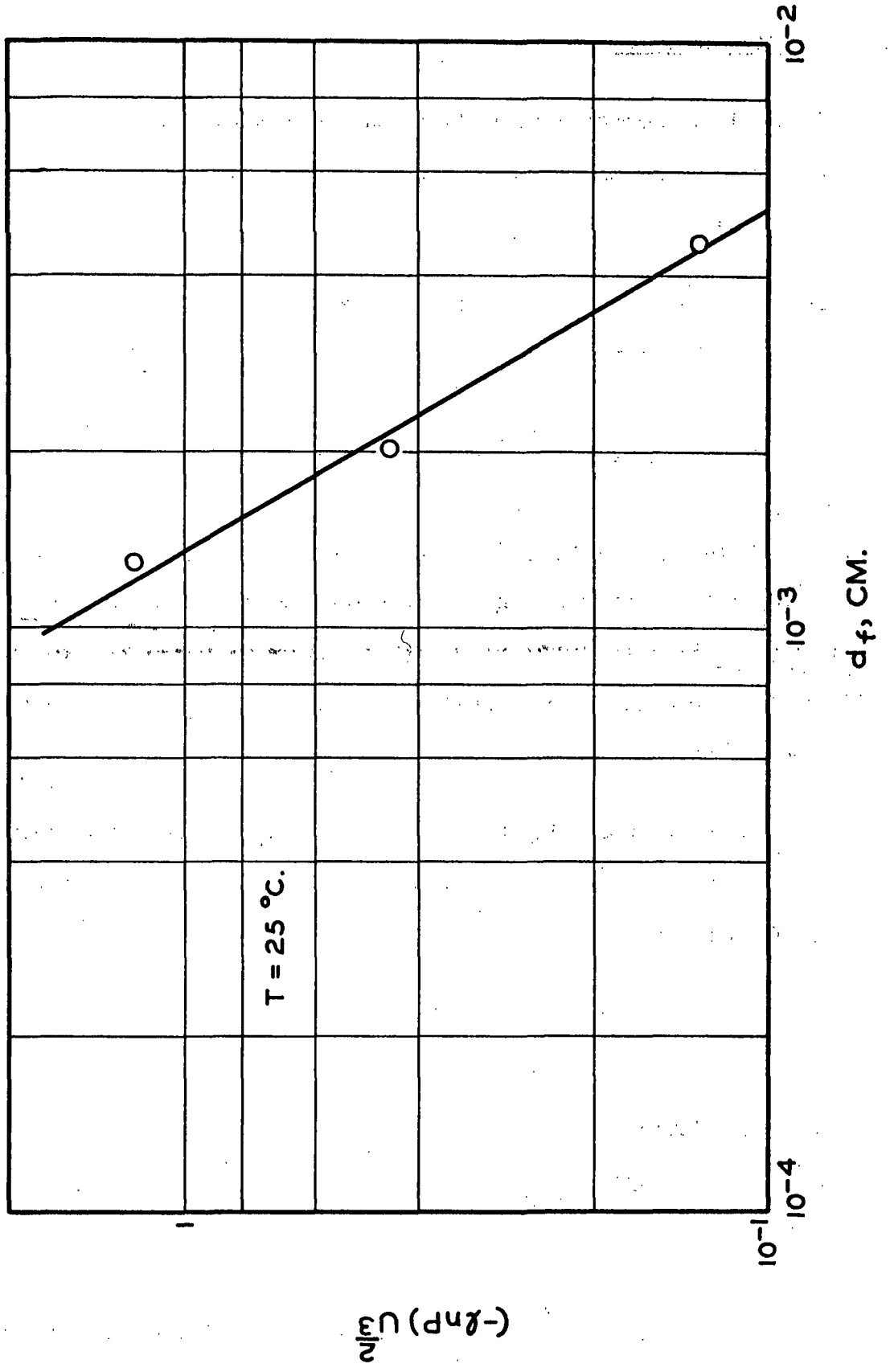

Figure A-7. Effect of Fiber Diameter on Retention

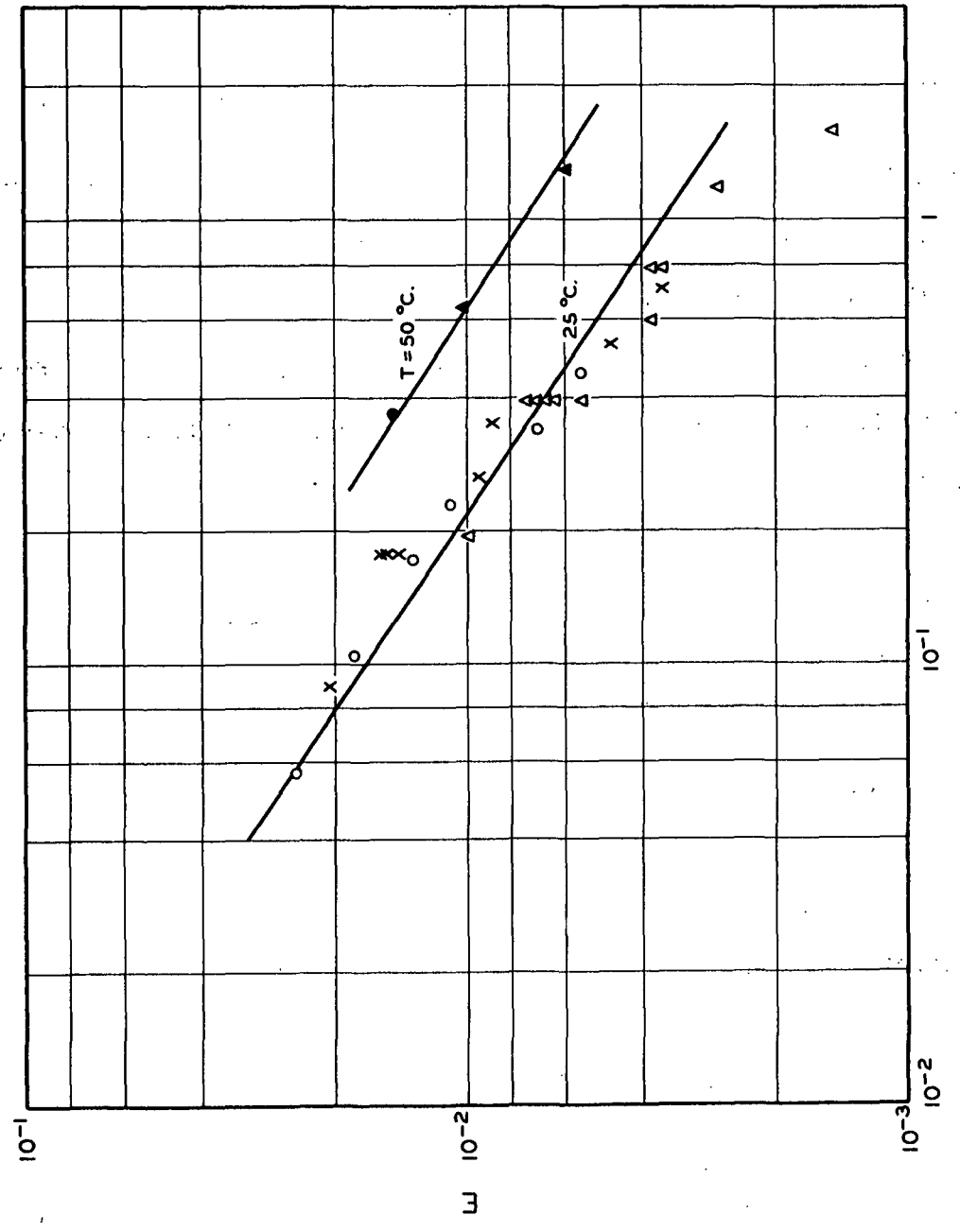

Figure A-8. Correlation of Collection Efficiency with Reynolds Number

suspended particles in a liquid (7), the diffusion coefficient of particles is related to the Stokes Law of viscous motion by

$$D = \frac{kT}{3\pi\mu d_p} \qquad \text{(A-36)},$$

where k is the Boltzmann constant (1.38×10^{-16} ergs per molecule per $^{\circ}$K.).

Johnson's retention experiments were carried out at two temperatures, 25 and 50°C. The high-temperature data consisting of only three runs are shown in Fig. A-8 as the upper line. In this plot of E vs. Re_f, the parameter separating the two parallel lines is the Schmidt number $(\mu/\rho D)$. It is found that E is directly proportional to the Schmidt number, again to the power of -2/3 as shown by the following evaluation:

T, °C.	$\mu/\rho D$, 10^{-5}	$(\mu/\rho D)^{-2/3}$, 10^{4}	E, at $Re_f = 1$, 10^{3}
25	1.83	3.0	3.6
50	0.65	6.2	7.4

Correlation

The functional relationship for Johnson's data at constant porosity is

$$E = \alpha \left(\frac{\rho d_f U}{\mu}\right)^{-2/3} \left(\frac{\mu}{\rho D}\right)^{-2/3}$$

$$= \alpha \left(\frac{D}{d_f U}\right)^{2/3} \qquad \text{(A-37)}.$$

This correlation, which is seen in Fig. A-9, is in agreement with the previous theoretical analysis for the simplest case of diffusional retention.

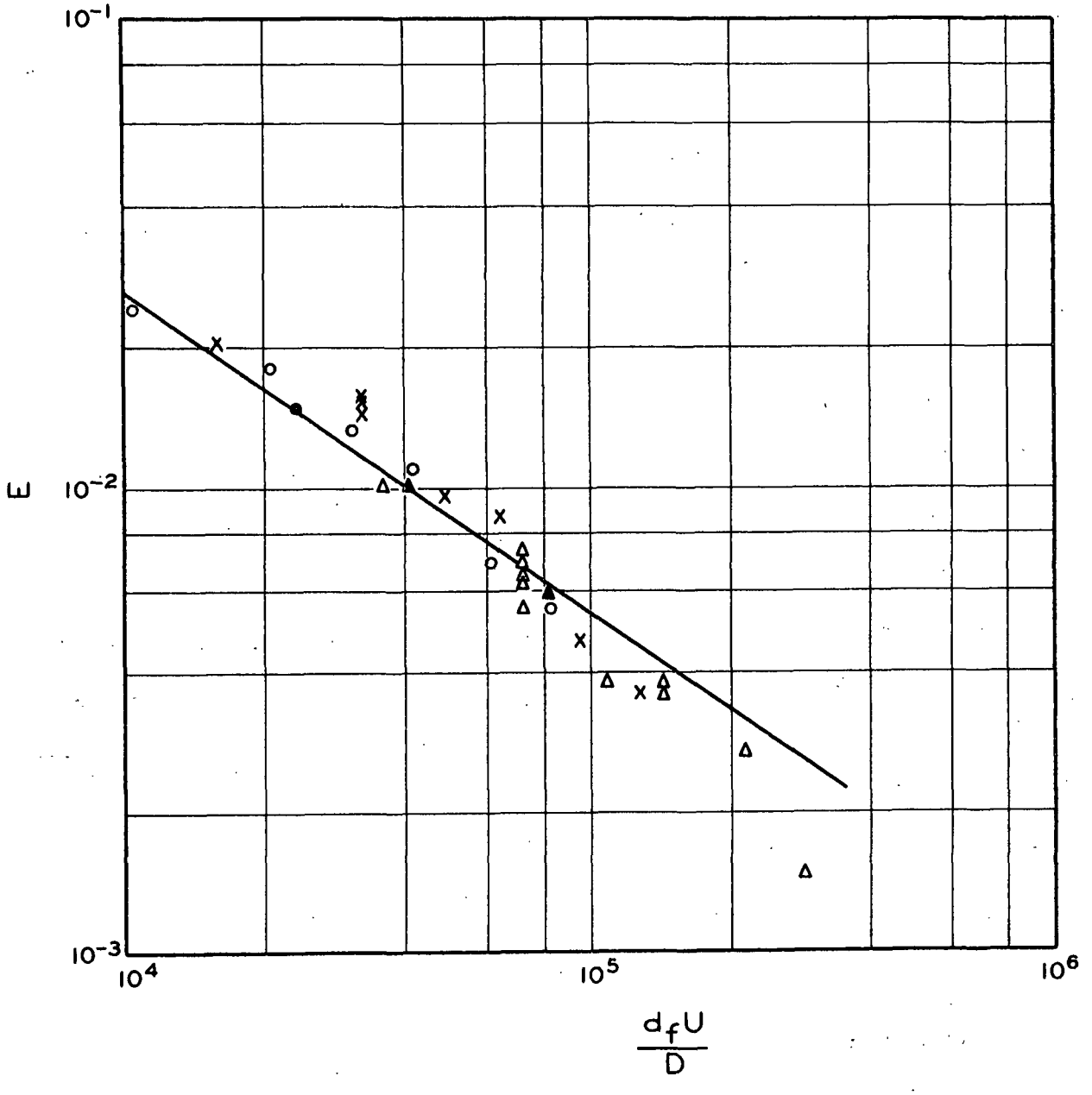

Figure A-9. Correlation of Collection Efficiency with Diffusion Number

The value of the dimensionless constant α is evaluated to be 11. In terms of penetration the correlation becomes

$$-\ln P = \alpha \frac{4(1-\epsilon)L}{\pi d_f} \left(\frac{D}{d_f U}\right)^{2/3} \qquad \text{(A-38)}.$$

The present correlation is limited to $\underline{Re}_f < 1$. The extension of the correlation to lower Reynolds numbers would probably be valid. We believe that Johnson's retention data represent the limiting case of pure diffusion in laminar flow.

Johnson also performed a few retention experiments with mats of different porosities. The results were inconclusive and therefore are not used here. At the same approach velocity the average velocity in the void space of a mat increases with decreasing porosity. This tends to reduce retention by diffusion. On the other hand, at smaller porosities the particles are closer to the fibers and would be captured more easily. As a result, the effect of porosity on diffusional retention is quite complex, presumably depending on the range of porosity. Recent experimental evidence in air filtration at the Institute indicated that collection efficiency is nearly independent of porosity below a porosity of 0.9. At high porosities Chen (8) demonstrated empirically that collection efficiency decreases linearly with increasing porosity.

In Johnson's experiments only a single particle suspension was used. The effect of particle size or rather the size distribution was not investigated. However, since the diffusion coefficient is inversely proportional to the particle diameter in a liquid suspension, the effect of diffusivity may be considered to be applicable to particle size; i.e., $\underline{E}$ should be inversely proportional to $\underline{d}_p^{2/3}$ in diffusional retention, provided that the particle radius is large compared with the mean free path of the fluid molecules.

The diffusion theory in its present state holds in the absence of fluid inertial effects. As the fluid velocity increases, the inertial effects become increasingly important even though the primary flow pattern may still be laminar. To account for the change in flow pattern, an additional parameter will be needed. The Reynolds number is the accepted parameter. With the use of the Reynolds number the correlation of diffusional retention may be generalized to include the fluid inertial effects:

$$E = \alpha \left(\frac{\mu}{\rho D}\right)^{-2/3} \left(\frac{\rho d_f U}{\mu}\right)^{-2/3} + \beta \left(\frac{\mu}{\rho D}\right)^{-n} \left(\frac{\rho d_f U}{\mu}\right)^{-n'} \qquad \text{(A-39)},$$

when β , n , and n' are to be experimentally evaluated. By crude considerations it appears that particle retention by diffusion would be more dependent on the previously hypothesized mixing process and less on the Brownian motion. Then the values of n and n' would be expected to be smaller than 2/3. Some evidence points to a value of 1/2 for n and 2/5 for n'. If the proposed correlation can be firmly established, the evaluation of collection efficiency of a practical system will be rendered quite simple. For a given system, Equation (A-39) may be simplified to

$$EU^{2/3} = A + BU^{-4/15} \qquad \text{(A-40)}.$$

Therefore,

$$\alpha = A\left(\frac{d_f}{D}\right)^{2/3} \quad \text{and} \quad \beta = B\left(\frac{\mu}{\rho}\right)^{1/10} d_f^{2/5} D^{-1/2} \qquad \text{(A-41)}.$$

The proposed correlation is amenable to further development. At higher velocities inertial impaction sets in. The simplest way to incorporate impaction is to add a third term. Impaction is probably proportional to U^2 (9). In this range the first term may become insignificant.

NOMENCLATURE

A	=	area of a mat, sq. cm.; a constant
B	=	a constant
b	=	width of a fluid stream, cm.
C	=	particle concentration, $cm.^{-3}$
$\bar{C}$	=	average particle concentration as defined by Equation (A-21), $cm.^{-3}$
C_L	=	downstream particle concentration, $cm.^{-3}$
C_o	=	upstream particle concentration, $cm.^{-3}$
D	=	diffusion coefficient, sq. cm./sec.
d_f	=	diameter of a fiber, cm.
d_p	=	diameter of a particle, cm.
E	=	collection efficiency, dimensionless
e	=	base of natural logarithm
exp	=	an exponential function of
F	=	particle-fiber diameter ratio, cm./cm.
f	=	a function of
g	=	acceleration due to gravitation, $cm./sec.^2$
h	=	thickness of a mat, cm.
I	=	impaction number, dimensionless
K	=	attenuation coefficient, $cm.^{-1}$
k	=	Boltzmann's constant, erg/(molecule)(^{o}K.)
L	=	thickness of a mat, cm.
L_f	=	thickness of a fiber, cm.
N_f	=	number of fibers per unit volume of mat, $cm.^{-3}$
n	=	exponent
P	=	penetration, dimensionless
Δp	=	pressure drop, dynes/sq. cm.

R = radius of a capillary, cm.

Re_f = Reynolds number based on fiber diameter, dimensionless

r = radial co-ordinate; radius, cm.

S = settling number, dimensionless

Sc = Schmidt number, dimensionless

T = temperature, $^{o}C.$ or $^{o}K.$

U = approach velocity, cm./sec.

U_o = velocity of a uniform stream, cm./sec.

u = velocity component in the z-direction, cm./sec.

u_o = axial velocity, cm./sec.

W = mass of fibers in a mat, g.

W_L = mass of particles penetrated through a mat, g.

W_o = mass of particles approaching a mat, g.

W_r = mass of particles retained in a mat, g.

x = x-co-ordinate

Z = a dimensionless parameter

z = z-co-ordinate; length of a capillary, cm.

z_o = attenuation distance, cm.

α = retention coefficient, dimensionless

α' = retention coefficient, dimensionless

β = retention coefficient, dimensionless

ϵ = porosity, cc./cc.

μ = viscosity of a fluid, poises

ρ = density of a fluid, g./cc.

ρ_f = density of a fiber, g./cc.

ρ_p = density of a particle, g./cc.

LITERATURE CITED

1. Wong, J. B. Ph.D. Thesis, Chem. Eng. Urbana, Ill., University of Illinois, 1954.

2. Gormley, P. G., and Kennedy, M., Proc. Roy. Irish Acad. 52, Sect. A:163-9 (May 3, 1949).

3. Johnson, R. C. A study of particle retention in relation to the structure of a fibrous mat. Doctor's Dissertation. Appleton, Wisconsin, The Institute of Paper Chemistry, 1962. 92 p.

4. Tomotika, S., and Soi, T., Quart. J. Mech. and Appl. Math. 3:140(1950).

5. Langmuir, I. O.S.R.D. Report No. 865. Washington, D.C., Office of Scientific Research and Development, 1942.

6. Stairmand, C. J., Trans. Inst. Chem. Eng. 28:130(1950).

7. Einstein, A., Ann. Physik 17:549(1905); 19:371(1906).

8. Chen, C. Y. Filtration of aerosols by fibrous media. Annual Report to U.S. Army Chemical Corps. Urbana, Ill., University of Illinois, 1954. 83 p.

9. Dorman, R. G. The role of diffusion, interception, and inertia in the filtration of airborne particles. In E. G. Richardson's Aerodynamic capture of particles. Proceedings of conference held at B.C.U.R.A., Leatherhead, Surrey, 1960. p. 112. New York, Pergamon Press, 1960.

APPENDIX II

COMPUTATION OF $\underline{p_s'}$ AND $\underline{E}$

The integrated retention equation is

$$m' = (m + m')_s\left(\frac{w}{W}\right) - \frac{(m + m')_s - m_s'}{K'}\left[e^{-K'\left(1 - \frac{w}{W}\right)} - e^{K'}\right]$$

$$= m_{t,s}\left(\frac{w}{W}\right) - \frac{m_{t,s} - m_s'}{K'}\left[e^{-K'\left(1 - \frac{w}{W}\right)} - e^{-K'}\right],$$

where by definition:

$$m' = -W\int_1^{1-(w/W)} p'd\left(1 - \frac{w}{W}\right),$$

$$m_s' = p_s'W,$$

and

$$m_{t,s} = p_{t,s}W.$$

Under the assumption of random errors, the best values of $\underline{m_s'}$ and $\underline{K'}$ may be obtained by the method of least squares if the retention equation is valid for the filtration experiments.

Let $\underline{R} = \sum(\underline{m'_{exp}} - \underline{m'_{calc}})^2$ for all cumulative layers of a mat. Since the calculated value of $\underline{m'}$ from the integrated equation, using certain arbitrarily chosen values of $\underline{m_s'}$ and $\underline{K'}$ must deviate from the experimental value by some differences in the chosen values from the best values of $\underline{m_s'}$ and $\underline{K'}$, we may include the effects of these differences by writing

$$m'_{calc} = m_{t,s}\left(\frac{w}{W}\right) - \frac{m_{t,s} - m_s'}{K'}\left[e^{-K'\left(1 - \frac{w}{W}\right)} - e^{-K'}\right] + b\Delta m_s' + c\Delta K' ,$$

$$b = \left(\frac{\partial m'_{calc}}{\partial m_s'}\right)_{K'} = \frac{1}{K'}\left[e^{-K'\left(1 - \frac{w}{W}\right)} - e^{-K'}\right] ,$$

and

$$c = \left(\frac{\partial m'_{calc}}{\partial K'}\right)_{m_s'} = (m_{t,s} - m_s')\left[\frac{1}{K'^2} e^{-K'\left(1 - \frac{w}{W}\right)} - \frac{1}{K'^2} e^{-K'}\right.$$

$$\left. + \frac{1}{K'}\left(1 - \frac{w}{W}\right)e^{-K'\left(1 - \frac{w}{W}\right)} - \frac{1}{K'} e^{-K'}\right] .$$

Therefore,

$$m'_{calc} = m_{t,s}\left(\frac{w}{W}\right) - \frac{m_{t,s} - m_s'}{K'}\left[e^{-K'\left(1 - \frac{w}{W}\right)} - e^{-K'}\right]$$

$$+ \frac{1}{K'}\left[e^{-K'\left(1 - \frac{w}{W}\right)} - e^{-K'}\right]\Delta m_s'$$

$$+ (m_{t,s} - m_s')\left[\frac{1}{K'^2} e^{-K'\left(1 - \frac{w}{W}\right)} - \frac{1}{K'^2} e^{-K'}\right.$$

$$\left. + \frac{1}{K'}\left(1 - \frac{w}{W}\right)e^{-K'\left(1 - \frac{w}{W}\right)} - \frac{1}{K'} e^{-K'}\right]$$

$$= a + b\Delta m_s' + c\Delta K' ,$$

and

$$R = \sum\left[m'_{exp} - a - b\Delta m_s' - c\Delta K'\right]^2 .$$

Upon partial differentiation, we obtain

$$\left[\frac{\partial R}{\partial(\Delta m_s')}\right]_{\Delta K'} = \sum -2b(m'_{exp} - m'_{calc}),$$

and

$$\left[\frac{\partial R}{\partial(\Delta K')}\right]_{\Delta m_s'} = \sum -2c(m'_{exp} - m'_{calc}).$$

By the theory of least squares,

$$-m'_{exp} \sum b + \sum ab + \Delta m_s' \sum b^2 + \Delta K' \sum bc = 0,$$

and

$$-m'_{exp} \sum c + \sum ac + \Delta m_s' \sum bc + \Delta K' \sum c^2 = 0.$$

Solving these two equations, we obtain

$$\Delta m_s' = \frac{\sum m'_{exp} - \sum ab - \Delta K' \sum bc}{\sum b^2}, \quad \text{and}$$

$$\Delta K' = \frac{\sum bm'_{exp} \cdot \sum bc - \sum bc \cdot \sum ab - \sum cm'_{exp} \cdot \sum b^2 + \sum ac \cdot \sum b^2}{(\sum bc)^2 - (\sum b^2 \cdot \sum c^2)}.$$

The computer program may be written in a manner such that when a set of arbitrary values of $\underline{m_s}'$ and $\underline{K}'$ is introduced, the values of $\underline{a}$, $\underline{b}$, and $\underline{c}$ corresponding to $\underline{m}'_{exp}$ will result. $\Delta \underline{m_s}'$ and $\Delta \underline{K}'$ are then calculated by the method of least squares indicated above, and the original values of $\underline{m_s}'$ and $\underline{K}'$ are corrected accordingly. The process is repeated until a desired level of precision is reached, for example, $\Delta \underline{m_s}'$ being less than 10^{-4}.